UNIVERSITY OF TWENTE.

Faculty of Engineering Technology
Civil Engineering and Management

A Framework for Standardized Assessment of Neighborhood Climate Adaptiveness and Derivation of Design Parameters under 2085 Climate Scenarios

Daniël B. van den Heuvel

Final thesis
August 21, 2019

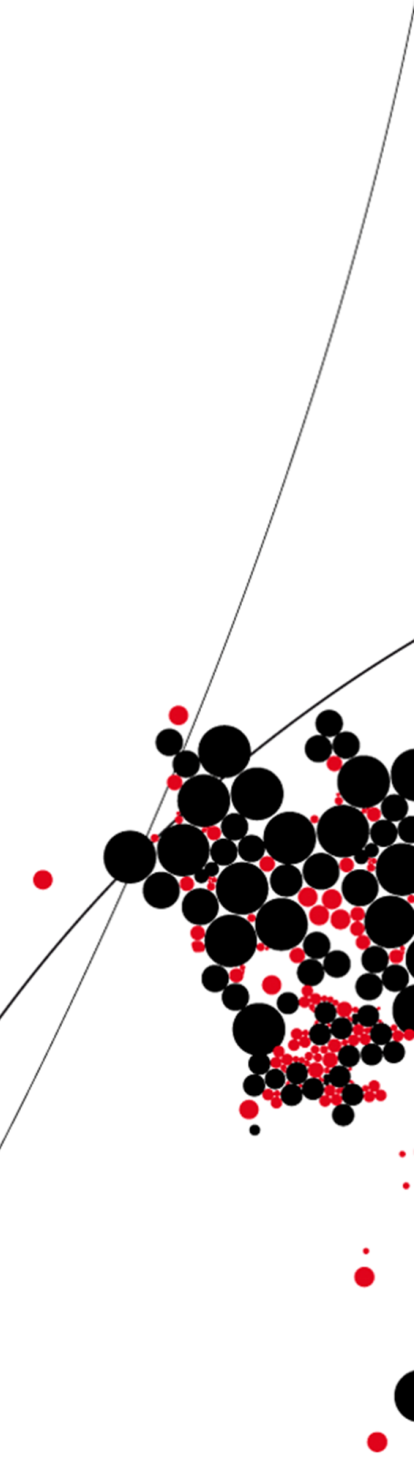

Witteveen + Bos

Supervisors:
dr. ir. M.J. Booij
dr. M.S. Krol
ir. S.F.M. Gijsbers

A Framework for Standardized Assessment of Neighborhood Climate Adaptiveness and Derivation of Design Guidelines under 2085 Climate Scenarios

Daniël B. van den Heuvel

A thesis submitted in partial fulfillment of the
requirements for the degree of
Master of Science

UNIVERSITY
OF TWENTE.

Department of Water Engineering and Management
University of Twente
Enschede, NL

August 21, 2019

Preface

Submitted in partial fulfillment for the requirements of the degree of Master of Science, this thesis marks the end of my time as a student at the University of Twente. It has certainly been a vivid period of my life during which I have gotten to know many great friends, shared countless unforgettable experiences and — sometimes — put painstaking efforts in my studies to get where I am now.

I would like to take this opportunity to thank several people who have been very helpful before and during my thesis project. In the first place, I would like to thank Martijn Booij and Maarten Krol for their excellent supervision from the University of Twente. Martijn's adequate feedback, scientific approach and ability to find every single misplaced comma in my writings have certainly helped me. In turn, Maarten's never-ending enthusiasm regarding the subject motivated me throughout my reserach even when things were not going so well. I honestly appreciate your time and the fruitful and intellectual discussions we had.

Of course, I would also like to thank Herman Mondeel and Stephanie Gijsbers from Witteveen+Bos. Herman provided me with the opportunity to work on my thesis at Witteveen+Bos. Stephanie continuously provided me with sharp-cut feedback and helped me keep track of the actual research aim and achieve it. I also render thanks to all the other colleagues I spent time with at the office of Witteveen+Bos in Deventer. Not only were they there to have lunch and share a laugh with me, they also never ever minded helping me whenever I got stuck with some computer model. I am definitely looking forward to work together with them on interesting projects starting the fall of 2019.

I hope you enjoy reading my thesis.

Daniël van den Heuvel
Deventer, August 21, 2019

Summary

As scientific evidence for climate change is mounting, so are the efforts to make neighborhoods and the public space in the Netherlands more resilient against the potential hazards caused by climate change. Municipalities and other Dutch governmental bodies have had numerous climate stress tests conducted in order to assess to what extent current and new neighborhoods are able to cope with a changing climate. However, these stress tests vary considerably in spatial and temporal resolution, climate change hazards considered (and indicators thereof) and methodology. Moreover, the results are always used locally only whereas it seems logical to generalize their findings to support the design of new neighborhoods in similar locations. The lack of standardization among stress tests is problematic as their methodologies are currently largely prescribed by the client and it jeopardizes comparability of assessments. As a result, stress test outcomes sometimes differ for a single neighborhood while there is no specific reason for this.

The aim of this research is twofold: (1) to develop and apply a more standardized framework to assess neighborhood-scale climate adaptiveness and (2) to prescribe coarse design guidelines for new neighborhoods of similar typology. Various assessment steps were included in the framework and indicators of climate change hazards and unacceptable values ("threshold values") thereof were determined under standardized climate change occurrences ("forcings"): extreme climate manifestations as projected by the KNMI for 2085. This time scale is unique as existing stress tests assume a 2050 time horizon that is too short for new neighborhoods. Several hazards were considered, being pluvial flooding, heat stress, high groundwater levels and drought-induced soil subsidence. The quantitative effects of the selected forcing events can be simulated with (computer) models and compared with the threshold values. The framework was applied in two cases: Wilderszijde (Rotterdam) and Hooghkamer (Voorhout), both in peatlands in the western part of the Netherlands. The framework was used to assess whether these neighborhoods can cope with the various hazards associated with climate change and to derive coarse design guidelines for other neighborhoods to be constructed in areas with similar characteristics.

The results show that neither Wilderszijde nor Hooghkamer is sufficiently adapted to withstand the worst-case climate conditions projected for 2085. Assuming their

current designs, both neighborhoods fail the assessments for almost all hazards considered. For each hazard, the effects of several possible measures were explored in an attempt to derive coarse design guidelines for neighborhoods yet to be constructed in Dutch peatlands. To mitigate pluvial flooding, it is recommended to increase the capacity of storage and infiltration facilities (e.g. stormwater sewage), reduce the amount and clustering of paved area and add more surface water to mitigate the flooding effects of extreme precipitation events. To combat heat stress, it is advised to add more greenery in the public space, to use light-colored, high-albedo construction materials and pavement, and to encourage (future) inhabitants to keep their gardens green and unpaved. Groundwater issues can be resolved by ensuring there is ample vertical space between the projected ground surface level and the highest maintained groundwater level, and by appropriately constructing drainage systems locally. It is also suggested not to have groundwater levels fluctuate too much during the summer so that soil-subsidence can be minimized.

This work contributes to the (standardization of) climate adaptiveness assessments of neighborhoods in the Netherlands. It also sheds light on what a new neighborhood should look like in terms of design guidelines for it to be sufficiently climate adaptive in the longer term and is one of the few works which actually quantify these design guidelines. While more standardization benefits the comparability of neighborhoods' climate adaptiveness, it remains difficult to prescribe the assessment methodology and design characteristics for each Dutch neighborhood. Especially drought-related problems will continue to require an approach tailored to the local situation as soil-subsidence problems largely depend on system parameters. The results of this research underline the dilemma between (potentially inaccurate) fully standardized assessments and (potentially costly) fully tailored assessments.

Contents

List of Figures

Chapter 1

Introduction

This introductory chapter serves to outline the motivation for this research, to describe the state of the art in this research field and to demarcate the project. The first section treats the scientific context in which this project takes place. Section 1.2 (State of the art) then provides an overview of recent insights into the field from scientific literature and current practice. The detected research gap is subsequently discussed in Section 1.3. This leads to the formulation of the research aims and questions in Section 1.4. The project is further demarcated in the Scope (Section 1.5). An outline of the remainder of this thesis can be found in Section 1.6.

1.1 Scientific context

Local weather patterns have been changing under the influence of large scale climate change and these changing patterns cannot be explained merely by inherent variability of climate (IPCC, 2001; Lindley et al., 2006). Scientific evidence that global scale climate change is largely anthropogenic is mounting. Changing weather patterns will have effects in all locations, but especially so in urban areas, for instance because of a high concentration of people, structures and infrastructure in cities. Due to these characteristics of urban areas, the impact of them being exposed to increasingly volatile weather conditions is relatively large. These risks are amplified by other factors than climate change: population growth, further urbanization and an overall increasing demand for water, food and energy all contribute to the risk of more unpredictable and intense weather events. In fact, Vörösmarty et al. (2000) have shown that the state of the world's water resources is largely defined by population growth, much more than by climate change. These developments will not form the subject of study here, and are not explicitly taken into account. One reason for this is the large number of scenarios and possible outcomes regarding population growth, urbanization and the resulting stress on the water system in ad-

dition to climate change. Therefore the focus here lies only on the effects of climate change as a whole, whether it be caused by excess greenhouse gas emissions or by inherent climate variability, on the risk of exposure to increasingly volatile weather conditions. Other influencing factors will thus be disregarded.

There is a wide variety of predicted long-term climate change effects which differ across locations. These effects need not necessarily be harmful, but many are considered to be potential hazards to liveability in cities (Ghoneem, 2016). These hazards include, but are not limited to: more and more severe urban flooding events, both pluvial and fluvial and/or coastal (Miller & Hutchins, 2017; Schreider et al., 2000), amplification of the urban heat island effect (McCarthy et al., 2010), and volatile and unpredictable changes in urban groundwater levels (Green, 2016). Many more aspects can be identified which are influenced by a changing climate, such as energy, mobility and agriculture. However, due to time constraints this work is limited to aspects related, either directly or indirectly, to water management and heat stress influenced by climate change in urban areas.

It is extremely difficult to estimate how future weather conditions will impact urban areas as induced by climate change, both due to the deep uncertainty concerning climate change developments (Casal-Campos et al., 2018; Marchau et al., 2019) and due to the strong local variation of impacts. There are still many plausible futures projected under climate change and as a result, no unambiguous strategy has been developed yet to cope with a changing climate in population centers. While it may be impossible to develop a single and universal strategy for climate adaptation measures, it is desirable to provide more standardization in assessment methodology for good comparability and efficiency.

There are several approaches available for decisionmaking under deep uncertainty (DMDU), many of which are elaborately explained in the work of Marchau et al. (2019). Two approaches which have received more attention recently, especially among Dutch scientists, are those of Dynamic Adaptive Planning (DAP) and Dynamic Adaptive Policy Pathways (DAPP) (Haasnoot et al., 2013). These methods have been used demonstratively in several cases regarding climate change adaptations, but mainly at the (sub-)national scale and delta regions and not in neighborhoods.

Many studies (e.g. Jabareen (2013); Hardoy and Ruete (2013)) have called for local measures in order to keep cities liveable. Because climate change effects are already manifesting themselves and because of the inherent uncertainty regarding further effects, they often call for adaptations to public space which are able to cope with a variety of climate scenario outcomes.

The Royal Dutch Meteorological Institute (KNMI) has researched climate change effects in the Netherlands and composed several climate change scenarios for the

country in particular (Klein Tank et al., 2015). Four scenarios were identified, both for a 2050 and 2085 (2070-2100) time horizon: G_L, G_H, W_L and W_H. The development of these scenarios depends on (1) the global temperature rise and (2) the change in circulation pattern. These worldwide developments are classified respectively as either low/small and high/large, which yields the total of four scenarios combined. This is depicted in Figure 1.1. For each scenario, quantitative indicators regarding the sea level at the North Sea coast, average temperature, total precipitation and solar radiation were estimated. A summary of the results of these estimations for the time horizon 2085 is shown in Figure 1.2. It is important to remark that these are average figures and that these projections are quite uncertain. This uncertainty is reflected by the broad ranges of projected values, even within the same scenario. Nonetheless, Figure 1.2 shows a trend of substantial sea level rise, an increase of average temperature and an increase of average precipitation. The incoming solar radiation is predicted to decrease or increase slightly. The KNMI specifically remarks that precipitation events are likely to become more extreme in all scenarios, as are heat waves and periods of drought (McCarthy et al., 2010). It is important to remark that the 2085 scenario does not exactly reflect the projected conditions for the particular year 2085, but rather for the period 2070-2100.

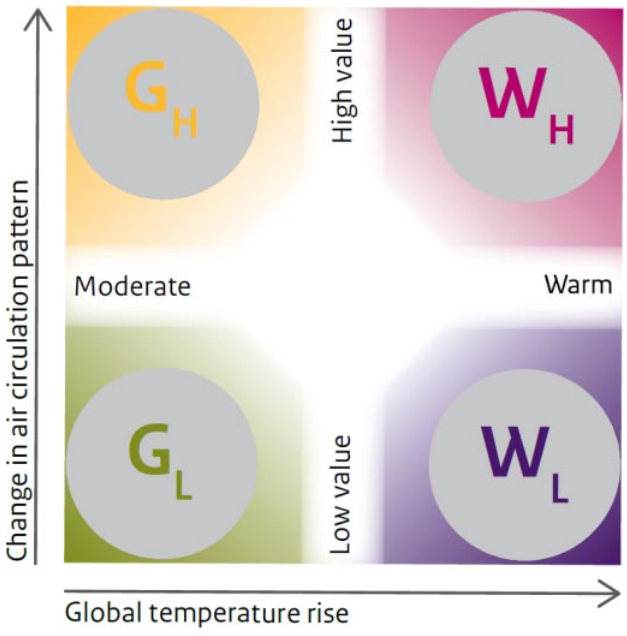

Figure 1.1: KNMI climate scenarios for the Netherlands

Variabele	Indicator	Climate 1981-2010	Scenario changes for the climate around 2085			
			G_L	G_H	W_L	W_H
Global temperature rise:			+1.5 °C	+1.5 °C	+3.5 °C	+3.5 °C
Change in air circulation pattern:			low value	high value	low value	high value
Sea level at North Sea coast	absolute level	3 cm above NAP	+25 to +60 cm	+25 to +60 cm	+45 to +80 cm	+45 to +80 cm
	rate of change	2.0 mm/yr.	+1 to +7.5 mm/yr.	+1 to +7.5 mm/yr.	+4 to +10.5 mm/yr.	+4 to +10.5 mm/yr.
Temperature	mean	10.1 °C	+1.3 °C	+1.7 °C	+3.3 °C	+3.7 °C
Precipitation	mean amount	851 mm	+5 %	+5 %	+7 %	+7 %
Solar radiation	solar radiation	354 kJ/cm²	-0.5 %	+1.1 %	-0.9 %	+1.4 %

Figure 1.2: Predictions of four KNMI climate scenarios for time horizon 2085

1.2 State of the art

Despite the clear hazards to cities and other densely populated areas posed by climate change, many cities have not yet developed climate change adaptation plans. Also, it is difficult to adequately compare adaptation agendas because of the large variations in the scale and nature of measures taken and the large local variety in adaptation strategies (Corfee-Morlot et al., 2011; Hunt & Watkiss, 2011). The absence of unambiguous and long-term climate adaptation strategies is caused by several factors, such as limitations in financial and human resources (Measham et al., 2011) and insufficient awareness of climate change hazards (Lehmann et al., 2015).

Where cities have paid attention to the effects of climate change, these efforts have often focused on the mitigation of climate change rather than on adaptation strategies (Hoppe et al., 2014). The former strategy is aimed at inhibiting the process of climate change itself through limiting the emission of green house gases by the city and its inhabitants. The latter is aimed at the mitigation of climate change effects by (re-)building cities and neighborhoods so that they are more resilient to

the expected future weather patterns as induced by climate change. While there seems to be strong scientific support for the pursuit of the mitigation strategy and reducing the emission of green house gases, the call for more elaborate adaptation strategies has gained momentum over the last two decades (Schipper, 2006). The primary reason for this shift seems to be the fact that already emitted green house gases and inertia effects will bring about climate change effects regardless of the chosen mitigation strategy.

In light of the increased attention for the climate adaption strategy, the Dutch Delta Program now includes a separate chapter on spatial climate adaptation (Deltacommissie, 2014). It specifically calls for the gradual development of "water robust" cities and urban areas, but does not provide a clear definition of the concept of water robustness. The definitions currently employed are limited to "shaping public space in such a way that the impact of, for instance, extreme precipitation events is limited" and "to alter areas in public space so that extreme weather conditions, a changing climate and associated increase in water-related burdens can be withstood" (Van de Ven et al., 2009). While it would seem that the concept of water robustness is aimed solely at water-related problems in the future, the authors also call for taking into account heat stress.

The Delta program requires all Dutch municipalities and provinces to have carried out a climate stress test to map potential vulnerabilities in the area under climate conditions as predicted for 2050, including their uncertainties. This requirement is no legal obligation, but all governmental bodies and the Delta Program have agreed on agendizing the issue and conducting stress tests (Deltacommissie, 2014). This stress test must at least address the aspects water hindrance, drought, heat and flooding. Water hindrance is defined broadly here and includes pluvial flooding, hindrance resulting from high groundwater levels and some water quality aspects. The aspect flooding here is purely aimed at fluvial and coastal flooding. The stress test thus takes into account both an increase in precipitation and flood risk, and more extreme dry spells. However, this requirement applies to the existing built environment and not to neighborhoods that are still in the planning phase. Moreover, the time horizon employed in these stress tests in 2050, while neighborhoods that were recently constructed or are currently being designed are supposed to be in place for a much longer time horizon. As it is most efficient to include measures which enable the living environment to withstand future climate conditions already during the design phase, it is desirable to be able to assess these designs while they are not yet definitive and have not yet reached the construction phase.

In an attempt to complement the recommendations of the Delta Program, the Dutch National Knowledge and Innovation Program Water and Climate (NKWK) identifies four main threats to the liveability of cities and neighborhoods: fluvial and

coastal flood risk, pluvial flooding, drought and heat (Rovers et al., 2014). In their report, these authors also emphasize the importance of small-scale, local measures to successfully adapt areas to climate change in addition to their vocal call for reducing the emission of greenhouse gases. They thus attempt to shift the focus of governmental bodies more from climate change mitigation towards adaptation.

Through the presentation of their reports, the Delta program and the NKWK have sparked growing interest among government bodies in climate adaptation measures. This has led to a strong increase in demand for climate stress tests and analyses, also because all municipalities have agreed on having stress tests conducted. There is an abundance of stress tests and quick scans available from engineering firms and consultants, and the Delta program has composed guideline for these stress tests to provide some standardization. This guideline is dubbed the Stress Test Light (STL). It mentions and describes several themes and aspects which must be present in each stress test (water hindrance, heat, drought and floods) and provides several examples of indicators to assess the degree of climate adaptation. However, it does not impose stringent rules on the methodology that should be employed, nor does it mention anything about the scale at which these tests should be performed or the desired level of detail. As a result, it seems that the STL does not provide much standardization in stress tests conducted by engineering firms. Also, this is not an actual stress test in that no quantitative indicators and threshold values are defined for the evaluated climate change hazards. The assessed study area can thus not pass or fail the test; rather it maps potentially vulnerable locations, based mostly on coarse simulations with a regional scale.

One aspect influenced by climate which receives relatively little attention is groundwater. Although the aspect of groundwater does receive brief mention in STL, it is not explicitly included as assessment criterion and categorized under “other potential climate change hazards”. Previous scientific works have shown the potential hazards of developments in groundwater levels under the influence of climate change. As the hydrological cycle is influenced by climate change through more extreme precipitation events and higher temperatures, so will be groundwater levels and the rate of groundwater recharge. Several attempts were made to assess the impact of climate change on groundwater levels and groundwater recharge in many locations (e.g. Australia (Barron et al., 2018) and the Great Plains in the USA (Crosbie et al., 2013)). While these studies have obtained meaningful findings regarding future groundwater simulations, the results show large variation and uncertainty. It is therefore difficult to predict how groundwater levels and recharge will develop in any given study area given estimations of precipitation and temperature. Groundwater levels and recharge rates are of importance to many cities and neighborhoods. Higher groundwater levels can lead to groundwater seepage into basements and

other subsurface structures, while lower levels may bring about soil subsidence and jeopardize certain economic activities. In contrast to precipitation and runoff, groundwater recharge is a relatively slow process and climate change effects on it therefore take place on another time scale than pluvial flooding for example.

The concept of water robustness as coined by the Delta Program remains ill-defined, as it is unclear whether issues not directly related to water management (such as heat stress) should be included. Van de Ven et al. (2009) base the concept of water robustness on future problems in the public space as predicted by the KNMI, but it is unclear what exactly is meant with the word "robustness" here. It suggests the preparation of public space to withstand future climate changes, but the temporal horizon is not explicitly mentioned, nor is the approach. Many scientific works make a distinction within climate change preparation efforts between (1) mitigation and (2) adaptation (Van Buuren et al., 2013). See also Section 1.1. Climate change mitigation as a strategy is not a part of this study. The adaptation strategy is further broken down into two categories: (1) the flexible approach and (2) the robust approach. The former refers to shaping the public space so that few definitive choices are made: there is still room to make further adaptations even after completion. This decision may be postponed until there is more certainty regarding the effects of climate change. One flexible planning strategy that aims to cope with deep uncertainty and is flexible is that of Dynamic Adaptive Policy Pathways. It is based on the implementation of short-term actions within a more elaborate framework of future actions. This strategy could be considered to be part of a new planning paradigm. DAPPs have been applied in numerous cases recently (for a comprehensive overview, see Haasnoot et al. (2013)), but chiefly on a regional scale. In contrast, the robust approach refers to designing the neighborhood so that no or few adaptations are necessary for it to remain climate adaptive.

To prevent confusion regarding the word robustness, the following concept of climate adaptiveness is proposed here, defined as *"the state of public space of being able to withstand future climate conditions regarding water management and heat stress as projected in scenarios"*. Climate adaptiveness can still be pursued through the two approaches mentioned before: the flexible and the robust approach.

It is assumed here that new neighborhoods are designed according to the robust principle. This means that they are put in place for the rest of the century and do not require any additional measures to be able to withstand future climate change effects. This allows for the usage of current data regarding neighborhood design without having to account for future changes to the neighborhood's spatial characteristics. While the flexible approach, and also the DAPP strategy, may be feasible in neighborhood design under climate change uncertainty, it was considered too cumbersome and difficult to deal with the dynamics of a flexible approach here. Instead,

the this research's aims are first pursued for the simpler robust approach.

The growing interest in climate adaptation measures has also manifested itself in the Dutch province of South Holland. A variety of stakeholders is unified in the "construction covenant South Holland" (Bouwconvenant Zuid-Holland) which stipulates the ambition to build all new neighborhoods in the province so that they are sufficiently climate adaptive, also in the longer term. Their mission is to collaboratively design and build neighborhoods to ensure (1) less pluvial flooding, (2) less heat stress, and (3) fewer negative effects from droughts. All municipalities in the province as well as several construction firms, banks, water boards and other stakeholders participate in the covenant.

1.3 Research gap

There is currently a gap in the approach for assessing climate adaptiveness and the desired situation in which the neighborhood design is based on (quantitative) results of a climate adaptiveness assessment. This desired situation requires the standardization of climate change hazards and indicators where possible under a clear and uniform definition of climate adaptiveness. Despite the mounting number of climate stress tests, there is no universally adopted definition by which neighborhoods are assessed and terms such as "water robust" and "climate adaptive" are often used interchangeably. Some definitions and assessment tools take only issues directly related to water quantity into account, such as flooding and droughts, while others also consider heat and water quality. There is thus very little standardization among climate stress tests, not only regarding methodology, but even regarding climate hazards and indicators thereof included in the test. As a result, it is conceivable that different stress tests yield different outcomes for one identical neighborhood under the same time horizon. While the STL attempts to provide some standardization in this matter, it remains merely a guideline and does not actually prescribe an unambiguous methodology or assessment indicators. Climate change adaptation in the Netherlands would benefit from a more standardized and demarcated approach to ensure good comparability.

Another drawback of the STL is its very coarse spatial resolution. For many considered and mapped indicators (e.g. groundwater, pluvial flooding) it utilizes regional or even national data as it is impossible or costly to obtain local data. As a result, its results are not sufficient for local decision making. The STL always has to be supplemented by local data and/or expert opinion to interpret its outcomes and to base decisions upon them. The resolution of the STL is thus not in accordance with the many calls throughout literature to focus more on local adaptation measures (see Section 1.2).

Moreover, currently all available stress tests, including the stress test light, employ a time horizon of 2050 for their assessment. This seems to be a reasonable time scale for already existing urban areas and neighborhoods, but there is no alternative assessment method for newer neighborhoods which are supposed to be inhabited long after the year 2050. In order to ensure that these homes and neighborhoods remain liveable in the longer term and will not encounter severe hindrance due to more extreme weather patterns, their ability to withstand the predicted climate conditions of 2085 should be quantitatively assessed. There is currently no such tool which includes multiple hazards related to water management and heat stress for the long term.

Also, there is no inclusive and comprehensive tool which assesses the degree of adaptiveness of neighborhoods in their design phase under future climate uncertainty. The availability of such a tool is desirable because urban planners are often confronted with objectives regarding climate adaptiveness on the one side and with budget and planning restrictions on the other side. In addition, developers often have an incentive to construct as many homes as possible in a neighborhood to increase their profits. The space necessary for construction competes with the space necessary for certain climate adaptation measures. A tool which takes into account a fixed set of climate change hazards and is able to quantify the climate adaptiveness of different design options may aid urban planners in the choice for their final neighborhood design.

In addition, the results of stress tests are always used locally. While useful, it may be possible to use the results of one climate stress test to derive coarse design guidelines for a similar type of neighborhood. It seems logical that similar neighborhoods with similar characteristics require similar designs in order to be sufficiently climate adaptive. After the framework has been applied in several similar cases, it may be possible to prescribe design guidelines for neighborhoods yet to be designed. Some work has been done to establish a standardized set of assessment criteria for different hazards, but these have not yet been translated to clear guidelines that can be used to design a new neighborhood.

These research gaps could be closed through:

1. Offering more standardization and demarcation regarding the climate change hazards included in the stress tests and the quantifiable indicators thereof;
2. Ensuring a good fit between the outcomes' spatial resolution and the assessment's objectives;
3. Choosing a longer time horizon in the case of recently constructed (e.g. from 2000) or yet to be constructed neighborhoods;
4. Designing a tool so that it fits the purpose of assessing the climate adaptiveness of neighborhoods still in the design phase;

5. Using that tool to derive coarse design guidelines for Dutch neighborhoods with similar characteristics to ensure they remain sufficiently climate adaptive under 2085 climate scenarios.

1.4 Research aim

The aim of this research is twofold: (1) to develop and apply a framework that can be used to assess quantitatively whether or not a neighborhood (either existing or still in planning) is sufficiently climate adaptive under the 2085 climate conditions as projected by the KNMI, and (2) to prescribe coarse design guidelines for new neighborhoods of similar typology (constituted by several system parameters; see Section 2.1.3 for a more elaborate explanation). These guidelines should ensure that newly constructed neighborhoods are climate adaptive and remain so in the long term. Table 1.1 provides an overview of the characteristics of the yet to be developed framework in comparison with existing stress tests and the STL. Various aspects as discussed in the Research gap (Section 1.3) are included. While it is possible to view the hazards' impacts on the neighborhood scale in the stress test light, these results are merely interpolations of models with coarser resolutions and need to be supplemented with local insights. Its spatial scale and applicability is therefore listed as regional only.

Table 1.1: Characteristics of the yet to be developed framework for climate adaptiveness assessment compared to existing stress tests and the stress test light. Each aspect is described in Section 1.3

Aspect	Existing stress tests	Stress test light	Framework
Standardized (hazards/indicators)	No/No	No/Yes	Yes/Yes
Spatial scale & resolution	Neighborhood or larger	Regional	Neighborhood
Time horizon	2050 (usually)	2050	2085
Construction phase	Construction finished	Construction finished	Design phase (and finished)
Applicability results	Locally only	Regionally only	Generically

The framework is thus more than a stress test as it also provides its users with the possibility of deriving coarse neighborhood design guidelines. Repeated application of the framework's steps can lead to a design direction of neighborhoods of similar typology. The neighborhood type is constituted by (1) system parameters specific to its location and (2) design parameters (see also Section 2.1).

As discussed in Section 1.1, multiple climate change hazards can be distinguished. There seems to be very broad consensus about the inclusion of pluvial floods in any climate assessment tool, both in literature and existing stress tests, including the STL. Although this hazard is sometimes categorized as a sub-aspect of water hindrance (or similar terms), it was decided to explicitly include pluvial flooding in the assessment framework.

Heat stress also forms a potential hazard stemming from climate change. Since it is related to water management but is not easily categorized as a sub-aspect of another climate change hazard, it will be a potential hazard on its own in the framework that is to be developed.

While most existing stress tests take into account some potential hazards of groundwater, it is often considered a part of other hazards (too high groundwater levels are usually a part of water hindrance, too low levels a part of drought or omitted altogether). Because changing groundwater levels may be an important hazard in neighborhoods in the future, and because the framework does not take water hindrance as a whole into account, groundwater is a separate hazard here. Both hindrance resulting from high groundwater levels and drought-induced soil subsidence are considered here.

This leads to the following list of hazards which will be used to assess the climate adaptiveness of neighborhoods, defined as *"the state of public space of being able to withstand future climate conditions regarding water management and heat stress as projected in scenarios"*:

1. Pluvial flooding;
2. Heat stress;
3. Groundwater: hindrance and drought-induced soil subsidence.

This list bears many similarities with the ambitions stipulated in the construction covenant (see Section 1.2).

The final assessment framework should be used to substantiate claims regarding the climate adaptiveness of newly designed or constructed neighborhoods using quantitative design characteristics. Possible weak spots in the design should immediately become clear after the assessment, because three hazards are evaluated. Conversely, it may be used to approximate the scale of adaptation measures necessary in order for the design to be sufficiently climate adaptive. The framework can thus also be used to generate coarse design guidelines for neighborhoods. Rather than prescribing norms or thresholds for climate adaptiveness, the framework attempts to derive the values of actual design parameters for the neighborhood specifically.

The standardization of climate adaptiveness seems to carry several dilemmas:

a fully standardized assessment overlooks local deviances from the average neighborhood, rendering its results less usable. A fully tailored assessment is costly and time-consuming.

The following research questions were formulated to guide the research:

1. Can the assessment of neighborhood climate adaptiveness be standardized in a framework, given its design and climate scenarios?
2. Can the outcomes of the framework assessment be used to derive coarse design guidelines for new neighborhoods?
3. Which design guidelines could contribute to making planned neighborhoods in Dutch peatlands sufficiently climate adaptive assuming a 2085 temporal horizon?

1.5 Scope and demarcation

This study assumes a long temporal horizon: the assessment framework should be applied to assess cities and neighborhoods climate adaptiveness to the climatic circumstances of 2085, as projected by the KNMI. While the climate scenario W_H is the most extreme scenario in that it assumes both a large increase in temperature and a strong change in circulation pattern, it is not certain whether this scenario will actually yield the largest impact on each of the four hazards. Not only average values are relevant, but also the extreme values. Multiple KNMI scenarios will therefore be considered, but the worst case outcomes for each hazard will be used.

In spatial terms, the framework's application is limited to the neighborhood scale; its goal is not to assess the climate adaptiveness of individual homes or entire urban areas. The following definition of a neighborhood is adopted here, as proposed by Barton et al. (2003), who define it as follows: "home patch, which is a cluster of dwellings grouped say around a street, but smaller than a city sector or district big enough to satisfy the full range of local needs such as a supermarket, secondary school and places of employment".

Within this spatial scope, the goal is to develop the framework so that it can be applied to a wide variety of neighborhoods in the Netherlands. The methodology prescribed by the framework should function regardless of the neighborhood's location in the Netherlands. However, the system parameters differ for each region, even within a small country such as the Netherlands. For example, the soil type, the proximity of surface water and the land elevation have a profound effect on the climate change hazards described. This necessitates different design guidelines for different types of neighborhood to arrive at a similar level of climate adaptiveness. Here the framework is only applied to cases located in the province of South Holland

to assess the climate adaptiveness of neighborhoods there and to prescribe coarse design guidelines for this type of neighborhood. These neighborhoods are characterized by the peatlands they are located in and this defines many of the system parameters. This was considered a suitable province, because (1) many new homes are to be constructed in the region, (2) the system parameters across the area are mostly similar (such as soil type and elevation) and (3) the construction covenant has formulated clear ambitions regarding three out of four climate change hazards considered in this work (pluvial flooding, heat stress, high groundwater levels and droughts) across the province. The design guidelines derived from these cases' results could be used to aid the design of neighborhoods in peatlands in other parts of the Netherlands as well.

1.6 Thesis outline

This thesis is further organized as follows. Chapter 2 describes the results of the preliminary literature research and the methodology employed to arrive at the research aim described. Results are presented in Chapter 3. Chapter 4 is dedicated to the discussion of this work and treats this research's potential and limitations in detail. Finally, the conclusions and recommendations for further research are to be found in Chapter 5.

Chapter 2

Methodology

This chapter presents the methodology that was employed to achieve the research aims of this study. Section 2.1 treats the methods and outcomes of the preliminary literature study. Section 2.2 shows the steps that were taken to set up the framework and describes the steps it comprises. The generic quantitative indicators used in the assessment framework are discussed in Section 2.3. Section 2.4 is dedicated to the choice of models and provides a brief description of the working of these models. Sections 2.5 through 2.7 respectively treat the generic forcings, generic threshold values and an overview of generic indicators, forcing and thresholds for each hazard. Sections 2.8 and 2.9 describe the research steps taken to obtain the results for the two case studies the framework was applied to. Finally, the methodology used to arrive at neighborhood design guidelines is discussed in Section 2.10.

2.1 Literature background

This section addresses several definitions and terminology about climate adaptiveness used throughout literature and practice. To this end, the questions below were drafted and answered. The answers to these questions are fundamental to the remainder of this thesis.

1. How can climate adaptiveness be defined and what does it include?
2. Which quantitative indicators are suitable to assess the extent of climate adaptation in a neighborhood?
3. Which quantitative design parameters that influence the aforementioned indicators are suitable to consider in the framework?

2.1.1 Definition of climate adaptiveness

Various names and definitions are being used to indicate the efforts to ensure neighborhoods can deal with future climate conditions, such as climate robustness, water robustness, and climate adaptation. For a more elaborate discussion, see Section 1.2. To prevent confusion regarding the word robustness, we here choose to adopt the concept of climate adaptiveness. It is defined as *"the state of public spaces of being able to withstand future climate conditions regarding water management and heat stress as projected in scenarios"*. Water management here refers to water hindrance resulting from pluvial flooding and too high or low groundwater levels.

2.1.2 Determination of possible quantitative indicators

To be able to assess neighborhoods' climate adaptiveness in a quantitative manner, it is necessary to have several indicators which describe the nature of each hazard. Quantitative values of these indicators can be compared with threshold values or norms to determine the extent of climate adaptiveness. To compose a list of possible quantitative indicators, insights from both practice and literature were used.

Indicators used in existing stress tests

First the included hazards, modeling approaches and underlying assumptions of four climate stress tests were analyzed. These stress tests were carried out by different renowned Dutch engineering firms in locations across the Netherlands: Noordwijk (Antea Group, 2018), the Gelderse Vallei (HydroLogic, 2015), Haarlemmermeer (Nelen&Schuurmans, 2018) and a more general guideline for stress tests by Wareco (Meijel, 2017).

All the considered stress tests base their assessment for pluvial flooding essentially on inundation depth. Some simply present the maximum inundation depth reached at various locations within the study area. Others also include the inundation duration or the locations of critical infrastructure, such as tunnels in main roads and accessibility for emergency services. However, the forcings used in the studies vary greatly: from precipitation events with return periods between 1 and 2 years to rarer events with a 2050 return period of 100 years.

Heat stress was only considered in the Noordwijk and Vallei cases. The indicator they use is different, however. In the Noordwijk case, the daily-averaged temperature difference in the neighborhood as compared to the countryside was mapped for a tropical day. The report does not provide insight in the simulation methodology. In the Vallei case, the primary indicator is the number of nights during which the temperature remains above 20 $^{\circ}$C.

Groundwater problems are included in multiple ways. All studies take into account critically low groundwater levels (such as future average lowest groundwater levels) in an attempt to assess drought stress. Most studies combine this with the presence of wooden pole foundations to assess for the risk of pole rot. These risks are not quantified, however. In the Vallei case and in Wareco's guideline, groundwater hindrance resulting from high groundwater levels is also included. They take into account the projected critically high groundwater levels and subsurface structures, and thus try to assess for groundwater hindrance.

Indicators used in literature

In literature, inundation depth is also an important indicator for the assessment of pluvial flooding. For instance, Zhou et al. (2012) present a framework with which the economic risks as a result of pluvial floods can be assessed. To quantify the adverse effects of pluvial floods, they use both inundation depths and inundation durations. These data are ultimately coupled to land use and vulnerability data to arrive at (potential) monetary damage as an indicator of pluvial floods. Moreover, in a flood risk assessment (both pluvial and fluvial flooding) of a site in India, Patra et al. (2016) combine several models to arrive at a range of outcomes (depending on forcing and the model chosen). Their primary criterion for risk assessment is also the inundation depth of flood-prone areas.

While not a scientific study, RIONED has formulated norms regarding water hindrance in the Netherlands (RIONED, 2006). These norms find their basis in inundation depths and duration, and their return period. For instance, water on the streets (not exceeding curbs) is accepted once every two years. The work by RIONED has also partly inspired the framework's generic forcing and threshold values, to be discussed in Sections 2.5 and 2.6 respectively.

In a study to determine the extent of the Urban Heat Island (UHI) effect across biomes in the United States, Imhoff et al. (2010) used remote sensing to obtain land surface temperatures of urban areas and surrounding rural areas. The criterion used to assess the degree of the UHI effect is the difference between these two temperatures. Schwarz et al. (2012) have attempted to combine multiple indicators for the amplified UHI effect. Traditionally, two approaches can be distinguished: quantification of the UHI effect through meteorological ground measurements of the air or through the remote sensing of land surface temperatures. In both cases, assessment of the extent of the UHI effect is done by comparing urban to rural temperature. In their concluding remarks, it is mentioned that a combination of both ground and air temperature measurements should be used to best show the extent of the UHI.

Apart from the change in local groundwater levels, many works have attempted to elucidate the effects of climate change on the recharge rate of aquifers (e.g. Rosenberg et al., 1999). Such predictions could prove useful in assessing the sustainability of groundwater extraction. However, the recharge rate of aquifers is simulated on a macro scale, both in space and time, and thus not very useful in the present study as it is concerned with the neighborhood scale. Several works have focused on the smaller scale and have, for instance, tried to model groundwater levels and streamflows locally. These studies (Allen, 2010; Croley & Luukkonen, 2003) show that climate change may locally affect the groundwater levels. This might thus be an interesting indicator for this possible hazard.

Summary of possible quantitative indicators

1. Pluvial flooding
    - Inundation depth;
    - Flood duration;
    - Inundation of critical infrastructure and accessibility;
    - Monetary damage.
2. Heat stress
    - Number of casualties;
    - Temperature difference between urban and rural areas;
    - Temperature of swimming water;
    - Number of warm nights (temperature exceeding 20 °C).
3. Groundwater
    - Average lowest/highest groundwater level;
    - Inundation of subsurface structures;
    - Groundwater level change to reference level;
    - Risk of damage from soil subsidence.

2.1.3 Determination of possible relevant design and system parameters

In modeling the climate hazards, it is important to incorporate the most relevant parameters of a neighborhood in the used modeling tools. A list of parameters that are possibly relevant to include in the various models was composed. Similarly to the list

of possible indicators, it was inspired by both scientific insights and the application of such system parameters in existing climate stress tests. A distinction is made between system parameters and design parameters. The former refer to neighborhood characteristics inherent to the area in which it is built. These are boundary conditions to which the design has to be adapted and which are not chosen or changed easily. Design parameters are those neighborhood characteristics which can be changed or chosen to a certain extent during the design phase. These parameters are pivotal in measures taken to ensure long-term climate adaptiveness.

Parameters used in existing stress tests

In all the analyzed stress tests, inundation depths were obtained with different hydrodynamic models. While the forcing differs in each case and each model is based on slightly different physical principles and assumptions, the used parameters seem to be mostly in line. Each model requires some input regarding land use in order to determine the runoff fraction. This information is combined with data about the sewage network (dimensions, location, capacity, roughness, etc.) and local elevation and soil type to simulate the inundation depths and durations at various locations. The sewage characteristics are a typical design parameter: these can be chosen given the set of boundary conditions and system parameters. Elevation and soil type are system parameters, although the elevation could be altered.

While all cases included some form of heat stress assessment, much remains unclear about the employed methods and simulation tools. The model in the Noordwijk case distinguishes several land use types, such as paved surface, buildings, sand, grassland, forest, water and trees. The model assigns a temperature amplification or dampening factor to each of these types and calculates the potential temperature difference compared to the countryside. Other methods do not take into account as many land use types, but also base their assessment largely on green land use versus paved surface. In the Wareco guideline, the height of structures is also taken into account (taller structures cause more heat stress) and most of the case studies also map the locations of especially vulnerable spots, such as hospitals and other places where many elderly people are located. It seems that these heat stress assessments are mostly based on design parameters, such as local land use and building density.

The Noordwijk case presents only output regarding groundwater. It simply refers to a study previously conducted by Deltares for these results and does not elaborate on parameter use. Something similar applies to the Vallei case. Simulated values of future groundwater levels are mapped, but it is unclear how these were obtained. The report also concludes that there is still a large knowledge gap in the effects of

climate change on groundwater levels. Little is known about the approach regarding groundwater employed in the Haarlemmermeer case. The report also refers to a study by Deltares to map the risk of rot in wooden pole foundations. For the remainder, it seems to be focused mainly on recent measurements of groundwater levels rather than simulations. It thus makes no further mention of parameters. Overall these reports provide little clarity regarding the modeling approach and parameters. While they all present maps with future groundwater levels, they do not mention how these were obtained or they simply refer to previous studies.

Parameters used in literature

The system and design parameters for heat stress found in existing stress tests are supported by scientific works (Stone & Rodgers, 2001; Arnfield, 2003). They mention that the UHI is largely a function of paved surface and high density areas and that green and blue areas may alleviate heat stress. Other factors may be at play as well, such as the structures' insulation and the number of heat-generating systems such as air conditioners, but their effects seem to be minor.

In a rather inclusive study on groundwater modeling, Carrera et al. (1989) present several core parameters in the simulation of groundwater levels and flows. These are all related to the soil. Important parameters are: the soil porosity, permeability, storage coefficient, packing, and transmissivity. In practice, this comes mainly down to the soil type (e.g. sand, clay, etc.) as the soil type largely governs the aforementioned parameters. The study mentions that in developed areas drainage, groundwater level management and abstraction also have a strong influence on groundwater behavior.

Summary of possible parameters

The following list presents several parameters which influence the aforementioned indicators for each hazard. Design parameters are printed in *italics*.

1. Pluvial flooding
    - *Land use and runoff fraction*;
    - *Sewage characteristics*;
    - *Overland storage capacity*;
    - Soil type;
    - Elevation (and *leveling*);
    - *Land use class* for monetary damages;

- *Locations of critical infrastructure*.

2. Heat stress
    - *Amount of paved surface*;
    - *Amount of greenery*;
    - *Amount of surface water*;
    - *Building density*;
    - *Albedo of used materials*.
3. Groundwater
    - Soil type;
    - *Groundwater level management*;
    - *Drainage characteristics*;
    - Elevation (and *leveling*).

2.2 Design of the framework

The preliminary study has laid the foundation for the framework to be used to assess neighborhoods' climate adaptiveness and to derive design parameters. The different steps of the framework are depicted in Figure 2.1 and subsequently described in more detail.

First the precise aim of the study and climate change hazards to be included in the research need to be agreed upon. The aim, and especially the choice for hazards to include in the study, are important in the choice for a set of suitable models that can be used to obtain meaningful simulations of the hazards' effects under a 2085 climate scenario. The model choice is also related to the availability of neighborhood data as different models may have different data needs. Should it appear that not sufficient data or not the right data are available, it may be decided to (1) alter the research aim so that it fits the available data, (2) choose another model that matches better with available data, or (3) acquire more data.

The neighborhood data comprise both system and design characteristics. The difference between these and many examples of both types were discussed in Section 2.1.3. These neighborhood data make up one part of the model input.

The other part of the input comprises forcing data, often inspired by the climate data for 2085 as projected by the KNMI. The KNMI has formulated four scenarios for the period 2070-2100 (see Section 1.1) which each feature different climatological circumstances. Here a decision has to be made on which KNMI scenarios are to be included and which forcings are suitable to impose on the models. These choices

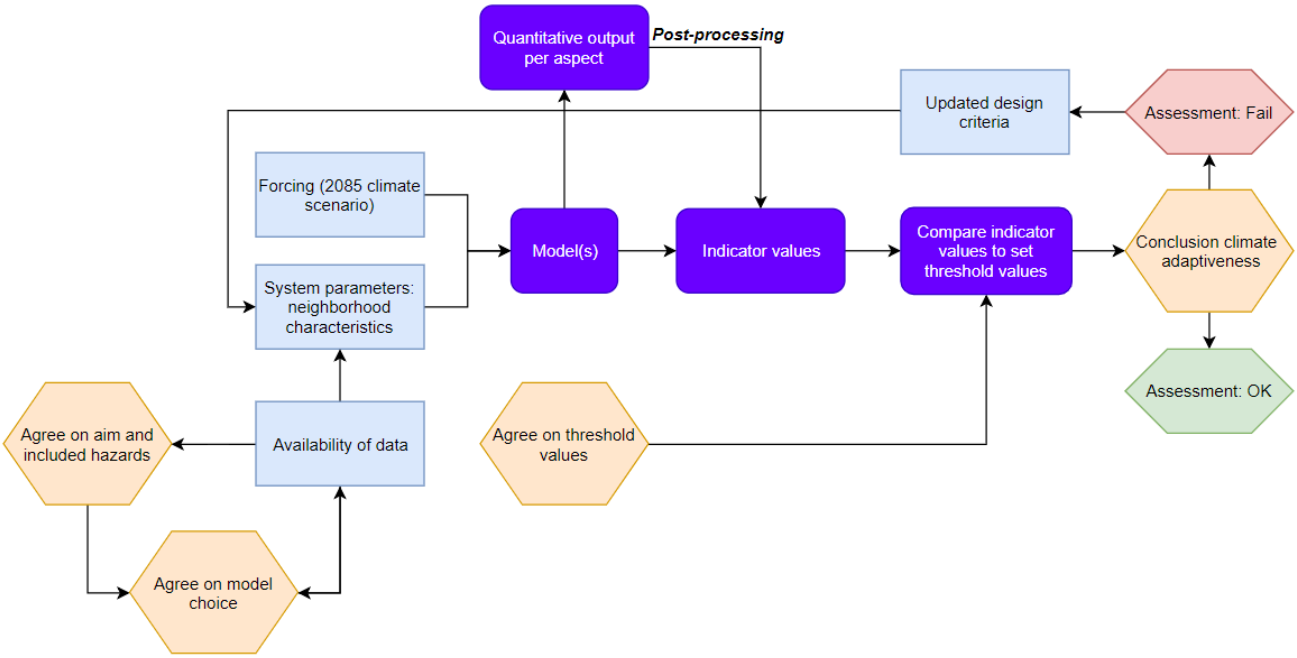

Figure 2.1: Overview of the proposed framework and the involved steps. The light blue rectangles refer to quantitative input data, (orange) hexagons to (management) decisions constituting the working of the framework and the outcomes and dark blue rounded rectangles to the modeling steps.

may also depend on the research aim, but the framework is accompanied by a set of generic forcings treated in Section 2.5.

The final decision that needs to be made before the models can be run is on the threshold values. Each hazard indicator should have threshold value(s) that can be used to draw conclusions as to the extent of climate adaptiveness in the neighborhood to that particular hazard. Again, these may be case-specific and depend on the area and research objectives, but several generic threshold values are proposed for each hazard indicator in Section 2.6.

To ensure the quantitative basis of the framework, computer models need to be run to obtain simulations of the hazard indicator values under a 2085 climate scenario for the specific neighborhood. In some cases the output of the models may directly be compared to the threshold values as they represent the same indicator. In other cases some post-processing may be necessary for good comparability. This varies for each case, chosen model and chosen indicators.

Comparison of the quantitative indicator values as obtained through simulations with the previously set threshold values leads to conclusions regarding the state of neighborhood adaptiveness to the climate change hazard considered. The conclusion is either that all indicator values are within acceptable threshold limits and the neighborhood is sufficiently climate adaptive, or that the neighborhood fails to meet

the criteria for a climate adaptive neighborhood on one or multiple hazards. If the latter is the case, the framework provides insight in the weak spots of the design and thus design guidelines can easily be derived. The updated design can be tested analogously.

One trait of the proposed framework is its unambiguity in that a neighborhood either passes or fails the assessment. This does contribute to the clarity of the assessment, but also introduces the problem of being too simplistic due to the binary assessment scale. Moreover, if a neighborhood fails to meet the criteria for one or more hazards in only few locations within the neighborhood, the outcome may be subject to debate. The question is whether a neighborhood is deemed climate adaptive when a certain portion of the neighborhood meets all criteria and small parts do not.

The framework presented here is merely a tool that supports local decisionmaking. While its outcomes may be used to substantiate claims regarding neighborhood climate adaptiveness and to derive local design guidelines, the final judgment on climate adaptiveness should lie with the engineer or policy maker who uses the framework.

2.3 Generic indicators

For each hazard, one or more indicators were selected to assess neighborhoods' climate adaptiveness. An educated choice was made from Section 2.1.2. The most important criteria for standardized indicators were (1) generic applicability in any neighborhood, (2) ease of modeling and (3) unambiguous interpretation of quantitative values. These generic indicators make up the standard indicators for the framework, but it may be decided to deviate from this if the research aim or available data necessitate so.

For pluvial flooding, it was decided to use the maximum inundation depth per location during and after a precipitation event as an indicator. This indicator provides a quick overview of weak spots within the neighborhood with regard to pluvial flooding, can be simulated at a sufficiently fine resolution for the neighborhood scale and is rather easy to simulate. Other possible indicators, such as the inundation of critical infrastructure, require much more detailed input and may not always be relevant if critical infrastructure is absent.

For heat stress the generic indicator is the daily-averaged Urban Heat Island (UHI) effect (in $^{\circ}$C). This indicator was chosen for its general applicability in any neighborhood, unlike the temperature of swimming water (may not apply to every neighborhood) and the number of casualties (depending on many other factors).

For groundwater hindrance the distance between the ground surface level and the groundwater level is used as a generic indicator. High groundwater levels directly result in groundwater hindrance.

For drought-induced soil subsidence the generic indicator is the soil-subsidence resulting from drought in a period of 60 years.

2.4 Climate hazard simulation tools

In order to provide the framework with a quantitative basis, simulated values of the used indicators are compared with threshold values. To obtain these simulations, several (computer) models were used throughout this work. The choice for models is first made and motivated in Section 2.4.1. A brief outline of the working of these models is given in Section 2.4.2.

2.4.1 Model choice

As mentioned in Section 2.2, the framework does not prescribe the use of specific models, since the model choice strongly depends on the case's objectives, the availability of data and the availability of models. However, because of time constraints and limited model availability, it was decided to fix the choice of models across the cases treated in this work. It would be too time-consuming to use multiple models for each climate hazard. Moreover, most software packages can only be used with licenses, which were not always available.

Although the model choice has been fixed in this research, the framework itself is sufficiently generic to allow the use of other models which may fit the research objectives better. The framework does not prescribe this but rather leaves this freedom to the user.

Pluvial flooding

To simulate the effects of pluvial flooding, several software packages were considered. A wide variety of flood models is available, but the model here should at least be able to simulate sewage flows (1D) and combine this with overland flow and runoff (2D) to arrive at the desired generic indicator inundation depth. This limited the list of possible choices to only a few models, being 3Di, SOBEK2, D-HYDRO and InfoWorks ICM. Both SOBEK2 and InfoWorks ICM are used within Witteveen+Bos, but InfoWorks is used most often for modeling pluvial flooding and water hindrance. It was therefore decided to use InfoWorks ICM as a software package to simulate the effects of pluvial flooding, partly based on a practical motivation.

Heat stress

As mentioned previously, heat stress modeling still is in its infancy. There are no dedicated software packages readily available and the quantitative basis for norms and model output is narrow. The discussion regarding standardization of heat stress modeling approaches has gained momentum in the Netherlands and is currently (2019) still ongoing.

Mirzaei (2015) distinguishes heat stress models according to their scale of application: building-scale, micro-scale and city-scale models. The former are limited to the heat stress in and around individual structures; the latter comprise entire cities. It here makes sense to choose a heat stress model at the micro-scale, suitable for a neighborhood. The scale of such micro-scale models is still too large to take into account air flows and turbulence, which leaves the option to make use of a simplified energy balance model.

Witteveen+Bos has co-developed their own heat stress model in collaboration with several institutes, called Urban Climate Assessment and Management (UCAM). The model is based on an energy balance and mainly takes into account land and material use and does not simulate fluid dynamics. It was specifically designed to assess heat stress at the neighborhood scale and its primary outcome is the quantification of the (daily-averaged) UHI effect. UCAM was the only available heat stress model fitting the neighborhood scale. Despite its limitations, it was decided to use UCAM here since it still gives a good impression of the heat stress experienced and shows potential vulnerable locations.

Groundwater

No groundwater computer models were used in this study due to time and practical constraints. Instead it was decided to use the analytical methods described by Hooghoudt (1940) and Bear (1979), and Koppejan (1942) to assess high and low groundwater levels respectively. These are classical groundwater equations which form the basis of various groundwater models. For the scale of application (neighborhood), it was considered justifiable to use these equations here.

2.4.2 Model descriptions

InfoWorks ICM

InfoWorks is a platform of water-related simulation models consisting of InfoWorks ICM (Integrated Catchment Model), SD (Stormwater Drainage), RS (River Systems) and CS (Collection System) among others. These models can be used separately

but can also be easily integrated. The description here focuses on InfoWorks ICM as this model was used to obtain simulations of the sewage system's behavior during and after precipitation events.

ICM has the possibility to integrate urban and river catchments in one model and is both a hydraulic and hydrologic model. It simulates the rainfall-runoff process in an urban environment through the allocation of subcatchment areas to drainage points (e.g. manholes). Within these subcatchments, a distinction is made between pervious and impervious areas (and their type, such as sloped or open or closed paved) in order to accurately model infiltration and runoff. For 1D infiltration, fixed characteristics for each subcatchment need to be specified. For 2D infiltration, ICM uses either (1) a fixed percentage of rainfall, (2) a constant infiltration rate based on saturated soil conditions or (3) a variant of the Horton Equation (Horton, 1933) over a 2D area.

Water which reaches the stormwater sewage is modeled using the 1D module of ICM; surface water flow is simulated using the 2D module. A more elaborate description of the modeling approach in InfoWorks ICM can be found in Appendix B.

UCAM

To simulate and assess local heat stress and air quality, the Urban Climate Assessment and Management (UCAM) model was developed (Witteveen+Bos, 2014; Tijdschrift Milieu, 2015). It was co-developed by Witteveen+Bos, Wageningen UR and the KNMI. The discussion about further standardization of heat stress modeling approaches and output to ensure better comparability among assessed areas is still ongoing.

UCAM's working is based on the effects of the heatwave that struck the Netherlands between July 14 and July 19, 2006 on a number of standard Dutch neighborhoods. To this end, the weather characteristics during this heat wave were used as input in the Weather Research and Forecasting (WRF) model (for a comprehensive overview, see Powers et al. (2017)) to simulate the energy balance discussed below. It was configured to account for small urban areas typical for the Netherlands and was validated using observations in the rural area Cabauw. The effects on the Urban Heat Island (UHI) effect (the air temperature difference between urban and rural areas) of several physical neighborhood parameters (to be discussed subsequently) were monitored and the sensitivity of the UHI effect to these parameters was determined. As a result, the model is able to approximate the extent of the UHI effect given that information about the relevant neighborhood parameters is available.

The model is governed by the following energy balance:

$$Q + AH = H + LE + G \tag{2.1}$$

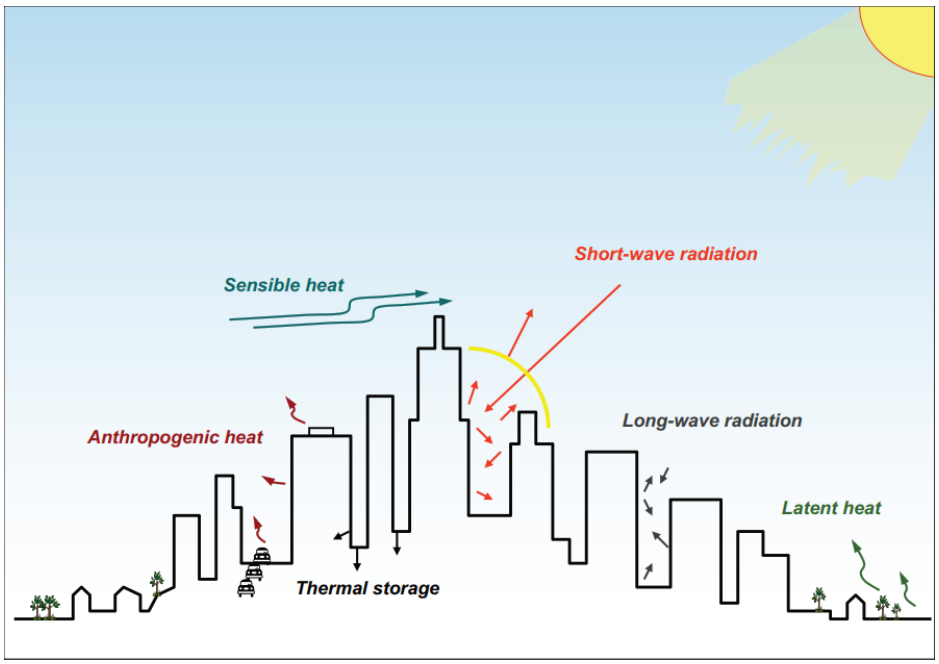

Figure 2.2: Illustration of the energy budget (Eq. 2.1) as used in UCAM. Adapted from Akbari et al. (n.d.)

where Q is (solar) radiation [M T^{-3}; usually W m^{-2}], AH anthropogenic heat, H the sensible heat in the area (UCAM's UHI output), LE latent heat, and G the storage of heat in the area. These parameters are illustrated in Figure 2.2.

During a heat wave, the solar radiation Q is at its highest. The energy balance in a city described by Eq. 2.1 differs from rural areas in the sense that (1) AH is larger because of more human activities, (2) urban areas are developed and feature low albedo values and ample opportunities for heat to be stored in buildings and (3) the amount of greenery is generally limited in cities, restricting the latent heat. As a result, much of the excess heat will be stored in buildings and roads (G). This storage term is eventually converted to sensible heat, which explains the strong UHI effect at night.

The model works with the Local Climate Zone classification system as described by Stewart and Oke (2012) for neighborhood types. The model differentiates between LCZ2 (compact midrise buildings), LCZ3 (compact lowrise), LCZ5 (open midrise), LCZ6 (open lowrise) and LCZ23 (a combination of LCZ2 and LCZ3; similar to typical Dutch row houses). Compact here refers to a low number of trees, largely paved land cover and the use of concrete construction materials; open refers to an abundance of vegetation and pervious land cover.

Moreover, the model accounts for the albedo-effect of the built-up area. Albedo can be considered the extent of the reflection of radiation and the albedo number varies between 0 (no reflection, maximum absorption) to 1 (maximum reflection, no

absorption) and as such is often expressed as a percentage. The albedo numbers of roofs, facades and roads are considered separately. As shown in Equation 2.1, anthropogenically generated heat contributes to the UHI, especially since urban areas often have many inhabitants. However, its effects are thought to be minor and it is difficult to approximate the degree of anthropogenic heat beforehand. It is therefore usually set to a default value. The amount of green surface area is another parameter that is taken into account. Greenery does not store heat, but rather converts it to latent heat (*LE* in Eq. 2.1), thereby lowering *H* and the UHI effect.

UCAM's primary input is the land use classified according to five categories, some with their own characteristic values. These categories are (parameter values bracketed): paved surface (road albedo), structures (roof and facade albedo and structure height), gardens (% unpaved/green), water and greenery. The study area is discretized into a grid and for each cell the model determines a LCZ based on the presence and relative position of these categories and structure height. The size of the entire area is also considered. The determination of LCZ requires semi-manual work of classifying the projected land use in the study area.

UCAM's primary output is the daily-averaged UHI effect (in °C); the sensible heat in the area (parameter *H* from Eq. 2.1). The daily average figure gives a good impression of both the amplified heat during the day in urban areas and the (lack of) cooling during the night. Also, the duration for which people are exposed to amplified heat is usually longer than just a few hours. To arrive at this value, UCAM first calculated the maximum UHI in each grid cell, based on its LCZ and the characteristics of the 2006 heat wave according to the WRF model. It then compensates the maximum possible UHI effect with reduction factors. Reductions in UHI effect due to albedo effects and greenery are subtracted from the maximum UHI effect. For example, a grid cell that contains only paved surface and no structures or greenery, will show the maximum UHI effect possible as there are no reduction factors at play. The role of water in heat stress is somewhat ambiguous: water may absorb heat and cause cooling through evaporation. However, surface water becomes warmer as the summer progresses, causing its mitigating effect on heat stress to dissipate or even become adverse. While it is very difficult to predict or simulate the temperature at a certain location with good accuracy, UCAM seems to give reasonable values for the UHI effect. Successful modeling studies with UCAM have already been undertaken in Ghent, Almere and Gouda.

Because the modeling of heat stress is still underdeveloped and no national standards exist, it is difficult to validate the model and assess a neighborhood with clear criteria. In an attempt to provide some assessment scale and allow for comparability across neighborhoods, UCAM works with the so-called heat-index. This index, which varies from 0 (no UHI) to 1 (large UHI effect; severe heat stress), is based on

the RIVM norms for ozone concentration in the air. The heat-index is linearly related to the UHI and a heat index of 1.0 corresponds roughly with a UHI effect of 3.3 °C (daily-averaged). This is the maximum value for the UHI effect that can be obtained in the simulations in a Dutch setting. This approach is based on the European WHO guidelines for ozone concentrations, because exposure to ozone peak values yields similar health risks as heat stress: both typically occur during heat waves and cause risks for the short term. The heat-index is used to formulate the final assessment in four categories: 0 through III. This classification is depicted in Table 2.1.

Table 2.1: UCAM heat stress categories according to the heat-index value

Category	Heat-index	Assessment	Interpretation
0.	0 - 0.29	Comfortable	No effects, no additional heat risks for the urban environment.
I.	0.3 - 0.57	Acceptable	Limited heat risks for the urban environment. Acceptable for a maximum of 25 days per year
II.	0.58 - 0.86	Risky	Additional heat risks for the urban environment. Comparable with the information threshold for ozone concentration.
III.	0.87 - 1.0	Unacceptable	Large additional heat risks for the urban environment. Comparable with the alarm threshold for ozone concentration.

It is important to remark that the UHI effect values calculated by UCAM are daily-averaged. In reality, the local deviation in temperature from the rural surroundings may reach much higher values. This is especially the case toward the end of the day as the sun has set and rural areas cool down faster than urban areas.

The UCAM GIS tool is supplemented by a spreadsheet in MS Excel. This can be used to compose a graph of the experienced temperature at a specific location (based on LCZ and vegetation percentage, as determined in the GIS tool) over the course of a hot day. The graph can provide more insight in the temperature difference between developed and rural areas at specific times, rather than just a daily-averaged figure.

Groundwater hindrance

The analytical formula of Hooghoudt (1940) was used to estimate the differential head between drains in the neighborhood. The formula can be written as follows:

$$m_0 = \frac{-8 \cdot K_2 \cdot d\sqrt{(8 \cdot K_2 \cdot d) - 4 \cdot 4 \cdot K_1 \cdot -s \cdot L^2}}{2 \cdot 4 \cdot K_1} \tag{2.2}$$

where m_0 denotes the differential head between two drains [L], K the hydraulic conductivity of soil layers 1 and 2 [L T^{-1}], d the equivalent depth [L; see Eq. 2.3], s the specific discharge to be drained [L T^{-1}] and L the distance between drains [L].

The equivalent depth d is a function of several other parameters, according to the following equation:

$$d = \frac{D}{1 + \frac{8D}{\pi L} \cdot \ln(\frac{D}{\pi r})} \tag{2.3}$$

in which D is the vertical distance between the drain and the impermeable layer (soil layer 1) [L] and r is the wetted perimeter of the drain [L].

In cases where the drainage levels on both sides are not identical, the following equation can be used to approximate the groundwater level (Bear, 1979):

$$h^2(x) = h_0^2 - \Big(\frac{h_0^2 - h_L^2}{L}\Big)x + \frac{s}{K}(L - x)x \tag{2.4}$$

where h is the groundwater level [L] as a function of the horizontal distance x [L] on the domain between 0 (left drain) and L (right drain). The maximum groundwater level can then be found graphically.

Drought-induced soil subsidence

In addition to water hindrance resulting from high groundwater levels, dry spells may cause the groundwater table to become much lower and induce soil subsidence and subsequent damage to property (Corti et al., 2009; Swiss Reinsurance Company, 2011). To quantify the extent of this phenomenon in the study area, we used the formula of Koppejan (1942). It combines the previously reported expressions for soil subsidence by Terzaghi et al. (1967) and Keverlingh Buisman (1940) and account for the duration of the soil loading or lowering of the water table. It can be written as follows:

$$S(t) = T\Big(\frac{1}{C_p} + \frac{1}{C_s} \cdot \log(t)\Big) \cdot \ln\Big(\frac{p_i + \Delta p_i}{p_i}\Big) \tag{2.5}$$

where S is the subsidence [L], t is time [T], T is the thickness of the layer subject to subsidence [L], C_p the consolidation constant for direct effect [-], C_s the consolidation constant for secondary effects [-] and p_i the intergranular pressure in the considered soil layer [M L^{-1} T^{-2}]. The intergranual pressure can be found by subtracting the

water pressure from the soil pressure at the bottom of the soil layer susceptible to subsidence.

Equation 2.5 can be used to estimate the subsidence of soils that are loaded, but also for soils where the water table is reduced as the effect on the intergranualar pressure is similar.

2.5 Generic forcing

Pluvial flooding

As described elaborately in Sections 1.1 and 1.2, the KNMI projects substantial increases in average precipitation and temperature for the period 2070-2100. In addition, most scenarios show that especially precipitation and temperature extremes are likely to be amplified as a result of climate change. Predictions for sea level rise and increases in river discharge are not considered here as the scope is limited to pluvial flooding only.

The choice for a certain precipitation event depends on the norm employed and what level of water hindrance is deemed acceptable. It is important to make a distinction between mild water hindrance where rainwater is temporarily stored on streets and excess ponding occurs, and large-scale inundation resulting from extreme precipitation causing lasting damage to property and impeding public life. The former is naturally accepted to occur more often than the latter. RIONED has attempted to compose norms regarding pluvial floods in Dutch neighborhoods (RIONED, 2006). Their guideline advises to use two separate precipitation events to assess whether a neighborhood is able to cope with extreme precipitation. An event with a return period of 2 years is recommended to assess the sewage system's capacity. This event should not cause large-scale problems and no excess water should be stored on the streets. The typical precipitation event used for this purpose under the current climate is dubbed "bui 08" ("Shower 08"). Its intensity varies within one hour, but the total amount of precipitation is 19.8 mm. Additionally a precipitation event with a return period of 100 years should be forced to gauge vulnerable locations and estimate large-scale damages. Here the choice is adopted to use precipitation events with return periods of 2 and 100 years as climate forcing. This ensures an assessment for both relatively frequent hindrance due to rainwater stored on streets and large-scale flooding.

In their recent work aimed at enhancing civil participation in climate adaptation endeavors, Kluck et al. (2017) pay much attention to climate adaptation criteria and precipitation events that can be used to assess climate adaptiveness. They acknowledge that there is no single standard precipitation event which can be used

across Dutch cities as each event is different and cities respond differently to extreme precipitation. However, they do underline the notion that precipitation events are defined by their return periods, duration and intensity. For the purpose of simulation urban pluvial flooding, Kluck et al. (2017) propose the use of an event that lasts one hour. Water travels about 360 m (at 0.1 m/s) during that period so that it can reach surface water. The forcings here therefore have a duration of one hour.

There is no standardization as to the type of forcing of precipitation events in stormwater modeling and STOWA does not have estimates of typical precipitation events in 2085 with a return period of 2 years (only for 10, 50 and 250 years). Current practices to take into account climate change in stormwater modeling vary greatly from applying a single factor to the current precipitation event to formulating own rules. The KNMI found that the total amount of precipitation in 2014 can be scaled by factors of 1.61, 1.65 and 1.67 respectively for the return periods 10, 50 and 250 years to obtain the precipitation amount projected for 2085 (Klein Tank et al., 2015).

STOWA (2018) has worked with several other organizations to estimate various precipitation characteristics for the long term. The amount of precipitation (in mm) for several precipitation events (defined by a return period and precipitation duration) is shown in Table 2.2.

Here it was decided to apply the current Shower 08 (current return period 2 years) scaled by a factor 1.65, in line with the scaling of other precipitation events. This yields a precipitation event with a 2085 return period of 2 years and a total amount of 33 mm. To obtain a precipitation event with a return period of 100 years and a duration of 1 hour, linear interpolation was applied to the figures shown in Table 2.2, which yields 69 mm in 1 hour. These two precipitation events are proposed as a generic model forcing.

Table 2.2: Precipitation amounts (in mm) for several event durations at different return periods as projected for the year 2085. **Bold** values were used as model forcing. Adapted from STOWA (2018)

Return period (years)	**Precipitation duration (minutes)**					
	5	**10**	**15**	**30**	**60**	**120**
2					**33**	
10	17	24	29	37	44	50
50	25	35	42	53	63	71
100					**69**	
250	-	48	58	73	86	94

Heat stress

As described in Section 2.4.2, UCAM does not work with a configurable forcing. Rather, the 2006 heat wave in the Netherlands is a fixed forcing and its traits cannot be modified. While limiting, the model currently does not support the configuration of a custom forcing event.

Groundwater

The KNMI reports current values and projections for the 10-day precipitation sum with a return period of 10 years. As groundwater dynamics are slower than surface water dynamics relevant for pluvial flooding, this was considered a better indicator than hourly or daily precipitation amounts for high groundwater levels. Current values and future projections of this forcing are provided in the KNMI climate change scenarios. In the reference climate this 10-day sum was 89 mm. For 2085 this amount is predicted to increase by up to 25% (111 mm) under the W_H scenario (most extreme). It was thus decided to set the generic forcing at 0.01 m d^{-1} (111 mm over 10 days yields 0.01 m per day). Seepage was disregarded here as its intensity is strongly location-dependent and even in extreme cases (approximately 0.2 m y^{-1} is considered extreme seepage) makes up a small portion of the forcing.

The generic forcing for drought-induced soil subsidence is also based on the W_H scenario. The KNMI's primary indicator for drought is the highest precipitation deficit with a return period of 10 years. In the reference climate, this deficit is 230 mm. It is forecast to increase by up to 50% under the W_H scenario (most extreme). However, the precipitation deficit is not a direct local indicator for drought as actual groundwater levels are also influenced by groundwater level management. The generic forcing is therefore not a fixed value, but rather the local decrease in groundwater level during the extremely dry year 2018 (return period 30 years (KNMI, 2019)) increased by 50%. The local lowest groundwater level in 2018 can be derived from monitoring wells in the vicinity of the study area. The same report mentions that the return period of such an extreme drought event may be 10 years by 2085 under the W_H scenario.

Naturally droughts with other return periods may occur as well, either more or less severe. It is difficult to estimate the occurrence and severity of droughts in the next decades, but based on the 2018 drought, the forcing here is set at ten events where the groundwater level is reduced by 50% for a duration of 30 days.

2.6 Generic threshold values

To draw quantitatively underpinned conclusions regarding a neighborhood's climate adaptiveness, indicator values for each hazard are compared with the threshold value associated with that indicator. These dictate what level of hazard occurrence is deemed acceptable in the neighborhood and are mostly based on norms or legal requirements.

2.6.1 Pluvial flooding

For pluvial flooding, there are two generic threshold values, depending on the forcing. With a forced precipitation event of 33 mm h^{-1} (T = 2 years), the threshold value for inundation is set at 0.10 m, measured from the street surface level. This value stems from the notion that the forced event is a scaling from the current shower 08 which may just cause the streets to be inundated and from the assumption that streets can store a maximum of 0.10 m water between curbs. For the event of 69 mm h^{-1} (T = 100 years), the threshold value is set at 0.30 m. At 0.30 m, houses will be struck by medium-scale flooding.

2.6.2 Heat stress

For heat stress, it was decided that the daily-averaged UHI effect must be within UCAM classes 0 or I across the study area to be deemed acceptable (see Table 2.1. This corresponds to a maximum daily-averaged UHI effect of 1.88 °C.

2.6.3 Groundwater

For hindrance from high groundwater levels, the minimum drainage head was set at 1.0 m, in line with the legal requirements for new neighborhoods (Van Wee et al., 2007).

While it seems logical to use the total subsidence over the neighborhood's lifetime as an indicator, it is difficult to assign a threshold value to it. This is due to several factors, among which the fact that the extent of acceptable subsidence differs in each case, depending on the damage potential and soil characteristics. Here the more or less arbitrary threshold value of 0.25 m of total drought-induced soil subsidence to the neighborhood during the period 2020-2085 is assigned.

2.7 Overview of generic framework indicators, forcing and thresholds

An overview of the generic indicators, forcing and threshold values for each climate change hazard as used in the framework is depicted in Table 2.3.

Table 2.3: Overview of generic framework indicators, forcing and threshold values for each hazard

Hazard	Indicator	Forcing	Threshold value
Pluvial flooding	Inundation depth	33 mm h^{-1}	0.10 m
		69 mm h^{-1}	0.30 m
Heat stress	UHI effect	2006 heat wave	1.88 °C
Groundwater hindrance	Drainage head	0.01 m/d	1.0 m
Soil subsidence	Total subsidence after 60 y	Varies	0.30 m

2.8 Case: Wilderszijde

2.8.1 Case choice and description

The case of Wilderszijde was chosen because (1) it is currently still in the design phase and the framework's outcomes can be used to adapt the design, (2) it is located in South Holland and thus the demands of the covenant apply and (3) abundant data about the neighborhood's design were available.

This subsection is structured as follows. First the study area is shown and a general description is given. The subsequent sections follow the structure of the framework as presented in Figure 2.1: the methodology of each involved step is treated for this case specifically, if applicable.

General description of study area

The neighborhood "Wilderszijde" is located in Bergschenhoek (just north of Rotterdam, Netherlands). Bergschenhoek is part of the municipality Lansigerland. The neighborhood was initially planned and designed around 2007, but its realization was indefinitely postponed due to the financial crisis at the time. The municipality has recently unveiled plans to start construction of the neighborhood, using its original 2007 design where possible.

The plans comprise the construction of approximately 2,650 homes and several facilities located south west of Bergschenhoek. The area is currently not very devel-

oped as it contains only few structures (a.o. a high school, several businesses and the Lansingerland city hall) and mainly agricultural area. The project area is roughly demarcated by the High Speed Line (HSL) to the west, the local road Wilderskade to the south and by the provincial roads N209 and N472 to the east and north. The area is shown in Figure 2.3 and is a typical Dutch peat meadow. We here consider only the sub-neighborhood “De Tuinen”. This is the first part of the neighborhood to be constructed.

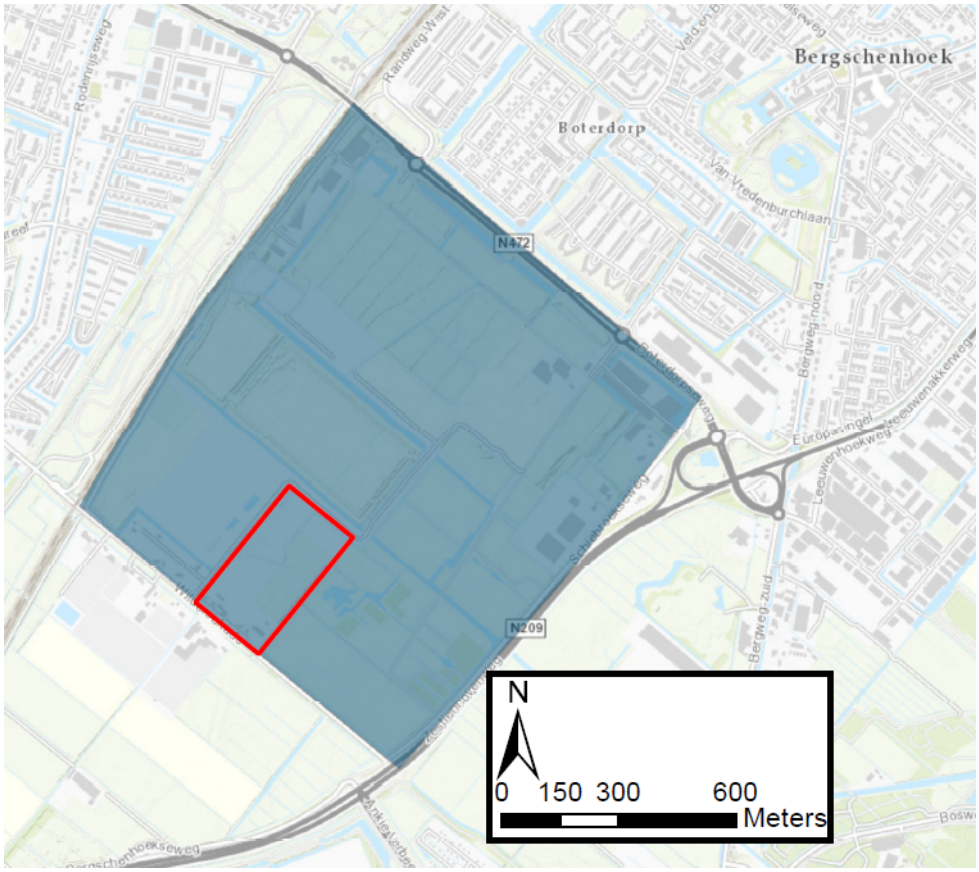

Figure 2.3: Location of the study area; nearby Rotterdam, Netherlands. Source of underlying map: Open Topo

For efficiency reasons, the municipality wants to hold onto the original 2007 design as much as possible. This design complied with the climate adaptation criteria that then governed. However, insights concerning climate adaptation have rapidly changed over the past decade and more information about the extent and effects of climate change has become available. It is therefore the question whether the original design is still sufficiently climate adaptive as previously defined. Moreover, the province has engaged in the construction covenant South Holland (Bouwconvenant Zuid-Holland; see also Section 1.2) which unifies several stakeholders in their ambition to construct “climate adaptive” neighborhoods. The parties in the covenant attempt to set regulations and guidelines for climate adaptive neighborhoods and

have formulated (specific) forcings and thresholds for some of the hazards considered here. These are mentioned in the relevant sections.

Data availability

Many design parameters were more or less readily available by virtue of the 2007 design. Neighborhood part “De Tuinen” was designed in great detail so that there was sufficient information available about the neighborhood’s demarcation, land use, building types, projected sewage system, pumps, drainage and projected surface level. Most designs were available in CAD-format, allowing them to be imported into a variety of software packages. Graphical representations of the design can be found in the urban allocation plan (Gemeente Lansingerland, 2008).

Moreover, many data about the projected water management system was described in the environmental assessment report (Milieu-effect rapportage; Gemeente Rotterdam (2005)). Combined with freely available data on system parameters such as soil type (from the Basisregistratie Ondergrond; BRO) and elevation (Algemeen Hoogtebestand Nederland; AHN), this allowed for overall good data availability.

Objectives and considered hazards

The wide availability of data allowed for a rather inclusive application of the framework. The purpose of this case study is thus twofold: (1) to assess if the original 2007 design is still climate adaptive enough to comply with the demands formulated by the construction covenant South Holland and (2) to propose adaptations to the design and derive design parameters for similar neighborhoods in peatlands.

To this end, the effects of climate change on the occurrence of pluvial flooding, heat stress and changes in groundwater level were included in the case study. The simulated effects of the included climate change hazards were compared with the generic threshold values and with specific values inspired by the demands issued in the covenant.

System parameters

Table 2.4 provides an overview of the system parameters in the study area of Wilderszijde. Five land use categories and their areas are shown in Table 2.5.

Table 2.4: Overview of system parameters in the Wilderszijde case

System parameter	Value(s)
Geology	0 to -0.8 m NAP: sand (K = 10 m d^{-1}) -0.8 to 12.8 m NAP: clay
Elevation	-5.0 to -6.7 m NAP Projected surface: -5.0 m NAP
Groundwater seepage	0.22 m y^{-1}
Current land use	Argi-/horticulture
Total area (De Tuinen)	11.4 ha

Table 2.5: Overview of land use categories and areas in Wilderszijde

Land use category	Area (m^2)	Percentage of total
Structures	17,485	15.3%
Water	14,580	12.8%
Pavement	22,120	19.4%
Gardens	36,870	32.3%
Greenery	22,931	20.1%
Public space	45,051	39.5%
Public space + water	59,631	52.3%
Private space	54,355	47.7%
Paved area	39,605	34.7%
Total area	113,986	100.0%

2.8.2 Pluvial flooding assessment

Forcing

Two types of forcing are distinguished: the framework's generic forcing as described in Section 2.5 and the case-specific forcing. Here the neighborhood of Wilderszijde is also assessed using the precipitation events stipulated in the construction covenant (and their respective threshold values; see next section). These are precipitation events of 30 and 120 mm h^{-1}. Their instensity in time here was scaled from shower 08. A total of four events is thus forced to this case: the generic forcings (33 and 69 mm h^{-1}) and the specific forcings (30 and 120 mm h^{-1}).

Threshold values

The generic forcings events of 33 mm h^{-1} and 69 mm h^{-1} are used here.

The construction covenant has formulated quite specific requirements for the

specific forcing events. An event of 30 mm h^{-1} should not lead to water storage on the streets (here interpreted as inundation $<$ 0.03 m). An event of 120 mm h^{-1} should not lead to large damage to new structures and infrastructure (in this case all structures and infrastructure). This is here interpreted as a maximum inundation depth of 0.30 m from the surface level. These threshold values are summarized in Table 2.6.

Table 2.6: Overview of forcings and threshold values for pluvial flooding assessment

Precipitation event	Forcing type	Threshold value
33 mm h^{-1}	Generic	$<$ 0.10 m
69 mm h^{-1}	Generic	$<$ 0.30 m
30 mm h^{-1}	Specific	$<$ 0.03 m
120 mm h^{-1}	Specific	$<$ 0.30 m

Model configuration

First the sewage network according to the CAD design was extracted, loaded into InfoWorks Asset and adapted and revised according to the design drawings where necessary. To this end, it was ensured that all manholes were assigned an elevation, shape (circular) and diameter, and whether they are part of stormwater sewage or wastewater sewage. All links were assigned a profile shape (circular), diameter, material (PVC for wastewater sewage; concrete for stormwater sewage), up and downstream levels, length and slope. It was also made sure that all links are connected to a node. Special constructions such as overflows were manually adapted according to the design. The network was then imported into InfoWorks ICM. The network was internally validated in the program to detect for faulty values or configurations. Where necessary the network was adapted to correct for obvious flaws in the design drawing (such as wrong signs and flow directions).

Subsequently the area draining onto each manhole was determined. The study area was divided using Thiessen polygons so that each point drains onto the nearest manhole. This was considered a reasonable approach as all manholes are projected at the same elevation. These areas make up the subcatchments in ICM. For each subcatchment, the area of closed and open paved area was determined in ArcGIS and assigned. It was assumed that gardens feature 40% of pervious land cover (as aspired in the construction covenant) and 60% of open paved area. In addition, the projected number of inhabitants in each subcatchment was determined and assigned, based on the assumption that a household comprises on average 2.5 inhabitants. Furthermore, the projected pump capacities and stormwater overflow dimensions were assigned. The pumps' switch on and off levels were not specified

in the design. Therefore the switch on level was assumed to be equal to the depth of the linked pipes and the switch off level one meter above. Figure 2.4 shows an overview of the sewage network and the assigned subcatchments.

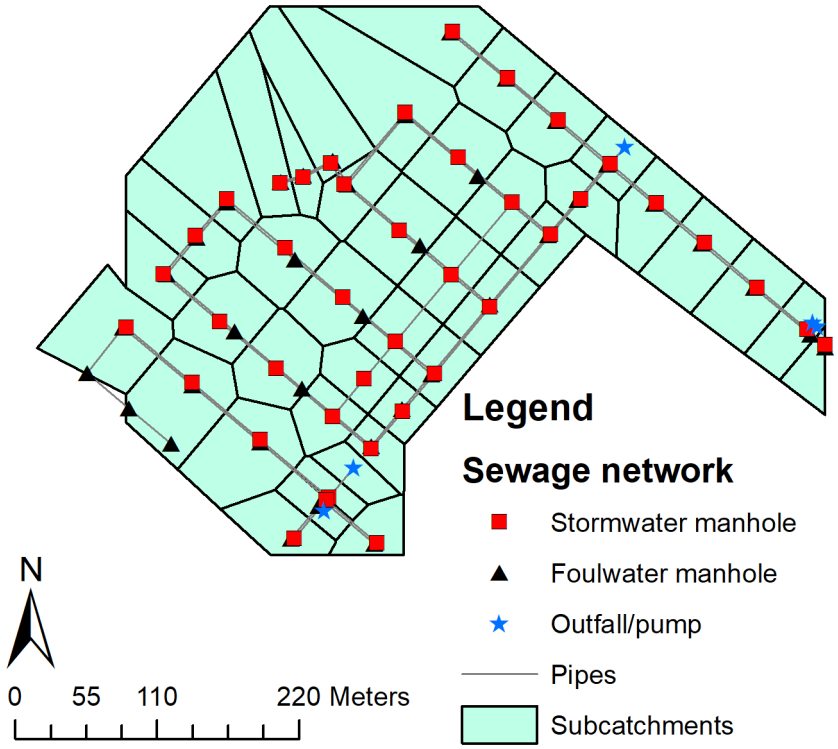

Figure 2.4: Overview of the Wilderszijde sewage network and assigned subcatchments

For the remainder the model was configured according to the Dutch "Leidraad Module C2100" (RIONED, 2004), a guideline and standardization for sewer and hydraulic modeling. This guideline stipulates rules for the modeling of inundation at manholes (the so-called cone-shape), and the modeling of water dynamics after precipitation has fallen. The latter refers to the amounts of water that evaporate, infiltrate, run off or are stored and is largely based on the assigned land use classes. Details are to be found in the Leidraad, but the most important aspects are briefly mentioned here.

Infiltration only occurs in (semi-)pervious locations. The soil type and soil moisture are among the most important parameters that determine the infiltration. The Leidraad follows Horton's approach to determine the course of the infiltration process; default values for each land use type can be found in the Leidraad.

Ponding in locations where no infiltration takes place can only disappear through evaporation. The model here assumes the monthly evaporation figures as found by the KNMI according to Penman. In its default setting, the model works with the average value (1.78 mm d^{-1}).

The nett precipitation, after subtraction of evaporation and infiltration, runs off. The discharge with which the rainwater enters the manholes [mm min^{-1}] is linearly dependent on the the amount of nett precipitation and a runoff factor [min^{-1}]. This factor varies between 0.1 and 0.5 min^{-1}; precise default values can be found in the Leidraad.

Moreover, all short pipes were assigned a minimum value of 5.0 m to prevent model instabilities. Surface water dynamics are not included in the model: it is assumed that outfalls have an infinite capacity and surface water cannot enter from the opposite direction. It was also assumed that the system is initially empty, so that the sewage system is at maximum capacity.

The model was first run using a 0 mm precipitation event (only waste water; results not shown and not relevant) to test for model stability. The different precipitation events were then forced with a total model run time of 5 hours. This was done to ensure that worst-case inundation, which may occur after rainfall has stopped, was included in the results.

Post-processing

The results, specifically the maximum inundation depth per manhole and maximum flood volume per manhole) were exported to ArcGIS in order to visualize these in maps. Inundation durations were directly accessed through ICM itself. Moreover, the total flood volume resulting from each precipitation event was converted to a storage deficit in mm for the entire neighborhood and for the total area of public and private domains.

Exploration of measures

The results were used to propose several measures that could help mitigate pluvial flooding in the neighborhood and explore their effects quantitatively. These measures are classified into (a) enlarging the capacity of the sewage network, (b) reducing the amount of paved surface, (c) finding additional storage facilities on private property, and (d) finding additional storage facilities in public space. In approaches (a) and (b), the design in InfoWorks ICM was adapted to compose what-if scenarios.

In approach (a), the sewage network was modified so that each pipe has a diameter 100 mm larger than the original design. In approach (b), the amount of paved (closed and open) surface was reduced by 10 and 20% in each subcatchment to investigate the influence of pervious versus paved surface. In approach (c) and (d), the flood volume was converted to amounts in mm of additional storage necessary and several measures to accomplish this were discussed.

2.8.3 Heat stress

Forcing

As mentioned in Section 2.4.2, UCAM does not work with variable climate forcings, but rather assumes the 2006 heat wave in the Netherlands as a forcing. This limits the possibility to impose more extreme heat waves onto the system or to simulate projected 2085 climate conditions.

Threshold values

No clear requirements were set for heat stress in the covenant, other than that "measures should be taken to prevent substantial warming of the study area". We here assume that the UCAM heat stress categories (see Section 2.4.2) 0 (comfortable) and I (acceptable) fall within this boundary. This means a maximum heat-index of 0.57 (see Table 2.1). This translates to a daily-averaged maximum UHI effect of 1.88 $^{\circ}$C.

Model configuration and simulation steps

To simulate heat stress in the neighborhood, the study area was first classified according to five land use classes: greenery, water, pavement, structures and gardens (see Figure 2.5). Greenery here includes greenery in the public space such as parks and unpaved roadsides and pavement refers to all paved areas in the public space, such as roads, paved paths, parking lots and squares. Structures includes all built-up structures within the area, but also storage sheds and walls. Gardens make up the remaining private space that is not allotted to structures. The classification was extracted from the neighborhood design CAD drawings.

The study area was discretized into a grid with cells of 50 x 50 m. In addition, each structure was assigned an estimated height. As the study area is primarily a residential area, a height of 10 m for main structures and homes and 3 m for storage sheds and walls was assumed. This served as the primary input in the UCAM tool developed for ArcGIS. The LCZ depends on the land use, building density and structure height in the area. The first step of this tool determined the LCZ for each grid cell based on this information.

For each structure's walls and roof an assumption was made regarding the material use for UCAM to estimate the albedo. For row houses, a default roof with a light-colored coating (albedo 50%) and default red brick walls (albedo 30%) were assumed, based on neighborhood artist impressions. For (semi-)detached homes, a combination of standard red roof tiles (22%) and red bricks (30%) were assumed.

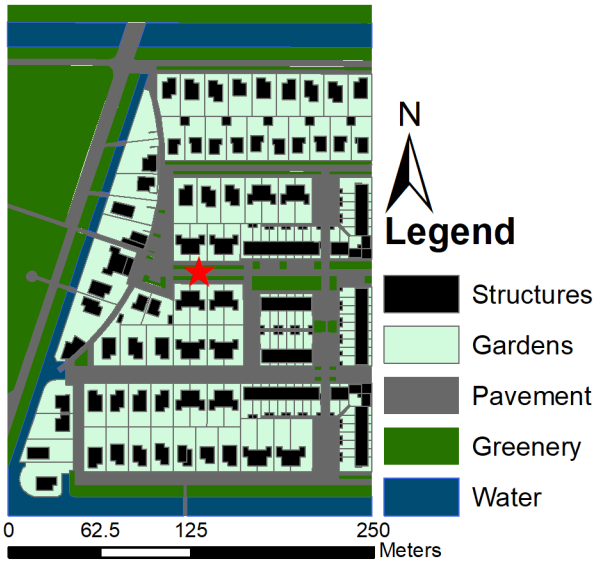

Figure 2.5: Land use in the neighborhood Wilderszijde, classified according to the five categories used by UCAM. The red star marks the fixed location where the UHI effect during a hot day was monitored

For storage sheds, the assumption of a roof with a light-colored coating and light-colored material for walls (40%) such as wood was used. Public pavement was assigned a universal material type of light-colored concrete (30%). It was assumed the gardens were on average covered with vegetation for 40%, in line with the ambition stated in the covenant.

The tool was run to determine the LCZ in the study area for each grid cell, determine the maximum UHI effect and the final daily-averaged UHI effect after compensation with albedo and vegeation reduction factors. These results were interpolated bilinearly to obtain a smoothed map of the daily-averaged UHI effect across the study area.

To gain more insight in the UHI effect over time on a hot day, a fixed point in the neighborhood (marked with a red star in Figure 2.5) was monitored and hourly values of the temperature were plotted. A distinction was made between fully paved gardens and fully green gardens. The rural situation (UHI effect 0 °C by definition) was added for reference. To this end, the local LCZ (6), local vegetation fraction (8 and 40%) and standard albedo factors (22, 30 and 30% respectively for roof, wall and road) were used in the MS Excel tool that supplements the UCAM GIS tool and is able to graph hourly values of the temperature.

Exploration of measures

To explore the effects on the UHI effect of the different input parameters, several sensitivity analyses were conducted. First the amount of vegetation in gardens was varied in a univariate sensitivity analysis (0, 40, 50 and 100%), keeping the material use constant according to the reference situation. Then the albedo values for the different materials were varied keeping the garden vegetation coverage constant. Finally the extremes (no/maximum garden vegetation, low/high material albedos) were used to check if this returned the minimum/maximum UHI effect in the neighborhood.

Based on the UCAM model outcomes generated using the original design, an alternative design was drafted. It was attempted to compose this design so that no construction lots would be lost, the neighborhood type would remain the same and the total number of parking lots would also remain more or less constant. The largest difference in the updated design was moving several parking areas from the center of the neighborhood, where much pavement was already present, to its outskirts where the UHI effect was low. The updated design was assessed for heat stress with UCAM using the same assumptions for material albedo and the percentage of greenery in gardens.

2.8.4 Groundwater

Forcing

For groundwater hindrance, the generic forcing value of 0.01 m d^{-1} was used.

For drought-induced soil subsidence the forcing was based on a nearby monitoring well. Analysis of the data provided by this well showed that the groundwater level was 0.40 m lower in the dry summer of 2018 as compared to average of all summers since 1980. As discussed in Section 2.5, this groundwater level reduction was multiplied by 50% to obtain the forcing: instantaneous 0.60 m groundwater level reduction for a duration of 30 days.

Threshold values

The construction covenant South Holland has tentatively decided that the drainage head (distance between the ground level and the groundwater level) must be at least 1.30 m. This is an ambitious demand, as the usual demand is 0.70 to 1.0 m (for major roads). Both threshold values were used here: 1.30 m as the specific value; 1.0 m as the generic value. For drought-induced soil subsidence only the generic threshold value of 0.25 m of total subsidence for the period 2020-2085 was

used.

Calculation method and assumptions

The geology and surface levels used for the assessment of groundwater problems are shown in Table 2.4, and Figures 2.6 and 2.7. According to the designs, the surface level in the entire project area is projected at -5.0 m NAP. This means that any areas with lower elevations need to be leveled with sand. This will cause settlement of the subsoil, requiring additional sand in order to reach the desired surface level of -5.0 m NAP. It was assumed that the areas already at -5.0 m NAP were elevated by 0.5 m to account for any settlement (total top layer 1.3 m sand; scenario 1). Low-lying areas of -6.7 m NAP are assumed to be elevated by 1.7 m + 0.5 m of sand to account for settlement (total top layer 3.0 m sand; scenario 2).

The maximum groundwater levels were calculated for both areas, with low and high elevations. The drainage head is then simply the distance between ground surface and maximum groundwater level. Cross sections of the subsoil and some other relevant parameter values can be found in Figures 2.6 and 2.7 respectively for the two scenarios. As the figures show, the drains are projected to be located at -6.30 m NAP and are located approximately 72 m apart. The highest maintained water level in the ditches is also -6.30 m NAP (winter level). The diameter of the drainage tubes is designed to be 160 mm.

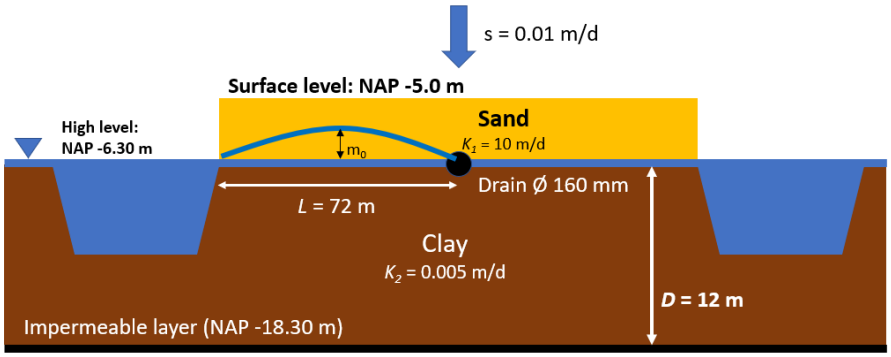

Figure 2.6: Cross section of scenario 1 (high-lying areas) with (assumed) parameter values underlying the groundwater level calculations

To show the effects of a dry spell on the soil level, Eq. 2.5 was used. It was assumed the groundwater level is instantaneously lowered by 0.60 m (see Forcing). The values for C_p and C_s were set at 12 and 80 respectively, based on the range of values presented in the work of de Glopper and Ritzema (2006). The intergranual pressure was calculated for the reference situation (annual average groundwater level) and the dry situation. This was done by subtracting the water pressure (density

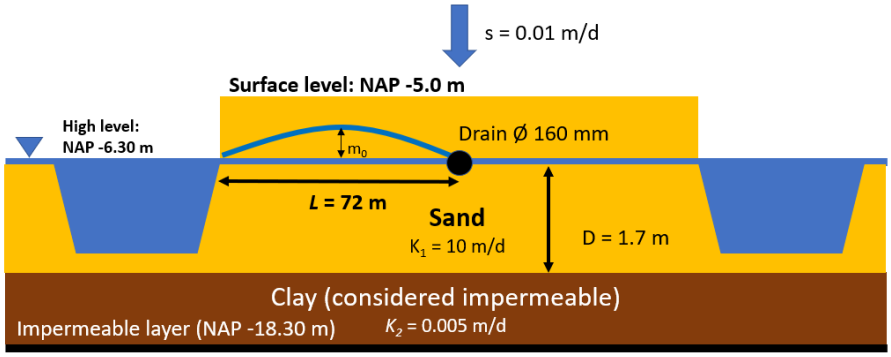

Figure 2.7: Cross section of scenario 2 (low-lying areas) with (assumed) parameter values underlying the groundwater level calculations

1,000 kg m^{-3}) from the soil pressure at the bottom of the soil layer. The porosity of sand and clay was assumed to be 0.30 and 0.65 respectively, and the density of the soil particles was set at 2,650 kg m^{-3}. These parameters are also shown in Figure 2.8.

Exploration of measures

To assess the influence of design parameters on local groundwater hindrance, the values for the highest acceptable surface water level and the location of the drains (both vertically and horizontally) was varied within reasonable design ranges. The drain diameter was not considered here because the indicator outcomes were found to be rather insensitive to this parameter. In the case of drought-induced soil subsidence only the lowest maintained water level was varied as there are no other design parameters.

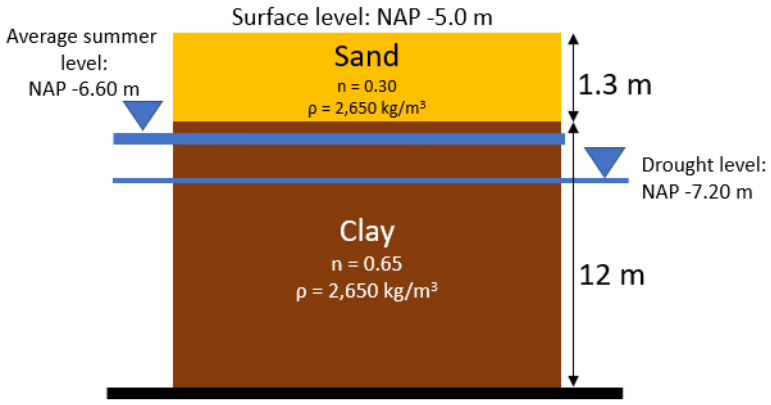

Figure 2.8: Cross section of the geology with (assumed) parameters underlying the drought-induced soil subsidence calculations

2.9 Case: Hooghkamer

2.9.1 Case choice and description

General description of study area

The second case treated in this work is the neighborhood “Hooghkamer”, north of Voorhout. It is located in the municipality Teylingen. Construction of the neighborhood has been planned since the early 2000s and has subsequently proceeded in three phases. The first phases were completed around 2012; the final phase is currently under construction and its completion is scheduled for 2020. In total, the neighborhood is projected to have around 900 homes.

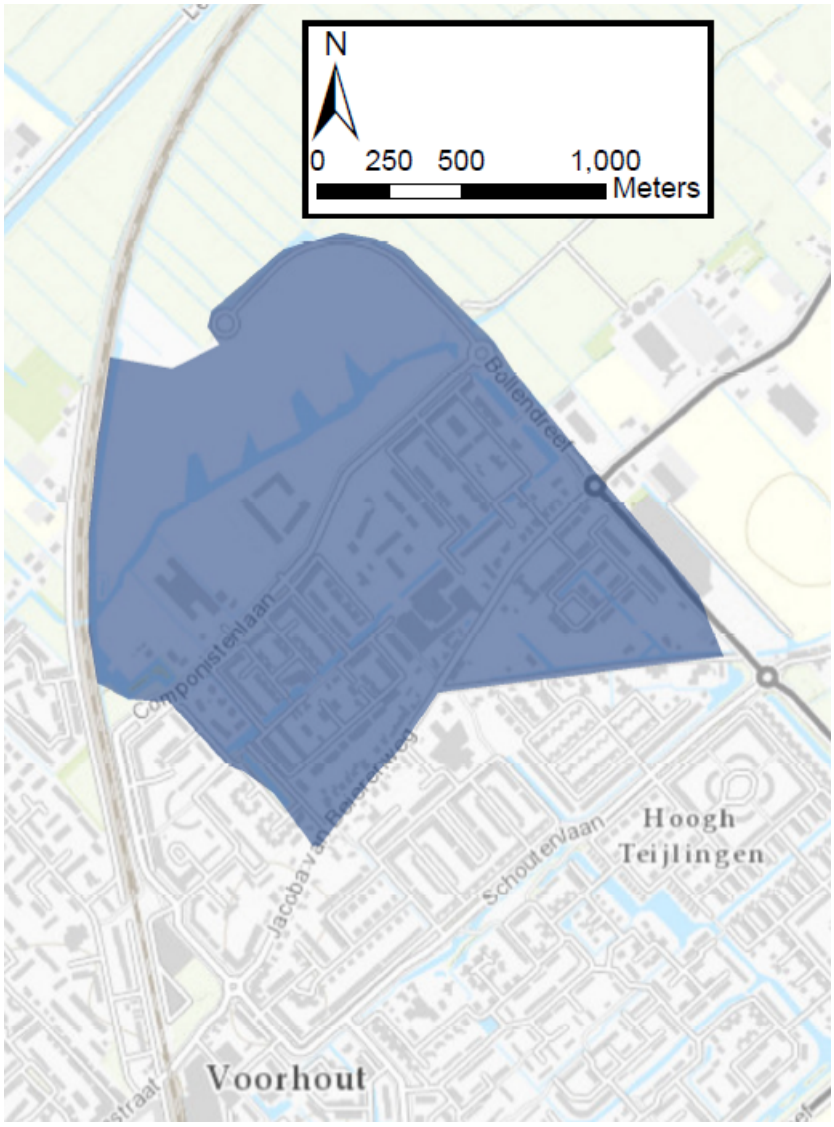

Figure 2.9: Location of the study area in the Hooghkamer case (near Voorhout, Netherlands). Source of underlying map: OpenTopo

The project area is depicted in Figure 2.9. It is roughly demarcated by the railway Leiden-Haarlem to the west, the existing developments of Voorhout to the south and the local road “Bollendreef” to the east and north.

Unlike the case of Wilderszijde, Hooghkamer is already under construction and outcomes of the framework cannot be considered in the final design. Nevertheless, this case is considered because (1) it boasts many similarities with Wilderszijde, both in neighborhood system parameters (peat meadow) and geographical location, (2) it is located in the province of South Holland so that the demands stated in the covenant are applicable, and (3) because of the availability of ample data regarding the neighboorhood’s design.

Data availability

As with the Wilderszijde case, many data were available in CAD-format, partially motivating the choice for this case. This entails a detailed plan of the neighborhood with sufficient information about the projected land use, building types, sewage system and other structures to define the projected design parameters.

System parameters could be derived from several environmental assessment and subsoil reports (NEXT Consultancy, 2015; IDDS, 2010). In addition, water management plans and permissions also provided valuable information. Overall the necessary data were available to obtain simulations of the climate change hazards.

Objectives and considered hazards

The objectives of this case study are (1) to assess the degree of climate adaptiveness in Hooghkamer and (2) to derive design parameters for neighborhoods in the province of South Holland to ensure their long-term climate adaptiveness. No extensive adaptations to the neighborhood design are proposed as the neighborhood has almost completely been constructed, but some measures were explored as was done in the Wilderszijde case. The climate change hazards pluvial flooding, heat stress and groundwater problems were considered here.

System and design parameters

Table 2.7 provides an overview of the system parameters in the study area of Hooghkamer. Table 2.8 gives an overview of the total areas of all land use categories in the neighborhood.

Table 2.7: Overview of system parameters in the Hooghkamer case

System parameter	Description
Geology	+0.20 to -1.10 m NAP: sand (K = 8 m d^{-1}) -1.10 to -2.50 m NAP: clay
Elevation	-0.40 to +0.20 m NAP Projected surface level: + 0.20 m NAP
Current land use	Pasture (north) Existing developments (south)
Total area	53 ha

Table 2.8: Overview of land use categories and areas in Hooghkamer

Land use category	Area (m^2)	Percentage of total
Structures	78,562	14.7%
Water	51,920	9.7%
Pavement	128,024	24.0%
Gardens	160,678	30.1%
Greenery	113,754	21.3%
Public space	241,778	45.4%
Public space + water	293,698	55.1%
Private space	239,240	44.9%
Paved area	206,586	38.8%
Total area	532,938	100.0%

2.9.2 Pluvial flooding

Forcing

Forcing for pluvial flooding was identical to the Wilderszijde case: the generic forcing (precipitation events of 33 (T = 2 years) and 69 mm h^{-1} (T = 100 years), and the specific forcings of 30 and 120 mm h^{-1} as described in the construction covenant.

Threshold values

The threshold values were also identical to the Wilderszijde case, see Table 2.6.

Model configuration

Several AutoCAD files containing the sewage network were available. However, each neighborhood part had separate definitive designs as they were constructed

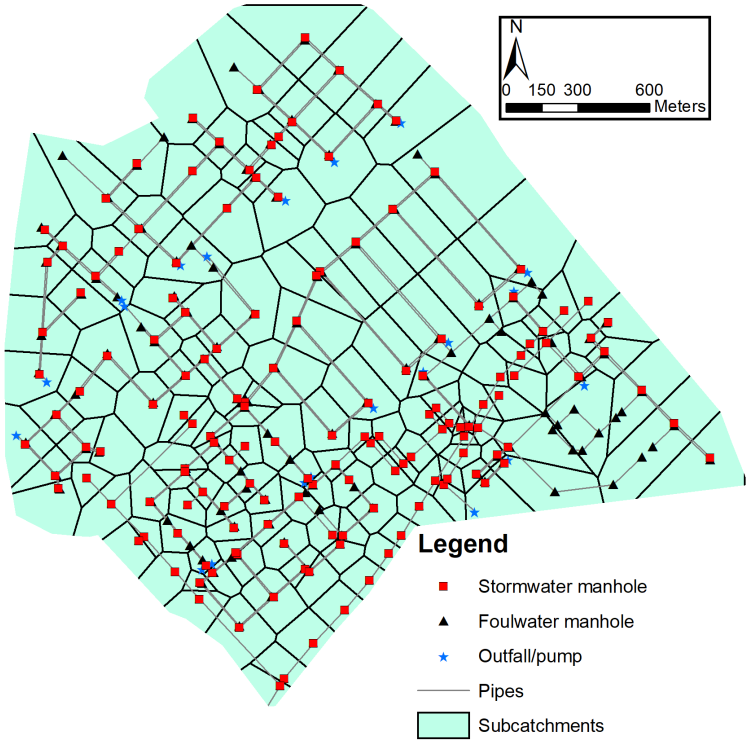

Figure 2.10: Overview of the Wilderszijde sewage network and assigned subcatchments

in phases. The designs were not always in accordance with each other at locations were different sewage networks come together. In these cases, a worst-case scenario for storage was assumed, for example the smallest pipe diameter.

For the remainder the model was configured in the same fashion as was done in the Wilderszijde case. The stormwater sewage of Hooghkamer and the subcatchments (Thiessen polygons around stormwater nodes) are shown in Figure 2.10.

2.9.3 Heat stress

Forcing and threshold values

The generic threshold value of UCAM class I (daily-averaged UHI of maximum 1.88 °C) was maintained here.

Model configuration and simulation steps

Hooghkamer was classified into the five land use classes used in UCAM (water, pavement, greenery, structures and gardens). The result is shown in Figure 2.11.

The area was discretized into a grid with cells of 50 x 50 m. All structures were assigned an estimated of 10 m (residential area), with the exception of several larger

Figure 2.11: Land use in the neighborhood Hooghkamer, classified according to the five categories used by UCAM. The red star marks the fixed location where the UHI effect during a hot day was monitored.

facilities such as super markets, schools and a medical center. These structures were assigned a height of 15 m. Based on the appearance of the homes already constructed, all homes were assigned a roof albedo value of 22% (standard red tiles) and a facade albedo of 30% (red bricks). Other facilities were assigned a roof albedo value of 8% (black tar) and a facade albedo of 30%. Analogously to the model configuration in the Wilderszijde case, it was assumed that gardens consist of 40% unpaved area and all public pavement has the same albedo of 30% (light-colored concrete).

The UCAM GIS-tool was run to classify each cell according to their LCZ and finally to obtain a daily-averaged value for the UHI. The results were interpolated according to the “bilinear” method to obtain a smoothed map of the results.

The UHI effect at a fixed location (a large supermarket and adjacent parking lot;

marked with a red star in Figure 2.11) was monitored over time on a hot day. To this end, its LCZ value, vegetation percentage and albedo values were entered in the MS Excel tool supplementing UCAM. The results were used to plot the simulated values of the UHI effect at a location theoretically very susceptible to heat stress.

Exploration of measures

To explore the effect of altering the design, UCAM was run with different settings for (1) the material albedo across the study area and (2) the amount of vegetation in gardens. The land use did not change and was identical to the original design. In variant 1, the roof albedo of all structures was set at the maximum value (82%; white ecoseal roof cover), the facade albedo at 40% (white bricks) and the road albedo to 50% (yellow clincker bricks). The amount of vegetation in gardens was kept at 40%. In variant 2, the material albedo was kept at the original design values, but the amount of greenery in gardens was set at 100%. UCAM was then run again with the new configuration.

2.9.4 Groundwater

Forcing

For groundwater hindrance, the generic forcing value of 0.10 m d^{-1} was used.

For drought-induced soil subsidence, the forcing was based on local information. Data from a nearby monitoring well were used to estimate the effects of droughts on the groundwater level. These showed the groundwater was up to 0.37 m lower during the dry summer of 2018 as compared to the average summer since 1994. This value was multiplied by 50% to obtain the forcing value of 0.56 m decrease in groundwater level.

Threshold values

Analogously to the Wilderszijde case, the threshold values for the drainage head were set at 1.0 m (generic) and 1.30 m (specific). The threshold for soil subsidence is also identical: 0.25 m subsidence in the period 2020-2085.

Calculation method and assumptions

Cross sections of the geology with (assumed) parameter values underlying the groundwater level and soil subsidence calculations are depicted in Figures 2.12 and 2.13 respectively.

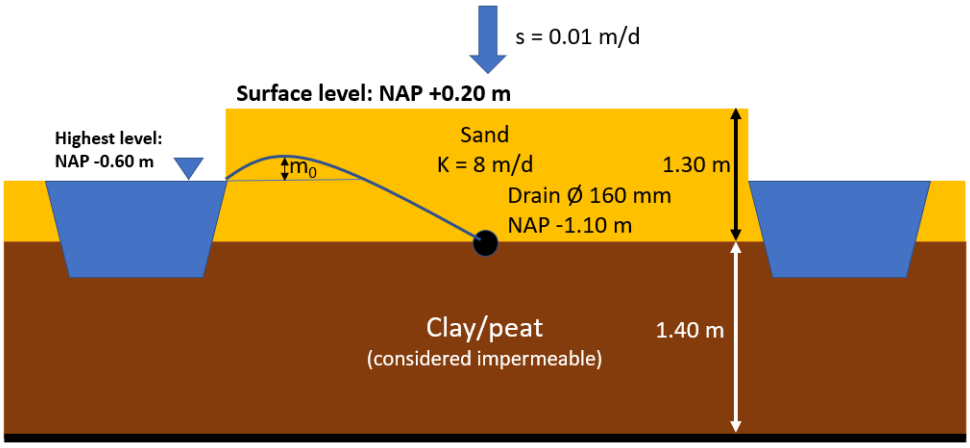

Figure 2.12: Cross section of the geology with (assumed) parameters underlying the groundwater level calculations

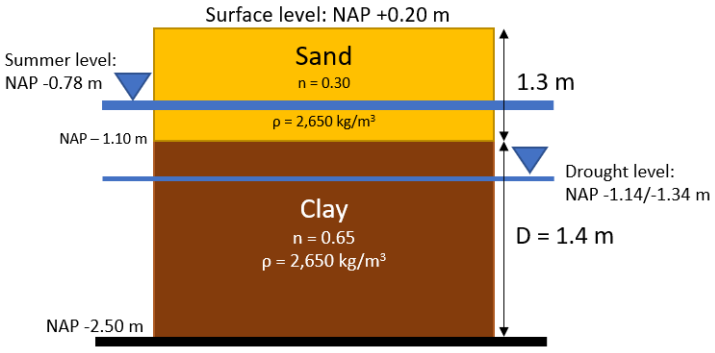

Figure 2.13: Cross section of the geology with (assumed) parameters underlying the drought-induced soil subsidence calculations

As the summer level in ditches (NAP -0.78 m) differs from the location of the drainage system (NAP -1.10 m), Eq. 2.4 was used to find the maximum water level. The soil permeability is 8 m d^{-1} and the distance between drains is 60 m according to the designs (see also Table 2.7).

For the drought calculations, the approach was identical as in the Wilderszijde case: Eq. 2.5 was used with values for C_p and C_s of 12 and 80. The other (assumed) parameter values were also the same.

2.10 Derivation of design guidelines

The results found here were used to derive coarse design guidelines for neighborhoods to be constructed specifically in peatlands. To this end, the results per hazard of both case studies were compared and the effects of possible measures were

analyzed. Differences in outcomes were explained using variation in the design parameters and this led to the formulation of several quantitative design guidelines for each hazard.

Additionally, the derived design parameters were compared to parameters mentioned in existing municipal neighborhoods design guidelines. Two municipal design guidelines were analyzed (Gemeente Hollands Kroon (2018); Gemeente Bunnik (2012)) and one scientific paper by Krumm et al. (2017), specifically about heat stress. The findings reported in these documents were compared to the results presented in this work.

Chapter 3

Results

This chapter is dedicated to the results of this study. First the climate adaptiveness assessment results are described and discussed in Sections 3.1 and 3.2 for the Wilderszijde and Hooghkamer cases respectively. The results for these cases are then compared in Section 3.3. Finally, results from both cases are used to derive coarse design guidelines for neighborhoods in peat meadow areas in Section 3.4.

3.1 Results case Wilderszijde

3.1.1 Pluvial flooding

The model results for pluvial flooding in the Wilderszijde neighborhood are depicted in Figures 3.1, 3.2 and 3.3. These show maximum inundation depths at stormwater manholes after precipitation events of 33 mm, 69 mm and 120 mm in 1 hour respectively. The results for the specific forcing of 30 mm h^{-1} are not shown here because they are very similar to the 33 mm h^{-1} event.

The results show that the designed stormwater sewage system is not able to adequately discharge all the water from the precipitation events. During and after the 33 mm h^{-1} event, no water is stored above surface level in most subcatchments that are nearby outfalls. However, a number of manholes experience substantial flooding in excess of the threshold value (and far beyond), especially in the western part of the study area and especially those far away from outfalls. In general, these manholes start to become flooded after 15 minutes of rainfall and flooding subsides to values below the threshold after 90 minutes. The total amount of water which cannot be stored in the sewage system is 815 m^3. The results obtained using the 30 mm h^{-1} event, mentioned in the construction covenant, are very similar.

As expected, the 69 mm h^{-1} event yields a similar but more extreme result. Several subcatchments are able to deal with the high amount of precipitation forced here, but the majority experience severe flooding, often exceeding the threshold of

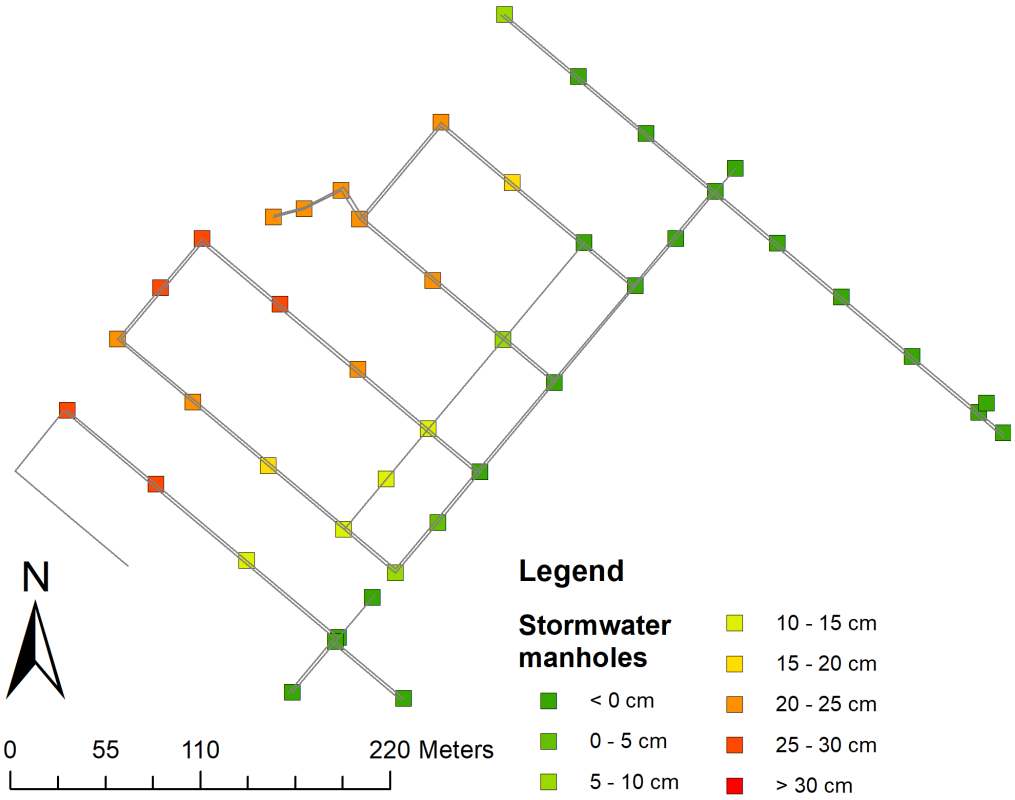

Figure 3.1: InfoWorks ICM results showing maximum flood depths at stormwater manholes for a precipitation event of 33 mm in 1 hour

30 cm inundation. This value is reached after approximately 45 minutes and subsides after approximately 135 minutes after the start of rainfall. The total amount of water which cannot be stored in the sewage system is 2,530 m^3.

The results for a 120 mm h^{-1} event are depicted in Figure 3.3. It shows extreme inundation depths of up to 0.46 m. The threshold value of 0.30 m is reached after about 35 minutes. The water takes a long time to recede: up to 4 hours and 15 minutes at the manholes struck by the worst flooding. The total amount of water which cannot be stored is approximately 6,000 m^3.

Overall the sewage network's performance during high-intensity precipitation events is poor. Even an event with a 2085 return period of about 2 years (33 mm h^{-1}) causes severe flooding of up to 0.26 m where the threshold value is only 0.10 m. The forced event with a future return period of 100 years (69 mm h^{-1}) causes more extreme flooding in multiple manholes (up to 0.36 m), also exceeding the set threshold value of 0.30 m.

One reason why the system functions inadequately may be the age of the design. The earliest designs for the sewage network of Wilderszijde were drafted around 2003 and design criteria were much looser in that period. Such designs used to be based on less extreme precipitation events (Shower 05 and 06 (Leidraad Riolering,

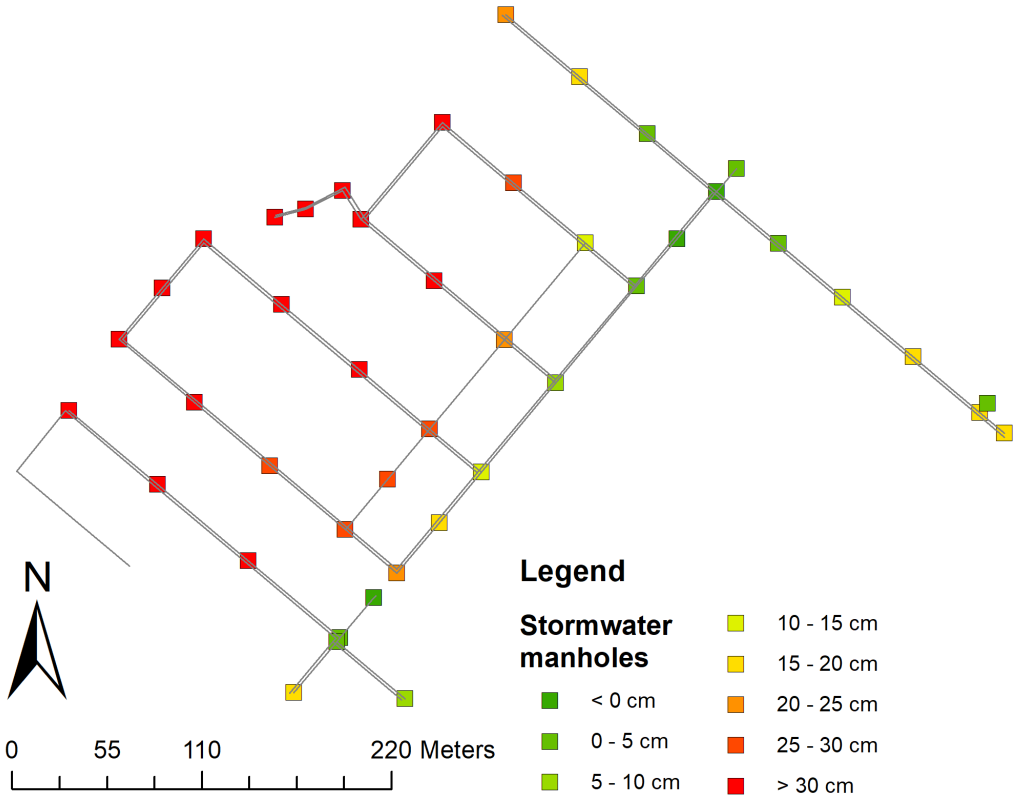

Figure 3.2: InfoWorks ICM results showing maximum flood depths at stormwater manholes for a precipitation event of 69 mm in 1 hour

2004)). It was decided to test the model by forcing these events on the network and it was found (not shown here) that no or very minor flooding ($<$ 3 cm) occurs when these events are forced. This supports the hypothesis that the design was composed using one of these precipitation events.

Exploration of measures

InfoWorks ICM was also used to explore possible measures to mitigate pluvial flooding. For clarity the results are not shown here graphically, but can be found in Appendix C. Table 3.1 gives an impression of the effects of these measures and presents the storage deficit — defined as the amount of water which cannot be stored in the sewage system — in each situation in mm.

Enhancing the sewage network's capacity by using larger pipes (diameter increase of 100 mm for all pipes) is effective in mitigating pluvial flooding, but not sufficient to reach inundation levels below the threshold value. In a 33 mm h^{-1} rainfall event, the vast majority of manholes does not flood, but several still reach too large inundation values. The total amount of flood volume does decrease substantially, from 815 m^3 (7.2 mm over total area) to about 315 m^3 (2.8 mm). The 69 mm

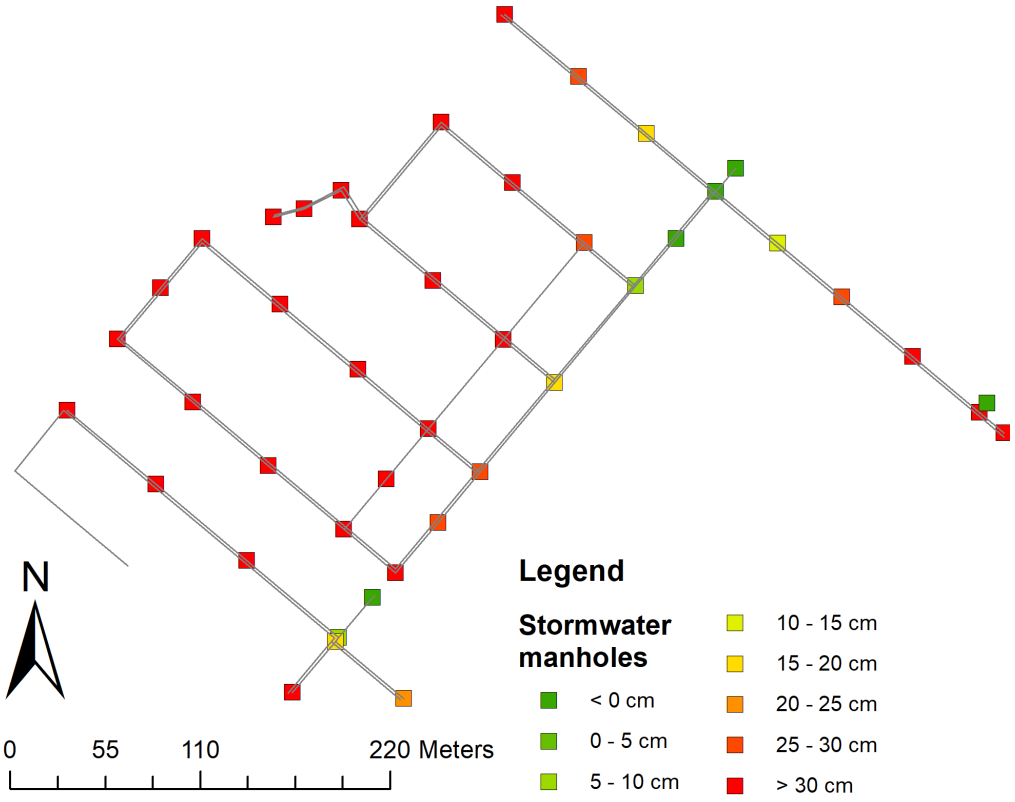

Figure 3.3: InfoWorks ICM results showing maximum flood depths at stormwater manholes for a precipitation event of 120 mm in 1 hour

h^{-1} event paints a similar picture: all manholes perform better in that their inundation depths are lower than under the original design, but six manholes still experience major flooding in excess of the threshold value of 0.30 m. The total flood volume decreases from 2,530 m^3 (22.2 mm) to 1,515 m^3 (13.3 mm).

While altering the design of sewage systems is often not a popular measure to take because it is deemed costly and causes much construction hindrance in existing neighborhoods, it may be a viable option in neighborhoods that are still in the design phase. The results here have shown that such a measure can greatly contribute to the total amount of rainwater storage in the neighborhood, although not quite sufficient in this case.

Approach (b) entailed the reduction of the amount of paved surface (both open and closed) in each subcatchment. If the amount of paved surface is reduced by 10%, the total amount of water not stored is 689 and 2,159 m^3 (6.0 and 18.9 mm) respectively for events of 33 and 69 mm h^{-1}. If the amount of paved surface is reduced by 20%, these figures are 550 and 1,877 m^3 (4.8 and 16.5 mm) respectively. The inundation depths for each manhole are graphically shown in Appendix C.

Table 3.1 also shows the implications when it is decided to store the storage deficit in either public or private space only. With the current design, each house-

hold should on average store an additional 15 mm of rainwater to prevent flooding altogether in the neighborhood in case of a 33 mm h^{-1} event.

Table 3.1: InfoWorks results of the exploration of measures. The storage deficit is the amount of water (m^3 / mm) which cannot be stored in the sewage system. The scenario names refer to the amount or precipitation forced in 1 hour and the measure taken

Scenario	Storage deficit (m^3 / mm)	Storage deficit - public space (mm)	Storage deficit - private space (mm)
33 - base	815 / 7.2	18.1	15.0
33 - sewage capacity	314 / 2.8	7.0	5.8
33 - 10% less pavement	689 / 6.0	15.3	12.7
33 - 20% less pavement	550 / 4.8	12.2	10.1
69 - base	2,530 / 22.2	56.2	46.5
69 - sewage capacity	1.518 / 13.3	33.7	27.9
69 - 10% less pavement	2,159 / 18.9	47.9	39.7
69 - 20% less pavement	1,877 / 16.5	41.7	34.5
120 - base	6,000 / 52.6	133.2	110.4
120 - sewage capacity	4,471 / 39.2	99.2	82.3
120 - 10% less pavement	5,253 / 46.1	116.6	96.6
120 - 20% less pavement	4,677 / 41.0	103.8	86.0

Extreme precipitation events also affect the levels in surface water. Outfalls are modeled in InfoWorks as if the surface water has an infinite capacity. In reality, however, the surface water level will increase. In extreme cases, the increase in level may cause local flooding from the ditches. For Wilderszijde, the maximum maintained surface level is NAP -6.30 m and the ground level is at -5.0 m. The water level increase for precipitation events of 33, 69 and 120 mm h^{-1} are 0.17, 0.51 and 0.88 m respectively. Even in the latter case, there is sufficient storage available in the surface water. However, it should be noted that in the future other neighborhoods will be developed which will also drain onto the same water body. Surface water level increases may then become problematic during and after extreme precipitation events.

If the current design were to be used, inhabitants would have to store a substantial amount of water on their private terrain: 15 mm or 46.5 mm to prevent flooding altogether under 33 mm h^{-1} and 69 mm h^{-1} forcing respectively. 15 mm comes down to 5.8 m^3 (or approximately 29 rain barrels or infiltration crates of 200 L) per private lot. Alternatively, the additional storage could be realized above the ground by sacrificing private lots. This would mean that approximately 2 lots cannot be developed,

assuming they are entirely turned into storage facilities with a maximum water depth of 1.0 m.

3.1.2 Heat stress

The results of the heat stress model UCAM are depicted in Figure 3.4, which shows the land use according to the design (left) and the projected daily-averaged and interpolated UHI effect (in °C) (right). All grid cells were classified as LCZ 6 (open low-rise). It reveals that heat stress, expressed in degrees UHI effect, manifests itself mainly in the center and the east of the study area. Roads and buildings are relatively prevalent here and there is little greenery and no surface water. The maximum daily-averaged UHI effect reached is approximately 2.27 °C, which is the temperature difference compared to rural areas. Conversely, in locations where no pavement or structures are present, such as in the northwest, the daily-averaged UHI effect is virtually zero. For an average grid cell to just satisfy the heat stress criterion (daily averaged UHI maximum 1.88 °C), the amount of green surface (both on private and public property) should be approximately 32%.

Figure 3.5 shows the same results, but classified according to the threshold value of 1.88 °C. It shows which locations do and which do not satisfy the previously determined threshold value. Again, this is especially the case in the center and eastern parts of the neighborhood.

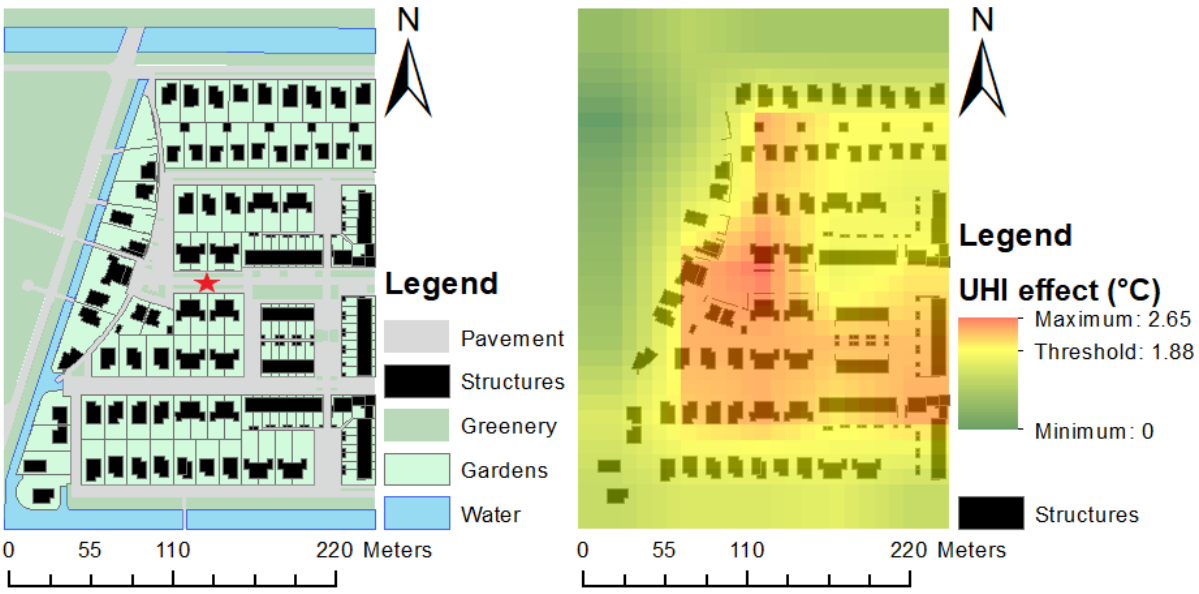

Figure 3.4: Left: land use in the study area according to the design. The red star indicates grid cell (3, 4). Right: UCAM model results showing the simulated Urban Heat Island (UHI) effect in °C across the study area.

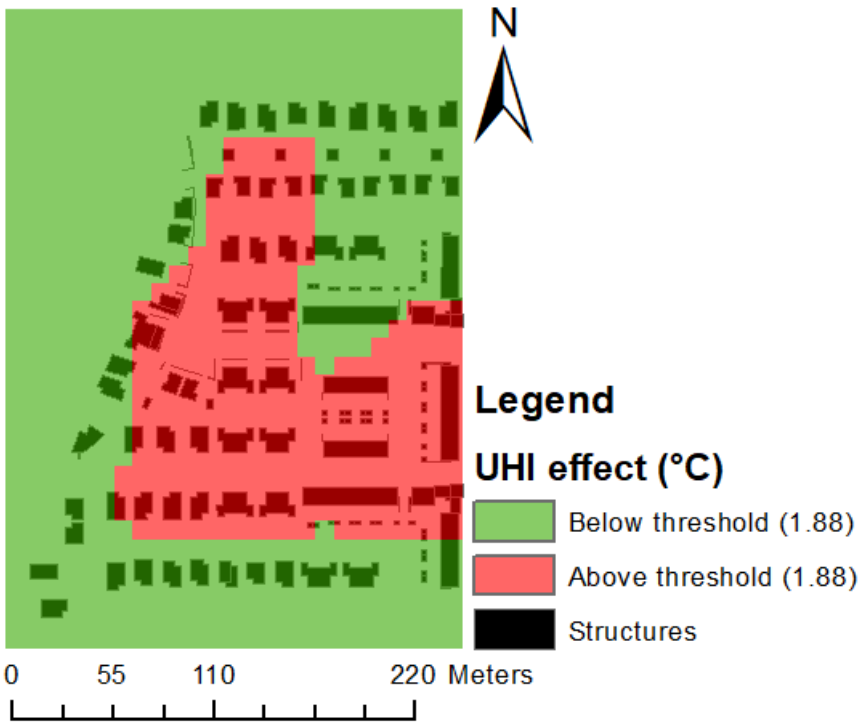

Figure 3.5: Detailed and interpolated heat assessment using a threshold value of 1.88 °C

These findings are in line with the expectation that more urbanized areas suffer more from heat stress than open or rural areas. The maximum UHI temperature reached is 2.27 °C higher than in surrounding rural areas. This corresponds with a heat-index of 0.69. According to Table 2.1, this falls within category II (risky). The current design which assumes gardens are paved for a maximum of 60% does not comply with the demands regarding heat stress as the heat-index exceeds the threshold value of 0.57 (1.88 °C).

Figure 3.6 depicts the simulated UHI effect at a fixed location (marked with a red star in Figure 3.4) as a function of time on a hot day. It differentiates between the situation where all gardens are fully paved, fully green and the rural reference situation. It shows clear differences in experienced temperature: the temperature is highest most of the time in the situation where all gardens are paved. Moreover, the figure shows that the UHI effect manifests itself mainly during the evening hours and early night, when the sun has set. Rural areas quickly cool down while more urban areas continue to suffer from the heat as much solar radiation has been absorbed during the day. In fact, the urban areas do not even completely cool down to the rural level before the next day starts.

Figure 3.6 also shows some inertia in the UHI effect. In the early morning, the rural areas heat up faster than urban areas as solar radiation is the primary source of warmth and is able to reach all locations. During these hours, much of the urban

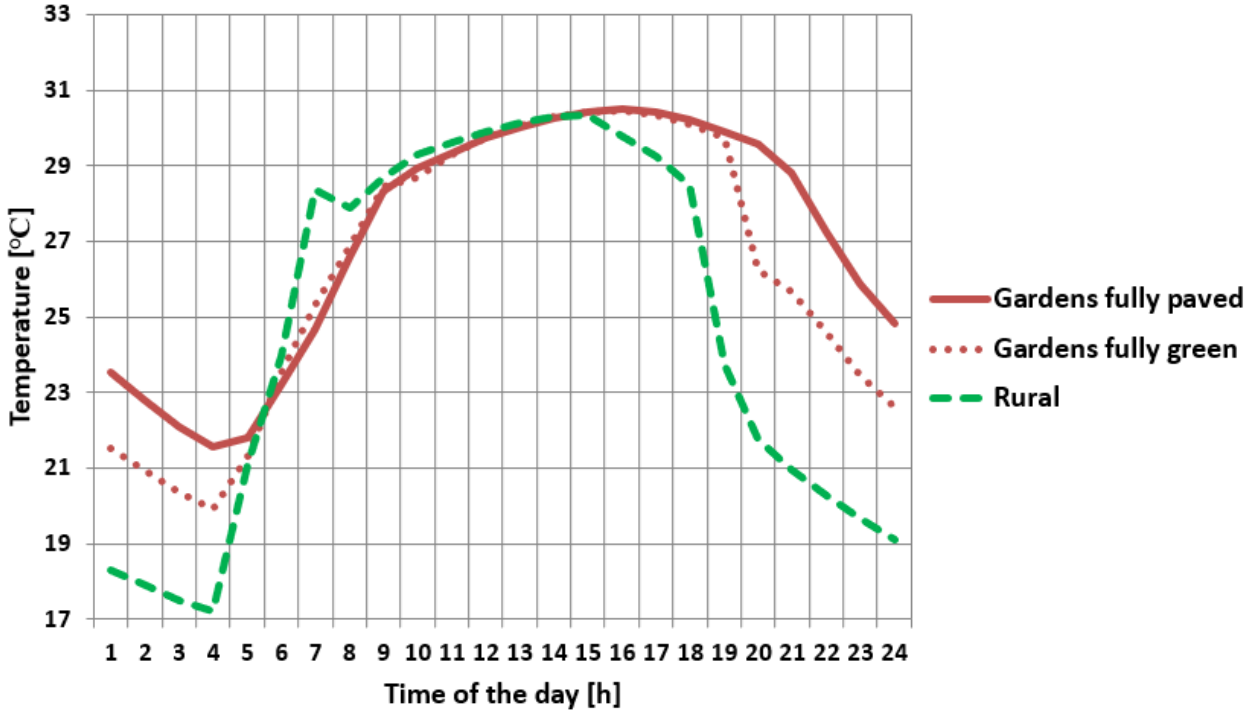

Figure 3.6: Hourly experienced temperatures at a fixed location (grid cell (3, 4); red star in Figure 3.4) in the neighborhood with fully paved gardens (red line) and fully green gardens (red dotted) during a hot day. The rural situation (green) included for reference

land is still covered by shadows and the built-up area has not absorbed much heat yet. In fact, between approximately 05:30 and 09:00, a negative UHI effect occurs as more heat is experienced in rural areas than in the neighborhood. The opposite effect is observed at night. A slightly alternative explanation for this phenomenon may be the thickness of the atmospheric boundary layer. This layer is generally thicker in urban areas because hot air rises. Due to its thickness, the boundary layer needs more time to cool down in the evening and warm up in the morning in urban areas. This phenomenon is described in detail by Oke (1995).

Exploration of measures

To investigate the effects of different design guidelines, UCAM was run for several scenarios where the amount of paved surface in gardens was varied (0-100%) as well as the material type for roofs, roads and facades. The results are presented in Tables 3.2 and 3.3 and are based on the maximum daily-averaged UHI effect reached in the hottest grid cell. The reference situation corresponds with 40% unpaved area in gardens and medium-colored materials.

Table 3.2: Results of the univariate sensitivity analysis of UCAM where the unpaved surface area in gardens (in %) was varied

Unpaved surface in garden (%)	**Maximum UHI (°C)**
0	2.62
40	2.27
50	2.12
100	1.74

Table 3.3: Results of the univariate sensitivity analysis of UCAM where the material type of the paved surface was varied

Material color	**Maximum UHI (°C)**
Dark-colored	2.47
Medium-colored	2.27
Light-colored	1.45

These sensitivity analyses reveal that both the amount of greenery in gardens and the buildings' material types have a profound influence on the daily-averaged UHI effect. If the gardens were 100% unpaved (medium-colored materials) *or* if all buildings featured light-colored materials (40% unpaved gardens), the maximum daily-averaged UHI would never exceed the threshold value of 1.88 °C.

The sensitivity analysis also suggests (not shown here) that the model outcomes are especially sensitive to the assigned roof albedo values, to a lesser extent to the road albedo and hardly to the facade albedo.

3.1.3 Updated design

The results of the original design were used to draft a design variant. This variant was also assessed for heat stress using UCAM. The land use classes and results are presented in Figure 3.7.

When the figure is compared to Figure 3.5, it shows that the portion of the neighborhood where the daily-averaged UHI effect is above the threshold, has been decreased substantially. Also, the maximum daily-averaged UHI effect reached is 2.10 rather than 2.25 °C, according to the model results.

These results show it is possible to improve the design through the framework assessment and iteration. Heat assessment according to the framework's methodology revealed locations where heat stress exceeded the threshold value and made it possible to propose specific measures to mitigate heat stress in specific locations. This attempt was at least partly successful.

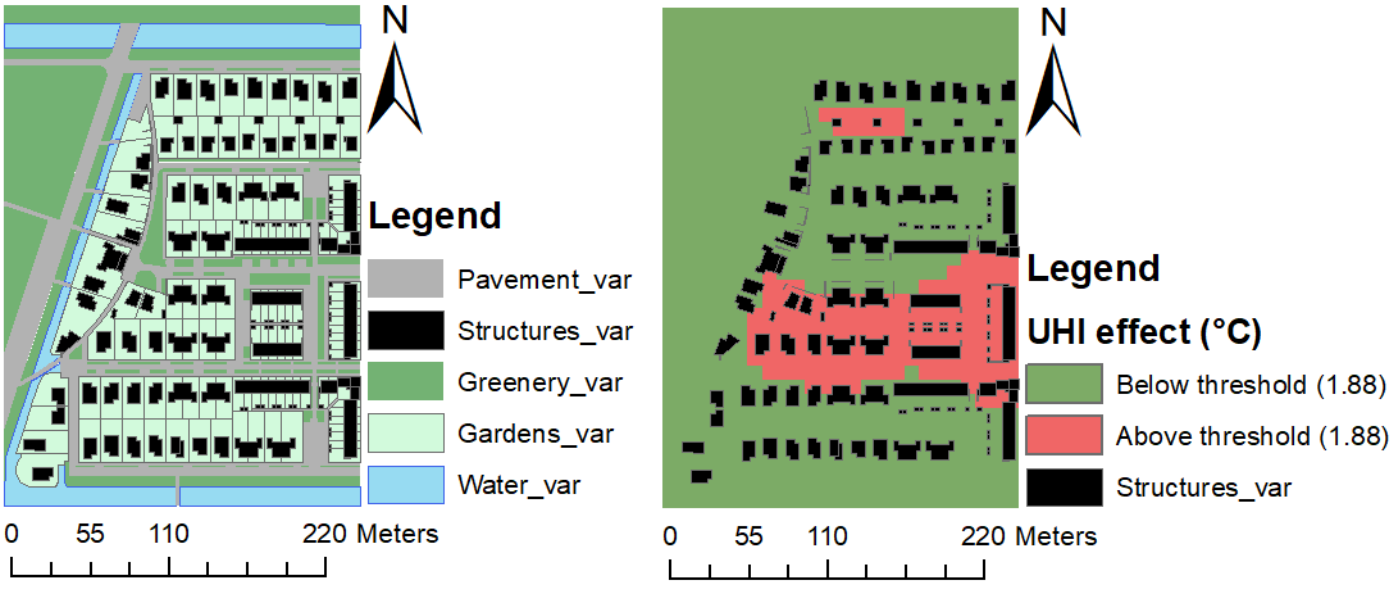

Figure 3.7: Left: land use in the study area according to the design variant. Right: Interpolated heat assessment results using a threshold value of 1.88 °C

3.1.4 Groundwater hindrance

Application of Eqs. 2.2 and 2.3 combined with the (assumed) parameter values listed in Figures 2.6 and 2.7 for the two scenarios respectively yields a groundwater level rise of 1.14 m for high-lying areas and 0.75 m for low-lying areas.

In the first scenario, the maximum groundwater level raise between drains is relatively high. This is caused by the relatively small amount of sand in which groundwater can be stored; the underlying clay layer is hardly permeable and the groundwater level between drains is thus high. In the second scenario, where much sand is added to level the area, the maximum groundwater level between drainage points is much lower as the soil's storage capacity is larger.

The groundwater levels in both scenarios are outside the acceptable limits. The drainage head is only 0.16 m and 0.55 m respectively, which is insufficient (thresholds 1.0 and 1.30 m). The results do show that additional sand is one way to mitigate groundwater hindrance by virtue of its larger water capacity.

Exploration of measures

The sensitivity of the groundwater level to realistic design values the surface water level (and depth of the drainage tubes) and *L* was tested in an exploration of possible measures to alleviate too high groundwater levels. The results are presented in Table 3.4. The sensitivity scenarios a through c have the following values for the surface water level (m -NAP) and *L* (m) of -6.10/30, -6.50/45, -6.70/90. The analysis is univariate: one parameter value is changed while the other is kept at the reference value.

Table 3.4: Results of the univariate sensitivity analysis in the case of low-lying areas showing critical drainage head (m). Variations of the surface water level and *L* for the four scenarios: -6.10/30, -6.50/45, -6.70/90 (m -NAP and m)

Parameter	**Sensitivity scenario**			
	a	**b**	**c**	**Reference**
Surface water level	0.0	0.36	0.56	0.16
L	0.83	0.59	0.35	0.16

These results show that both measures can be successful in the mitigation of local groundwater hindrance. However, none of the proposed measures suffices to ensure local groundwater levels remain within the threshold limits alone. A combination of the two seems to be required. Setting the distance between drains *L* at 30 m *and* decreasing the surface water level annex drain depth to -6.50 m NAP would

be enough to comply with the generic threshold value of 1.0 m drainage head. Another possible measure would be to elevate the entire neighborhood with additional sand. Its effect would be similar to lowering the surface water level.

3.1.5 Drought-induced soil subsidence

Using the assumptions shown in Figure 2.8 and Eq. 2.5 it was found that the clay soil may subside by approximately 2.7 cm during a single forced drought event. This yields a total of 0.27 m over ten of such events. The calculation (sub-)results are summarized in Table 3.5.

These results show that droughts and subsequent soil subsidence pose a serious hazard to the structural integrity of buildings. The total subsidence of 0.27 m is higher than the threshold value of 0.25 m and the neighborhood is thus not yet considered sufficiently climate adaptive for soil subsidence. However, these results are to be approached critically as the forcing and thresholds are quite arbitrary and the methodology is based on an analytical formula.

Table 3.5: Overview of parameters and outcomes for the drought-induced soil subsidence calculations

Parameter	Reference	Drought
Relative GW level [m]	- 0 m	-0.60 m
$P_{i,\,tot}$ [kPa]	94.47	96.57
Delta $p_{i,\,tot}$ [kPa]	-	2.1
Subsidence [cm y^{-1}/total]	-	2.7/27

3.1.6 Summary of results

A summary of the climate adaptiveness assessment for the neighborhood Wilderszijde is provided in Table 3.6.

Table 3.6: Summary of the climate adaptiveness assessment of the Wilderszijde neighborhood

Hazard	Threshold value	Indicator value	Fail/pass
Pluvial flooding (33 mm)	0.10 m	0.26 m	FAIL
Pluvial flooding (69 mm)	0.30 m	0.36 m	FAIL
Heat stress	$<$1.89 °C	2.25 °C	FAIL
Drainage head	$>$1.0 m	0.16 m	FAIL
Soil subsidence	$<$0.25 m	0.27 m	FAIL

3.2 Results case Hooghkamer

3.2.1 Pluvial flooding

The InfoWorks model results for 33 mm h^{-1}, 69 mm h^{-1} and 120 mm h^{-1} events forced onto the Hooghkamer case are depicted in Figures 3.8, 3.9 and 3.10 respectively.

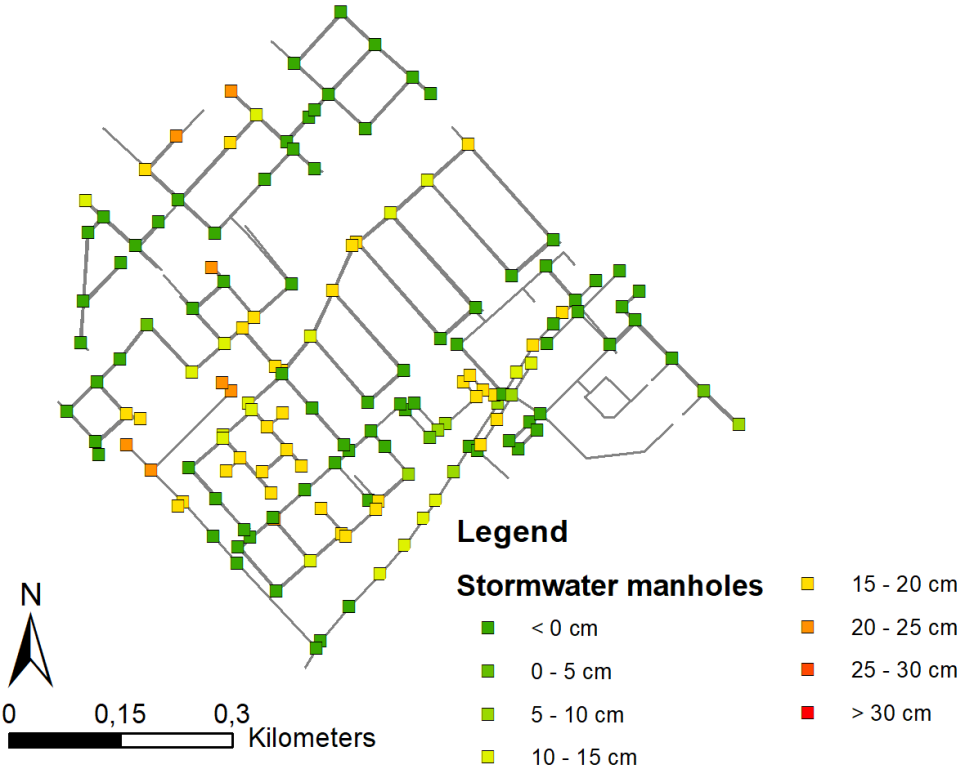

Figure 3.8: InfoWorks ICM results showing maximum flood depths at stormwater manholes for a precipitation event of 33 mm in 1 hour in Hooghkamer

The results show large spatial differences across the neighborhood: the sewage system is able to process the 33 mm h^{-1} well in some areas as no water needs to be stored on the streets. In general this applies to the (north)western parts of the neighborhoods which are yet to be constructed. In other places, however, inundation depths north of the threshold value of 0.10 m are reached. This is especially the case in locations with large amounts of paved surface (see Figure 2.11 for an overview of land use). Most manholes start to become flood after approximately 15 minutes and flooding subsides generally an hour later. 1,140 m^3 of water could not be stored within the sewage system.

The results for an event of 69 mm h^{-1} paint a similar yet more severe picture. Flooding occurs at approximately half of the manholes with unacceptable ($\geq$ 0.30 m) flooding occurring at 25 manholes. The flood duration is a little over 1 hour and

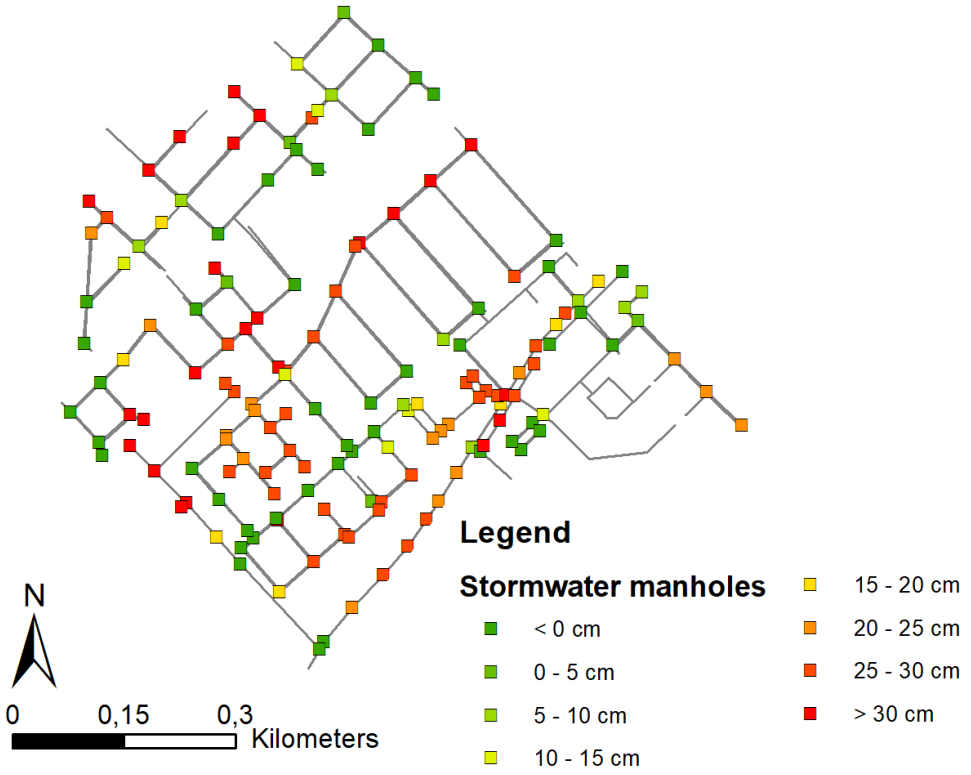

Figure 3.9: Identical to Figure 3.8, but for a 69 mm h^{-1} event

15 minutes: between 12 minutes and 1 hour and 15 minutes. The total amount of water not stored in the sewage system is about 6,700 m^3.

In the extreme event of 120 mm of rainfall within 1 hour, practically all manholes experience severe flooding. The flood duration is also substantial as the inundation depth remains above 0.10 m for almost two and a half hours. The total flood volume is 18,050 m^3.

Under all forcings, the threshold values of 0.10 and 0.30 m respectively are exceeded in multiple manholes. The neighborhood thus fails the pluvial flooding assessment.

Exploration of measures

As with the Wilderszijde case, several possible measures to mitigate pluvial flooding were explored. For clarity the results are not shown here, but can be found in Appendix D. The results of the exploratory analyses conducted with InfoWorks are summarized in Table 3.7.

Enlarging the sewage capacity by increasing each pipe's diameter by 100 mm has a positive effect on reducing floods. In a 33 mm h^{-1} precipitation event, the total flood volume reduced to only 15 m^3 so that all hardly any water accumulates on

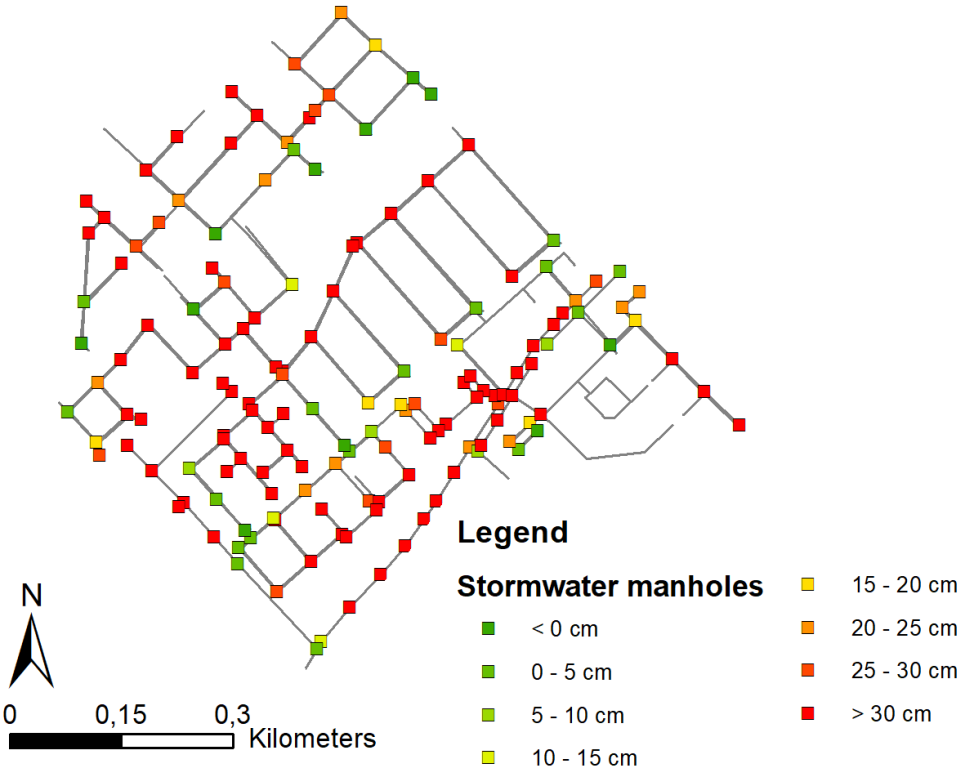

Figure 3.10: Identical to Figure 3.8, but for a 120 mm h^{-1} event

the streets. Under 69 and 120 mm h^{-1} forcings, this value is 2,200 and 10,270 m^3 respectively.

Reducing the amount of paved surface by 10 and 20% also has a positive influence on the mitigation of pluvial flooding. However, it seems unlikely that flooding can be prevented entirely through this measure as it would probably require unrealistically high efforts of reducing the amount of paved surface.

Rainwater which runs off causes increases in the surface water level of 0.23, 0.65 and 1.13 m respectively in the 33, 69 and 120 mm h^{-1} precipitation events. In summer, the maximum maintained level is NAP -0.78 m and the ground level is at +0.20 m. There is thus sufficient storage available in surface water for the 33 and 69 mm h^{-1} events. In the extreme event of 120 mm h^{-1}, the surface water will flood or water will enter the outfalls in reverse direction.

Table 3.7 also shows the storage deficit – defined as the amount of water which cannot be stored in the sewage system and thus causes flooding – in mm. It also differentiates in storage deficit in the public and the private space. For instance, households have to store an additional 4.8 mm on average on their terrain to prevent flooding in a 33 mm h^{-1} event under the current design.

This figure implies each household would have to purchase and use approximately 10 rain barrels or infiltration crates with a capacity of 200 L. Alternatively,

Table 3.7: InfoWorks results of the exploration of measures. The storage deficit is the amount of water (m^3) which cannot be stored in the sewage system. The scenario names refer to the amount or precipitation forced in 1 hour and the measure taken

Scenario	Storage deficit (m^3 / mm)	Storage deficit - public space (mm)	Storage deficit - private space (mm)
33 - base	1,139 / 2.1	4.7	4.8
33 - sewage capacity	15 / 0.0	0.1	0.1
33 - 10% less pavement	833 / 1.6	3.4	3.5
33 - 20% less pavement	563 / 1.1	2.3	2.4
69 - base	6,707 / 12.6	27.7	28
69 - sewage capacity	2,199 / 4.1	9.1	9.2
69 - 10% less pavement	5,724 / 10.7	23.7	23.9
69 - 20% less pavement	4,780 / 9.0	19.8	20.0
120 - base	18,047 / 33.9	74.6	75.4
120 - sewage capacity	10,272 / 19.3	42.5	42.9
120 - 10% less pavement	15,949 / 29.9	66.0	66.7
120 - 20% less pavement	13,896 / 26.1	57.5	58.1

about 2.5 lots would have to be sacrificed to store the deficit in the 33 mm h^{-1} event in a dedicated storage facility of 1 m water depth.

3.2.2 Heat stress

The results from heat stress model UCAM are graphically presented in Figure 3.11. The figure shows large differences in daily-averaged UHI effect values across the study area, varying between 0.4 and 3.06 °C. Low UHI effect values are observed in parks and green areas; high values at strongly developed locations with large structures.

The highest value observed (3.06 °C daily-averaged) corresponds with a heat-index of 0.92, which is in UCAM class III (unacceptable). The assessment according to the threshold value is shown in Figure 3.12. It shows that approximately half of the neighborhood does not satisfy the threshold value of 1.88 °C and that there are substantial heat stress risks in large portions of the study area.

The experienced temperature at a fixed location as a function of time is shown in Figure 3.13. It shows that the experienced temperature throughout the day in the grid cell with the highest UHI effect is substantially higher than the rural reference situation (up to 8.2 °C around 21:00). This grid cell is almost entirely covered by

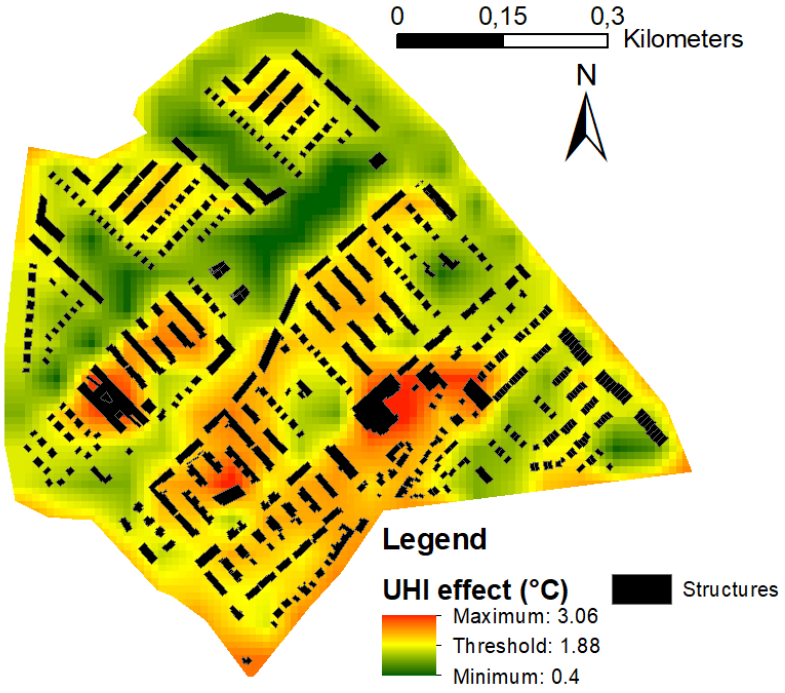

Figure 3.11: UCAM model results showing the simulated daily-averaged UHI effect in °across the study area. It was assumed that gardens feature 40% unpaved area

Figure 3.12: Detailed and interpolated heat assessment using a threshold value of 1.88 °C

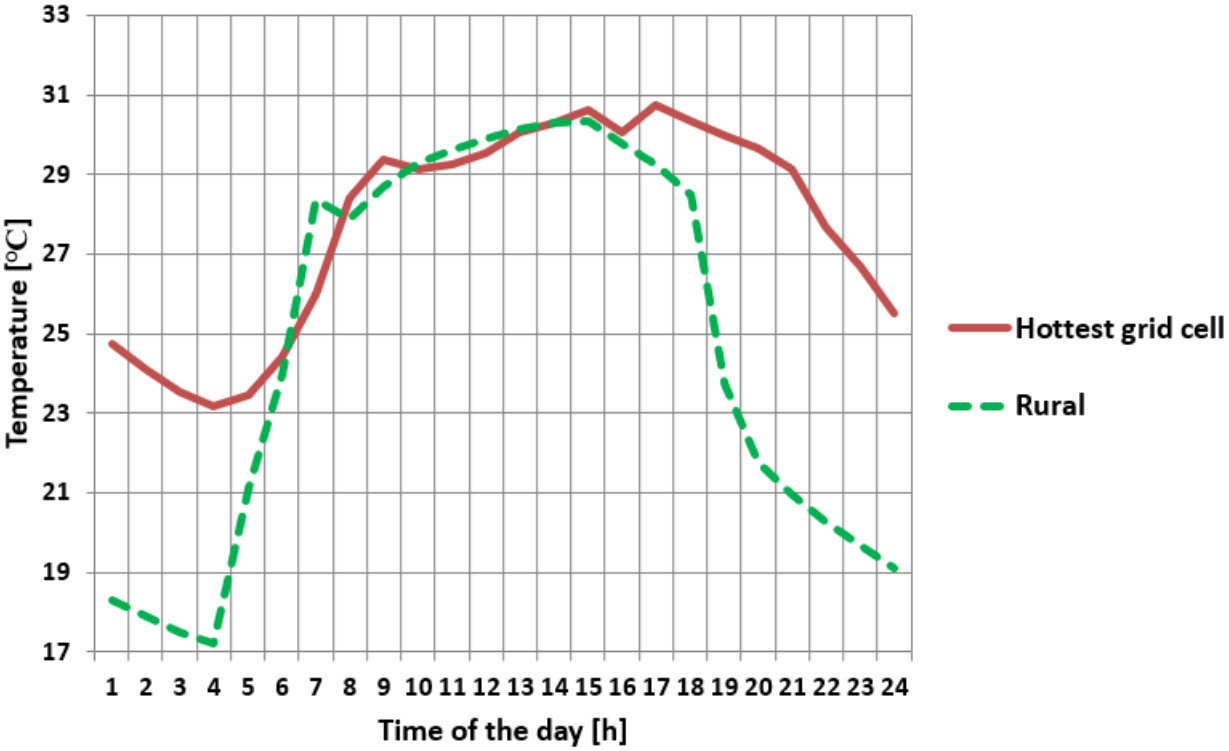

Figure 3.13: Hourly experienced temperatures in the hottest grid cell (red star in Figure 2.11 in the neighborhood (red line) during a hot day. The rural situation (green) included for reference

medium rise buildings (15 m) with low material albedo and no greenery.

Exploration of measures

For clarity, the results of the heat stress assessments with the design variants 1 (maximum material albedo) and 2 (maximum garden vegetation) are shown in Appendix D. Both variants show a substantial reduction in local heat stress. In variant 1, the daily-averaged UHI effect remains below the threshold value of 1.88 °C in almost all locations. The maximum value reached is 2.50 °C in locations with no greenery and with tall buildings. In variant 2, more areas experience a daily-averaged UHI effect above the threshold value and the maximum value reached is exactly as high as in the original design (3.06 °C; in a location without gardens), but it is still a strong overall improvement over the original design.

These outcomes show that both design options can have a strongly mitigating effect on the heat stress. In fact, it is possible to reduce the heat almost completely to values below the threshold through the use of high-albedo materials.

3.2.3 Groundwater hindrance

Application of Eq. 2.4 combined with the (assumed) parameter values presented in Figure 2.12 yields the groundwater level as a function of the horizontal distance x. The maximum of this function is NAP -0.45 m at approximately x = 26 m (distance from the left drain). As the surface level is at NAP +0.20 m, the drainage head is only 0.65 m. This is less than the threshold values of 1.0 and 1.30 m; the design fails the demands.

Exploration of measures

The surface water level, distance between drainage tubes L and the vertical drain depth were varied to assess the effects of modifications on the groundwater level. Their values in scenarios a through c are respectively: -0.88/-0.98/-0.68 m NAP, 30/45/75 m and -1.2/-1.3/-1.0 m NAP.

Table 3.8: Results of the univariate sensitivity analysis in the case of low-lying areas showing the critical drainage head. Variations of the surface water level, L and the drain level for the four scenarios: -0.88/30/-1.20, -0.98/45/-1.30 and -0.68/75/-1.0 (m -NAP, m and m -NAP)

Parameter	**Sensitivity scenario**			
	a	**b**	**c**	**Reference**
Surface water level	-0.72	-0.79	-0.57	-0.65
L	-0.95	-0.82	-0.44	-0.65
Drain level	-0.70	-0.75	-0.59	-0.65

With the surface level at +0.20 m NAP, none of the proposed measures suffice to ensure there is at least 1.0 m between the highest groundwater level and the surface level. The measures can be easily combined, however, to mitigate groundwater hindrance.

3.2.4 Drought-induced soil subsidence

The results of the drought-induced soil subsidence calculations for Hooghkamer are summarized in Table 3.9. It shows that the area is susceptible to additional soil subsidence resulting from severe droughts in the order of 1 cm per drought event.

Table 3.9: Overview of parameters and outcomes for the drought-induced soil subsidence calculations

Parameter	Reference	Drought
Relative GW level [m]	- 0 m	-0.53 m
$P_{i,\,tot}$ [kPa]	29.96	32.935
Delta $p_{i,\,tot}$ [kPa]	-	2.975
Subsidence [cm y^{-1}/total]	-	1.4/14

3.2.5 Summary of results

A short summary of the assessment results for the Hooghkamer neighborhood is provided in Table 3.10.

Table 3.10: Summary of the climate adaptiveness assessment of the Hooghkamer neighborhood

Hazard	Threshold value	Indicator value	Fail/pass
Pluvial Flooding (33 mm h^{-1})	$<$0.10 m	0.23 m	FAIL
Pluvial Flooding (69 mm h^{-1})	$<$0.3 m	0.47 m	FAIL
Heat stress	$<$1.89 °C	3.06 °C	FAIL
Groundwater hindrance	$>$1.0 m	0.65 m	FAIL
Soil subsidence	$<$0.25 m	0.14 m	PASS

3.3 Comparison of case studies

This section is devoted to discussing differences and similarities in the framework assessments of both cases. The hazards are treated in their typical order.

3.3.1 Pluvial flooding

In both cases, the designed sewage system is not able to adequately cope with the amount of rainfall. In all precipitation events, severe flooding occurs at multiple manholes exceeding the set threshold values. Proposed measures to adapt the neighborhoods' designs, either by altering the sewage capacity or decreasing the amount of paved surface, seem promising as they show a mitigating effect on pluvial flooding. These adaptations can be supplemented with measures in the private space to further reduce the risk of pluvial flooding.

An important difference between the Wilderszijde and Hooghkamer cases is projected storage deficit (in mm) as compared to the designed land use. The land use in Wilderszijde seems more favorable to withstand extreme precipitation as the total paved area is smaller than in Hooghkamer and thus less rainwater runs off. Also, there is more surface water projected in Wilderszijde and the area per manhole (2,715 m^2) is smaller than in Hooghkamer (3,460 m^2). However, the neighborhood performs worse than Hooghkamer judging by the storage deficits in mm under various scenarios. The reason for this probably lies in the design of the sewage network: Wilderszijde's network was clearly designed with more lenient forcing criteria (shower 05 or 06), where Hooghkamer is (almost) able to handle shower 08. This remains a hypothesis, however. Moreover, the number of outfalls in Wilderszijde is much smaller: only 3 compared to 21 in Hooghkamer. As a result, many manholes drain onto the same outfall in Wilderszijde, while the pipes do not have much larger dimensions. This causes bottlenecks in the sewage network nearby outfalls, causing excess flooding upstream in the manholes farther away from outfalls.

3.3.2 Heat stress

The heat stress assessment results are similar in that most results can be explained using UHI theory and are in line with expectations. For instance, more developed and paved areas generally feature larger daily-averaged values for the UHI effect while entirely green grid cells remain relatively cool. Also, in both cases approximately half the study area does not pass the assessment in the original designs.

The most notable difference between the cases is the much larger daily-averaged UHI effect attained in the Hooghkamer case (3.06 °C versus 2.27 °C; and much larger during the UHI peak in the evenings). This difference seems to stem from the more developed character of some areas within Hooghkamer. Hooghkamer features several locations with large and tall (15 m) structures and adjacent parking lots (such as a super market). UCAM classifies these areas as LCZ 2 (compact midrise) rather than LCZ 6 (open low rise). This results in higher UHI effect projections. The solely residential areas of Hooghkamer are better comparable to Wilderszijde.

3.3.3 Groundwater

The results for groundwater hindrance are similar in both cases. The drainage head is much too small (0.16 m in low-lying Wilderszijde, 0.55 m in high Wilderszijde en 0.65 m in Hooghkamer). In fact, it seems almost impossible to suffice the threshold values — especially the specific one of 1.30 m — without ensuring a larger difference between the surface water *and* the ground level and reducing the distance between

drains *L*.

3.4 Derivation of coarse design guidelines

In this section, an attempt is made to derive coarse design guidelines for Dutch neighborhoods in peatlands. These are based on the two climate adaptiveness assessments for Wilderszijde and Hooghkamer in the province of Zuid-Holland.

3.4.1 Pluvial flooding

The current designs of both neighborhoods did not comply with any of the threshold values. However, a number of possible measures were found that help mitigate flooding problems. One of the most effective measures appeared to be increasing the sewage capacity. Increasing all pipe diameters by 100 mm (mostly from the standard diameter of 300 mm to 400 mm; locally different) strongly enhances the storage capacity and even eradicates flooding altogether in the Hooghkamer case under a 33 mm h^{-1} event. However, this measure is only recommended in neighborhoods that are yet to be constructed as adapting the sewage system in existing developments is a costly matter that causes nuisance. Both designs featured standard pipe diameters of 300 mm; it is recommended to maintain a standard diameter of at least 400 mm.

The case studies have also revealed that the relative number of outfalls to surface water may have an effect. Hooghkamer performs better than Wilderszijde in spite of its less favorable land use, probably due to its sewage network having more outfall points. It is recommended to connect a maximum of 10 manholes to a single outfall; such sub-networks perform best in Hooghkamer.

Another helpful measure is reducing the amount of paved area in the public space. Roads, parking lots and roofs greatly contribute to the amount of water running off to the sewage system and excessive pavement should thus be avoided as much as possible. The results show that a reduction of paved surface to approximately 30% of the total area helps mitigate pluvial flooding. Reducing or spreading out strongly developed areas helps, as well as green roofs, grass parking tiles and other measures which promote infiltration rather than runoff in the public space.

While it did not play an important role in the case studies presented here, it is important to ensure the surface water has sufficient capacity to store extreme precipitation. Rainfall enters the surface water system through the sewage outfalls, which has a limited capacity. Assuming surface water makes up 10% of the study area, a margin of 0.70 m between the maximum maintained surface level and the

projected ground surface level should be sufficient to prevent overland flooding from the surface waters in the extreme precipitation event of 69 mm h^{-1}.

Additional measures can be taken on private property. Possible measures and their effects were discussed previously. At least citizens can be encouraged to reduce the amount of paved surface in their gardens. If necessary, municipalities have the right to issue “reasonable” demands regarding storage on private terrain.

The specific design guidelines can be summarized as follows:

1. Increasing sewage capacity, especially nearby outfalls (if neighborhood is still in design). Increase standard diameter to 400 mm;
2. Maintaining a minimum number of outfalls in the sewage network: preferably maximum 10 manholes per outfall;
3. Reducing the total amount of paved area in the public space (pavement and structures) to a maximum of 35%. Also spreading out strongly developed and paved locations;
4. Ensuring there is sufficient capacity in the projected surface water: the highest maintained surface water level should be at least 0.70 m below the ground surface level;
5. Encouraging or forcing measures in the private space: reducing paved area and/or an obligatory storage demand.

3.4.2 Heat stress

Neither Wilderszijde nor Hooghkamer performed well in the heat stress assessment. In both neighborhoods, approximately half of the study area did not comply with the set threshold value and experienced more heat stress than allowed. In the Wilderszijde case, a sensitivity analysis revealed that *either* adding more green (in the public and private space) *or* constructing all structures with light-colored materials would be sufficient for the entire neighborhood to stay below the threshold value and pass the heat stress assessment. A similar approach in the Hooghkamer case has shown that the use of high-albedo materials has the potential to reduce heat stress under the threshold value in almost every location. The effect of entirely green gardens is also mitigating, albeit slightly less so since some areas still suffer from heat stress above the threshold.

It seems that a total vegetation percentage of 30% is the minimum value for the heat stress assessment in both cases, given all other neighborhood characteristics. This percentage refers to the amount of green surface in each UCAM grid cell (50 x 50 m), the total of public and private space (gardens).

While a thorough estimation of costs for the alternative is outside the scope of this work, it seems that choosing construction materials with high albedo values

is a more cost-effective solution than additional greenery in the public space. On the other hand, greenery may also be used as additional water storage in pluvial flooding. This measure thus has co-benefits other than reducing heat stress.

The recommendation formulated here is therefore to make use of high-albedo construction materials throughout the neighborhood. Clusters of tall buildings should be avoided as these have more potential to store heat during the day. Where possible, the public space should be enhanced with additional greenery and (future) residents should be encouraged to arrange their gardens with much vegetation and avoid pavement.

These are summarized as follows:

1. Making use of high-albedo materials (light-colored) as much as possible.
2. Adding greenery in the public space where possible
3. Encouraging (future) inhabitants to design and maintain green gardens;
4. Avoiding dense clustering of tall structures: spread out where possible.

3.4.3 Groundwater

There were especially large gaps between the indicator and threshold values for groundwater hindrance in both cases. There are only two design parameters which can be altered to mitigate groundwater hindrance: the vertical distance between the projected ground surface level and the surface water/drain level, and the horizontal distance between drains.

The former measure also helps reducing the risk of flooding, as it increases the storage capacity of surface water as a co-benefit. If the vertical distance between the ground surface and surface water is 1.10 m, there is ample opportunity to store even the most extreme precipitation events and the risk of groundwater hindrance diminishes. In this case, drains need to be installed every 30 m (horizontal) so that the groundwater rise is less than 0.10 m. This ensures the neighborhood can pass the generic threshold of 1.0 m between surface and groundwater level. This can be achieved through lowering the surface water levels or leveling the area that is to be developed with a permeable soil type.

To avoid large problems with soil-subsidence, it is recommended to prevent the groundwater level from fluctuating too much during the summer. The results here have shown that an instantaneous reduction of 0.40 m in groundwater level may lead to severe soil subsidence. A maximum reduction of 0.20 m is recommended to mitigate the risk of excessive drought-induced soil subsidence. This only applies if the soil is susceptible to subsidence (thick clay and/or peat layers), but this is generally the case in peatlands.

Summarized:

1. Ensuring a minimum distance between ground level and projected surface water/drain level of 1.10 m (permeable soil type);
2. Installing drainage points every 30 m (or less, if measure 1 cannot be implemented);
3. Limiting the groundwater level reduction in summer to 0.20 m (if soil is susceptible to subsidence).

3.4.4 Comparison with existing design guidelines

The design guidelines derived in the previous sub-sections were compared with several existing documents comprising municipal design guidelines for new neighborhoods.

The most important finding is that the guidelines in existing reports are often in fact no actual guidelines but rather threshold values. The documents prescribe certain values and norms for pluvial flooding and groundwater hindrance which should not be exceeded (defined as threshold values in this work). These works and reports do not attempt to translate these thresholds to actual design values.

For example, the guidelines used by two municipalities (Gemeente Hollands Kroon, 2012; Gemeente Bunnik, 2014) do prescribe norms for pluvial flooding (e.g. water storage on streets is considered acceptable once every two years) and groundwater hindrance (minimum distance between floor level and groundwater level of 0.70 m), but do not stipulate measures on how to achieve this. This is where the present work's results differ from existing guidelines: forcings and threshold values are generalized as much as possible here and translated to actual, quantified design guidelines.

The paper by Klemm et al. (2018) focuses on a broader application of measures against heat stress than just the municipal scale. Various measures are discussed which can be implemented on the city, park and street scale, but these merely give qualitative direction and are not quantified.

Kleerekoper (2018) has made a concrete attempt at setting threshold values and quantifying neighborhood design parameters aimed at reducing heat stress. She finds that the amount of paved surface and greenery (both in the public and private space) should be approximately equal. The fraction of paved surface in the two cases studies treated in this work is about 35%. An equal vegetation share would thus be in line with the design guideline of 30% vegetation at minimum presented here.

Chapter 4

Discussion

The results and implications of this study are discussed in this chapter. It first treats the potential and contribution of this work in Section 4.1. As in every research, several limitations of the methodology and overall study were detected and these form the subject of Section 4.2.

4.1 Potential and interpretation

This work has proposed a framework for a more standardized approach in climate adaptiveness assessments, thereby partially closing the research gap described in Section 1.3. Unlike many existing stress tests, it employs a standardized methodology to assess neighborhoods while leaving some room for deviations necessitated by the local situation. This standardization manifests itself through (1) the inclusion of up to three climate change hazards and several indicators thereof, (2) underpinned proposals for 2085 climate change forcings for each of these hazards, (3) proposals for generic threshold values used to reach final assessment of each hazard (in part based on existing norms and legal requirements), and (4) its particular design for the neighborhood scale. Despite the standardization, the framework methodology itself leaves sufficient room to deviate from the generic forcings and threshold values, and even the time horizon, if the user desires. Moreover, its long temporal horizon (2085) enables the user to quantitative substantiate claims regarding climate adaptiveness even for neighborhoods which have just been completed or are still in the design phase.

Due to these characteristics, the framework presented here differs from existing stress tests. These are demand-driven in that they treat only those topics and hazards which the client has shown interest in. They almost always employ a 2050 time horizon that is too short for neighborhoods yet to be constructed and their results can only be applied locally. The framework is also distinct from the stress test

light. While the STL proposes several hazard indicators, it does not provide as much quantitative basis in the form of forcing and threshold values. One reason for this is its coarse spatial scale and resolution: its results are best interpreted regionally and not at the neighborhood scale.

Not only the entire approach of assessing climate adaptiveness was standardized in the framework, but also the forcings and thresholds of several hazards. For pluvial flooding and groundwater hindrance, the generic forcings used here were based on worst case 2085 climate projections. These were coupled with educated threshold values that were based on existing norms (pluvial flooding), the UCAM heat management program (heat stress) and legal requirements (groundwater hindrance). These forcings shed light on the adaptation efforts necessary for 2085, regardless of framework application. However, it must be noted that these forcings mostly correspond with the W_H-scenarios currently available. These are surrounded by large uncertainties, partly because of the long time horizon.

The framework also boasts the possibility to derive coarse design guidelines for similar neighborhood types using the assessment results. The design guidelines may be used in the design of alike neighborhoods to efficiently ensure their climate adaptiveness for the longer term. This feature of the framework was applied here to two neighborhoods in South Holland, inspired by the construction covenant. The results may be used to draft the design of similar neighborhoods in peatlands as the system parameters probably do not differ much. Eventually the framework can be applied to multiple types of neighborhoods featuring different system parameters. This would yield coarse guidelines or conditions for the design of any new neighborhood in the Netherlands, depending on its projected location and system parameters. The detailed quantification of design guidelines is novel: guidelines used in municipal design protocols to design new neighborhoods have been limited to qualitative descriptions, such as “increase the amount of vegetation for a cooler city” and “reduce the amount of paved area to limit runoff and decrease pluvial flooding”. These lack the specification of the quantitative extent of such measures. Where design guidelines were quantified, such as in the work by Kleerekoper (2018) regarding heat stress, the findings were in line with the results presented here.

The degree to which design guidelines and measures could be derived differs for each hazard. It appears that heat stress is a rather generic hazard in the Netherlands and measures to mitigate it also seem universally applicable. Heat stress is not influenced by neighborhod system parameters and there are multiple design parameters available to reduce it. As a result, the findings presented here seem more or less readily applicable to other neighborhood types as well. Something similar applies to pluvial flooding, but to a lesser extent. The effects of pluvial flooding seem to be governed by both system and design parameters (e.g. infiltration capacity and

elevation as system parameters versus sewage capacity and land use as design parameters). The role of system parameters limits the general applicability of measures. However, it seems logical that the results obtained are similar across cases with similar system parameters, as are the most fruitful measures to be taken and the design guidelines.

Of the three considered hazards, it appears most difficult to derive unequivocal design guidelines for groundwater hindrance and, even more so, droughts. This is even the case for a specific neighborhood type. These hazards are largely influenced by soil type (system parameter) and (regional) groundwater level management. While groundwater level management is technically a design parameter, it is governed at a larger scale than the neighborhood and can thus not always be used to mitigate groundwater problems. As a result there is no set of design parameters that can be used to mitigate drought-induced soil subsidence. This risk will have to be assessed locally and accounted for through the (ground)water management plan at a larger scale.

Several measures aimed at mitigating a climate change hazard also have a positive influence on another hazard (co-benefits). These are (1) reducing the amount of paved area [pluvial flooding and heat stress], (2) increasing the distance between surface water level and maximum groundwater level [pluvial flooding and groundwater hindrance], and (3) increasing the amount of greenery, both in the public and private space [pluvial flooding and heat stress]. These measures may be especially interesting if a neighborhood fails the assessment on multiple hazards. The measures may have even more co-benefits, for example in improving air or water quality, or in general well-being, but these were not considered here.

Another insight provided by the application of the framework is that the covenant's demands and thresholds seem excessively ambitious and strict. This applies to the pluvial flooding demand that a precipitation event of 120 mm h^{-1} may not cause damage to structures. There is a large difference between the generic forcing event of 69 mm h^{-1} derived here (T = 100 years in 2085) and the 120 mm h^{-1} stated in the covenant. This figure seems to lack a solid scientific basis, has been the subject of much criticism from multiple engineering firms and is likely to be softened. The drainage head difference demand of 1.30 m is another strict demand that requires much effort to achieve in practice. It is also substantially more ambitious than the legal requirement of 1.0 m. The large differences between the indicator values presented throughout this work and the specific thresholds mentioned in the covenant underline this.

4.2 Limitations

4.2.1 Framework limitations

While the framework's methodology itself was successfully standardized, it remains difficult to standardize the choice of models, their forcings, hazard indicators and their threshold values. The choice for models often depends on the availability of data and practical considerations, which vary across cases. Political choices also play a role, for example in the decision on which hazards should be considered in the study. The design of the framework allows for such freedoms, but it was not possible here to compose a single tool with fixed choices for hazards, indicators and threshold values (only proposed generic values). As a result, the assessment outcomes may still depend on (arbitrary) choices made. More importantly, the variety of possible model choices and configurations may jeopardize the possibility to derive design guidelines for each neighborhood type due to a lack of comparability. In other words: to be able to accurately derive design guidelines, the underlying choices of framework case applications must not differ too much. This was not the case in this work, but is a limitation for future case studies.

In addition, it appeared impossible to reach the desired level of standardization of each hazard's forcing and threshold values. This was especially the case in drought-induced soil subsidence. It was attempted to generalize and standardize the forcings and thresholds of this hazard, but this would not allow for the desired level of detail and would impair a thorough assessment. As a result, only the method to arrive at a forcing is standardized; its precise value still depends on the local situation. Full standardization of climate adaptiveness assessment thus seems not possible; there should be some room for tailored application.

Another point for discussion, and possibly a limitation of the framework, is the large amount of uncertainty inherent with the used climate scenarios. The employed time horizon is long and this implies the amount of uncertainty is high. Not only is there uncertainty in the development of temperature and circulation pattern (the four KNMI climate scenarios), but also within each scenario most indicators show broad bandwidths. The framework attempts to assess current neighborhood designs under the climate conditions projected for 2085. The degree of climate adaptiveness and extent of necessary measures is thus also very dependent on how climate change unfolds and manifests itself in the future. In its current design, the framework is not fully able to account for these uncertainties as it assumes worst case climate projections. It also assumes neighborhoods are designed and constructed according to a robust approach and spatial characteristics are not altered during the time horizon. This may result in the costly exaggeration of climate adaptation efforts. In reality, it

may be possible to change certain design parameters depending on climate change developments, even without incurring high costs or much hindrance. An example is (ground)water level management. Alternatively, a neighborhood could be designed conservatively in that the initial design should comply with the framework assessment. Should it appear that the effects of climate change are modest, the design parameters imposed may be relaxed. For instance, space may be left available for greenery initially, but this space can be taken by additional developments if climate developments allow for it.

While the derivation of generic neighborhood design guidelines has provided some insight in relevant design parameters and desired values thereof, costs or other benefits were not included here. As a result, the outcomes presented here do not directly reflect optimal solutions for each neighborhood. The cost-effectiveness may differ across cases. The framework would benefit from a more inclusive discussion in which the implications of measures in terms of costs and co-benefits also receive attention.

4.2.2 Hazard simulation limitations

In this work, InfoWorks ICM was used to obtain simulations of pluvial flooding. The results seem credible as application of the forcings by which the networks were designed returns no or minor flooding. However, it was necessary to make some assumptions, probably at the cost of model accuracy. A major assumption is the use of Thiessen polygons to determine which location drains to which manhole. This approach was considered justifiable here, especially because there are no designed variations in ground surface level, but it does not entirely reflect reality. Moreover, the study areas were divided into five land use categories: open/closed paved, flat/inclined roofs and pervious area, each with their own runoff coefficients programmed within InfoWorks ICM. If no runoff occurs (for instance in pervious locations), it is assumed that all rainfall infiltrates. In reality this does not seem reasonable, especially given the extreme precipitation events that were forced and the fact that the soil types in this neighborhood type allow for limited infiltration only.

This study has also once again revealed that the modeling of heat stress is still underdeveloped. While UCAM was successfully used to simulate heat stress at the neighborhood scale and obtain plausible results, it lacks the configuration possibilities of programs used for other hazards and desired to perform a thorough assessment. For instance, UCAM does not allow the configuration of forcing: it is merely based on the characteristics of a 2006 heat wave. The model was usable to give an impression of the heat stress experienced in the cases, but could not be used to find the absolute local effects under 2085 climate conditions. Moreover, the model is

simplistic in that it works with only 5 land use classes whose characteristics can be altered only to a certain extent. For example, all greenery in the area is reduced to a single aspect without the ability to differentiate for the precise type of vegetation and the effect of shadows. Nevertheless the model functioned sufficiently well to explore the effects of several measures, but the absolute outcomes must be considered critically.

For groundwater hindrance, the formula of Hooghoudt (Eq. 2.2) was used. Its application was considered acceptable on the neighborhood scale, but the results do stem from an empirical formula that assumes homogeneous geology and hydraulic conductivities across the study area. This will not be the case in reality and subsurface structures may impede the groundwater flow, which is not included in the equation. This approach was used conservatively to obtain an impression of the extent of groundwater hindrance in the area, but the actual situation is inevitably going to be different from the results presented here. The neighborhood scale may actually still be too large for good application of Hooghoudt's formula; it would be better to consider each subsystem of drains separately. Alternatively, the area could be modeled in a suitable software package.

The formula of Koppejan (Eq. 2.5) was used to estimate drought-induced soil subsidence. It was not possible in this study to provide a very thorough and local value of soil subsidence for the long temporal horizon. As described previously, soil subsidence is strongly dependent on local groundwater level management and geology. The forcing is therefore more specific than generic and based on local groundwater levels during droughts. Also, soil may subside under other forces than droughts, such as autonomous soil subsidence and the extraction of subsurface natural resources. These were not included here, but can be relevant in neighborhood design and construction.

4.2.3 Impact of limitations on the results

The limitations mentioned in the previous sections have inevitably had an impact on the results of this study and their accuracy. While simulations have shown the mitigating effects of several measures on the climate change hazards, their precise extent must be approached with caution, due to uncertainties in (1) 2085 climate projections (forcing), (2) neighborhood system parameters and (3) abstractions and assumptions used to facilitate simulations. Considering the extent of the uncertainties, the only way to robustly design a neighborhood that will require minimum future spatial adaption is to use the conservative design guidelines derived here. These guidelines are coarse and will need to be reviewed as more certainty regarding climate change becomes available. However, they do provide a clear direction in the

neighborhood design parameters necessary for climate adaptiveness in peatlands.

The limitations have also had an effect on the derivation of design guidelines. The sheer amount of uncertainty associated with the quantitative output makes it impossible to determine the extent of measures at the neighborhood level very accurately. This is one reason why it is recommended to leave sufficient open spaces in new neighborhoods: these can be turned into various land uses depending on how climate change unfolds.

Chapter 5

Conclusions & recommendations

This final chapter is dedicated to the conclusions drawn from this study and several recommendations for subsequent research and for practice in application of the framework.

5.1 Conclusions

The research aim of this work was twofold: (1) to develop and apply a framework that can be used to assess quantitatively whether or not a neighborhood suffices the climate adaptiveness objectives under the 2085 climate conditions as projected by the KNMI, and (2) to use its results to prescribe coarse design guidelines for new neighborhoods. The research was guided by the following research questions:

1. Can the assessment of neighborhood climate adaptiveness be standardized in a framework, given its design and climate scenarios?
2. Can the outcomes of the framework assessment be used to derive coarse design guidelines for new neighborhoods?
3. Which design guidelines could contribute to making planned neighborhoods in Dutch peatlands sufficiently climate adaptive assuming a 2085 temporal horizon?

The systematic approach and various steps in the framework have been essential in the standardization of climate adaptiveness assessments. Actual standardization was achieved through the formulation of underpinned generic forcing events, quantitative indicators and threshold values. These standardization attempts are novel and can be helpful even outside the application of the framework presented here. The choice to include certain hazards (and excluding others) also contributes to the standardization endeavor. Furthermore it was important to distinguish design parameters from system parameters; the latter were more or less considered

boundary conditions depending on the geographical location and connected to the neighborhood typology.

The choice of models was fixed for the cases treated in this work, based on their applicability on the neighborhood scale and on practical motivation. The design of the framework allows for the application of different models. It does not seem realistic nor necessary to prescribe the choice for certain models within the framework. However, the simulation tools should comply with certain criteria regarding (1) the resolution (neighborhood), (2) the ability to provide quantitative values of the (standardized) indicators and (3) the ability of modifying both the climate forcing and design parameters in the model. The resolution of the simulations of the climate change hazards was sufficient to propose specific measures locally. For each hazard, several possible measures and their effects were investigated. This allowed for the coarse derivation of design parameters in neighborhoods with similar system parameters.

This study has shown that the developed framework is able to guide the assessment of a neighborhood's climate adaptiveness. The various steps of the framework have supported a systematic approach in the two case studies. The choice to include several hazards has contributed to standardization and the threshold values in conjunction with simulated indicator values provided the means to assess climate adaptiveness quantitatively. With sufficient data about a neighborhood's system and design parameters, it is possible to substantiate claims regarding its climate adaptiveness. Moreover, the framework is unique in that it is designed to assume a long temporal horizon (2085; although other forcings can be freely applied) and the used models provided simulations with a spatial resolution fitting the neighborhood scale application. This scale is much smaller than the scale employed in the stress test light, whose results are often presented on a coarse scale only. Also, the framework does not simply lead to a single conclusion about climate adaptiveness, but specifically includes an iteration loop to update the design should a neighborhood not pass the assessment. This makes the framework a suitable starting point for future neighborhood designs.

This research has also shed light on the possibility of standardizing forcings, indicators and threshold values for the hazards considered. The extent to which these could be derived differed strongly across the hazards. Moreover, it has appeared that some hazards are influenced more by system or design parameters than others. As a general rule of thumb, the smaller the influence of system parameters on the hazard's indicator values, the easier it was to derive generic design guidelines for that hazard. Table 5.1 provides a summary of these findings.

It appeared well possible to standardize forcing events, find a suitable indicator and determine educated threshold values for the hazard of pluvial flooding. This

hazard has also received much attention in the past, both in literature and in practice. While the effects of pluvial flooding can be mitigated through certain design parameters (such as sewage capacity and lay-out, and infiltration facilities), there are also several system parameters that influence its effects (most importantly local geology and elevation). As a result, it was possible to derive some design guidelines regarding pluvial flooding, but their applicability depends on the neighborhood typology because of the system parameters' influence.

Heat stress seems to be a quite generic climate change hazard in the Netherlands: its forcing and thresholds can be easily standardized and extent of the hazard is mainly dependent on a number of design parameters and not on system parameters. System parameters such as geology, elevation and location within the country have no or minimum effect on heat stress, while there are many design parameters involved, such as amount of vegetation, building density and color of construction materials. Its effects can thus easily be mitigated through neighborhood design.

While it appeared possible to determine a rather specific forcing, indicator and threshold for groundwater hindrance, this was not the case for drought-induced soil subsidence. The forcing and threshold are both arbitrary for the latter hazard, making it difficult to derive generic design guidelines. Both groundwater-related hazards depend strongly on the local geology and this further decreased the possibility to determine generic design guidelines. Nevertheless, some guidelines were derived in the cases considered here which may be able to give some direction in the design of neighborhoods in peatlands. These hazards do require much local input, hindering full standardization.

Table 5.1: Summary of standardization possibilites and genericity of derived design guidelines for each hazard

	Pluvial flooding	**Heat stress**	**GW hindrance**	**Drought**
Standardization of forcing	Standardized	Standardized	Standardized	Limited: local information
Standardization of indicator	Standardized	Standardized	Standardized	Arbitrary
Standardization of threshold value	Standardized	Standardized	Standardized	Arbitrary
Influence of system parameters	Medium	Minor	Major	Major
Genericity of design guidelines	Medium	High	Low	Low

High genericity as listed in Table 5.1 means that the derived design guidelines are

applicable to virtually any Dutch neighborhood. Medium means that the guidelines are applicable to neighborhoods of similar typology: if the system parameters are similar, the design guidelines are applicable. Low genericity means that the guidelines provide some direction regarding the design in neighborhoods of similar typology, but that the final design still must be tailored to the local situation as the governing system parameters are decisive. The design thus also requires local tailored assessment.

5.2 Recommendations

Here several recommendations which may help improve the framework and the subsequent derivation of design guidelines are presented. First some general recommendations are made, then some specifically aimed at Witteveen+Bos and affiliated parties.

5.2.1 General recommendations

While uncertainty is inherent to climate change projections, especially for such a long term, it would be beneficial for the framework to emphasize this uncertainty explicitly and show its implications in the quantitative output. For instance, the uncertainty ranges for each hazard's forcing could be included in the simulations to obtain bandwidths of possible outcomes in indicator values. This would also help the framework's users appreciate the uncertainty of the projections.

The current version of the framework is rather static as it assumes a neighborhood to be designed robustly in that no major adaptations are to be implemented during its lifetime. This was done for simplicity, but it is not very likely that a neighborhood's spatial characteristics do not change over time. Costs associated with adaptations may be minimized if works are combined with regular maintenance. One way to make the framework more dynamic and to account for some uncertainties in climate change predictions would be to follow a DAPP-like approach (see Chapter 1. In that way the costs and benefits of multiple measures are considered for each hazard and each measure is allocated a tipping point.

As treated in Chapter 4, it was found that heat stress is the most generic climate change hazard in the Netherlands as its forcing, threshold values and design requirements can be used across the Netherlands. Despite its potential to be fully standardized, heat stress modeling is still in its infancy and approaches vary greatly across cases. It would be beneficial to further standardize the assessment of heat stress to provide more insight in the possible and necessary design choices that mitigate heat stress.

5.2.2 Recommendations for practice

The derivation of design guidelines has been limited to presenting possible measures and quantifying their effects. A next step which would aid neighborhood designers would be to include costs of measures so that they can make more educated choices regarding neighborhood design.

Currently the framework assumes a robust neighborhood design in that the neighborhood is fully constructed according to the design and is not changed for its lifespan. To help cope with uncertainty in climate change, some decisions regarding neighborhood design may be desirable to postpone or altered until there is more clarity regarding climate change developments. Again, this is similar to the DAPP-approach treated previously.

Another recommendation is to conduct more case studies using the framework. The results presented here give some direction as to the design parameters necessary to achieve a sufficient level of climate adaptiveness in the long term, but the findings are based on only two case studies. More cases in peatlands can help validate these findings and may yield more results and new additional insights. Moreover, it is recommended to apply the framework to planned neighborhoods of other typology (e.g. “high” Netherlands with sandy soils and high elevations) and explore what design characteristics are required in order for them to be sufficiently climate adaptive. It would be interesting to compare the findings across neighborhood types in the Netherlands.

The framework currently supports the inclusion of pluvial flooding, heat stress and several groundwater problems as climate change hazards. Other issues that threaten the liveability of neighborhoods, such as air and water quality issues, may also be mitigated by many of the measures mentioned throughout this work. It may be worthwhile to explore the potential of including such issues as well in subsequent versions of the framework.

References

Allen, D. (2010). Historical trends and future projections of groundwater levels and recharge in coastal British Columbia , Canada. In *21st salt water intrusion meeting* (pp. 267–270). Azores, Portugal.

Antea Group. (2018). *Klimaatbestendig ontwikkelen wijk Bronsgeest - Noordwijk* (Tech. Rep.). Deventer: Antea Group.

Arnfield, A. J. (2003). Two decades of urban climate research: A review of turbulence, exchanges of energy and water, and the urban heat island. *International Journal of Climatology*, *23*(1), 1–26. doi: 10.1002/joc.859

Barron, O., Crosbie, R., Dawes, W., Pollock, D., Charles, S., Mpelasoka, F., ... Wurcker, B. (2018). *The impact of climate change on groundwater resources: The climate sensitivity of groundwater recharge in Australia* (Tech. Rep.). CSIRO: Water for a Healthy Country Report to National Water Commission. Retrieved from http://link.springer.com/10.1007/978-3-319-92459-5{_}22 doi: 10.1007/978-3-319-92459-5_22

Barton, H., Grant, M., & Guise, R. (2003). *Shaping Neighbourhoods, A Guide for Health, Sustainability and Vitality*. London, UK: Spon Press.

Bear, J. (1979). *Hydraulics of groundwater* (Vol. 3) (No. 4). New York: McGraw-Hill. doi: 10.1016/0309-1708(80)90046-9

Carrera, J., Medina, A., Heredia, J., Vives, L., Ward, J., & Walters, G. (1989). Parameter Estimation in Groundwater Modelling: From Theory to Application. *Groundwater Contamination: Use of Models in Decision-Making*, 151–169. Retrieved from http://www.springerlink.com/index/10.1007/978-94-009-2301-0{_}15 doi: 10.1007/978-94-009-2301-0_15

Casal-Campos, A., Sadr, S. M., Fu, G., & Butler, D. (2018). Reliable, Resilient and Sustainable Urban Drainage Systems: An Analysis of Robustness under Deep Uncertainty. *Environmental Science and Technology*, *52*(16), 9008–9021. doi: 10.1021/acs.est.8b01193

Corfee-Morlot, J., Cochran, I., Hallegatte, S., & Teasdale, P. J. (2011). Multilevel risk governance and urban adaptation policy. *Climatic Change*, *104*(1), 169–197. doi: 10.1007/s10584-010-9980-9

Croley, T., & Luukkonen, C. (2003). Potential Effects of Climate Change on Ground Water in Lansing, Michigan. *Journal of the American Water Resources Association*, *39*(1), 149–163.

Crosbie, R. S., Scanlon, B. R., Mpelasoka, F. S., Reedy, R. C., Gates, J. B., & Zhang, L. (2013). Potential climate change effects on groundwater recharge in the High Plains Aquifer, USA. *Water Resources Research*, *49*(7), 3936–3951. doi: 10.1002/wrcr.20292

Cunge, J. A., & Wegner, M. (1964). Intégraton Numérique Des Equations d'Écoulement de Barré de Saint-Venant par un Schéma Implcite de Différences Finies. *La Houille Blanche*(1), 33–39.

de Glopper, R., & Ritzema, H. (2006). Land Subsidence. In H. Ritzema (Ed.), *Drainage principles and applications* (pp. 477–512). Wageningen.

Deltacommissie. (2014). *Deltabeslissing Ruimtelijke Adaptatie* (Tech. Rep.). Den Haag: Ministerie van Infrastructuur en Milieu. Retrieved from https://www.deltacommissaris.nl/deltaprogramma/deltabeslissingen/deltabeslissing-ruimtelijke-adaptatie

Fan, Y., Ao, T., Yu, H., Huang, G., & Li, X. (2017). A Coupled 1D-2D Hydrodynamic Model for Urban Flood Inundation. *Advances in Meteorology*, *2017*, 1–12. doi: 10.1155/2017/2819308

Gemeente Bunnik. (2014). *Programma van Eisen Voor het inrichten van de Openbare Ruimte Gemeente Bunnik* (Tech. Rep.). Gemeente Bunnik.

Gemeente Hollands Kroon. (2012). *Handboek Inrichting Openbare Ruimte* (Tech. Rep.). Gemeente Hollands Kroon.

Ghoneem, M. Y. M. (2016). Planning for Climate Change, Why does it Matter? (From Phenomenon to Integrative Action Plan). *Procedia - Social and Behavioral Sciences*, *216*(October 2015), 675–688. Retrieved from http://linkinghub.elsevier.com/retrieve/pii/S1877042815062400 doi: 10.1016/j.sbspro.2015.12.060

Green, T. R. (2016). Linking Climate Change and Groundwater. In *Integrated groundwater management* (1st ed., chap. 5. Linking). Springer International Publishing. Retrieved from http://link.springer.com/10.1007/978-3-319-23576-9 doi: 10.1007/978-3-319-23576-9

Haasnoot, M., Kwakkel, J. H., Walker, W. E., & ter Maat, J. (2013). Dynamic adaptive policy pathways: A method for crafting robust decisions for a deeply uncertain world. *Global Environmental Change*, *23*(2), 485–498. Retrieved from http://dx.doi.org/10.1016/j.gloenvcha.2012.12.006 doi: 10.1016/j.gloenvcha.2012.12.006

Hardoy, J., & Ruete, R. (2013). Incorporating climate change adaptation into planning for a liveable city in Rosario, Argentina. *Environment and Urbanization*, *25*(2), 339–360. doi: 10.1177/0956247813493232

Hooghoudt, S. (1940). Algemeene Beschouwing van het probleem van de detailontwatering en de infiltratie door middel van parallel loopende drains, greppels, slooten en kanalen. *Bijdrage tot de kennis van eenige naturkundige grootheden van den grond*(7), 515–707.

Hoppe, T., van den Berg, M. M., & Coenen, F. H. (2014). Reflections on the uptake of climate change policies by local governments: Facing the challenges of

mitigation and adaptation. *Energy, Sustainability and Society*, *4*(1), 1–16. doi: 10.1186/2192-0567-4-8

Horton, R. (1933). The Role of Infiltration in the Hydrological Cycle. *Trans. Am. Geophysical Union*, *14*, 446–460.

Hunt, A., & Watkiss, P. (2011). Climate change impacts and adaptation in cities: A review of the literature. *Climatic Change*, *104*(1), 13–49. doi: 10.1007/s10584-010-9975-6

HydroLogic. (2015). *Stresstest voor Klimaatbestendige Ruimte PWVE* (Tech. Rep.). Author.

IDDS. (2010). *Rapport betreffende verkennend en nader bodemonderzoek op de locatie Hooghkamer te Voorhout* (Tech. Rep.). Author.

Imhoff, M. L., Zhang, P., Wolfe, R. E., & Bounoua, L. (2010). Remote Sensing of Environment Remote sensing of the urban heat island effect across biomes in the continental USA. *Remote Sensing of Environment*, *114*(3), 504–513. doi: 10.1016/j.rse.2009.10.008

IPCC. (2001). *Claimte Change 2001: The Scientific Basis* (Tech. Rep.). Retrieved from `https://www.ipcc.ch/ipccreports/tar/wg1/pdf/WGI{_}TAR{_}full{_}report.pdf` doi: 10.1256/004316502320517344

Jabareen, Y. (2013). Planning the resilient city: Concepts and strategies for coping with climate change and environmental risk. *Cities*, *31*, 220–229. Retrieved from `http://dx.doi.org/10.1016/j.cities.2012.05.004` doi: 10.1016/j.cities.2012.05.004

Keverlingh Buisman, A. (1940). *Grondmechanica*. Delft, NL: Band IV.

Kleerekoper, L. (2018). *Ontwerprichtlijnen voor de hittebestendige stad* (Tech. Rep.). Amsterdam: Hogeschool van Amsterdam.

Klein Tank, A., Beersma, J., Bessembinder, J., Van den Hurk, B., & Lenderink, G. (2015). *KNMI Climate Scenarios for the Netherlands* (Tech. Rep.). De Bilt: KNMI.

Klemm, W., Lenzholzer, S., Brink, A. V. D., Klemm, W., Lenzholzer, S., & Brink, A. V. D. (2018). Developing green infrastructure design guidelines for urban climate adaptation Developing green infrastructure design guidelines for urban climate adaptation. *Journal of Landscape Architecture*, *12*(3), 60–71. doi: 10.1080/18626033.2017.1425320

Koppejan, A. (1942). A Formula Combining the Terzaghi Load-Compression Relationship and the Buisman Secular Time Effect.

Lehmann, P., Brenck, M., Gebhardt, O., Schaller, S., & Süßbauer, E. (2015). Barriers and opportunities for urban adaptation planning: analytical framework and evidence from cities in Latin America and Germany. *Mitigation and Adaptation Strategies for Global Change*, *20*(1), 75–97. doi: 10.1007/

s11027-013-9480-0

Lindley, S. J., Handley, J. F., Theuray, N., Peet, E., & Mcevoy, D. (2006). Adaptation strategies for climate change in the urban environment: Assessing climate change related risk in UK urban areas. *Journal of Risk Research*, *9*(5), 543–568. doi: 10.1080/13669870600798020

Marchau, V., Walker, W. E., Bloemen, P. J. T. M., & Popper, S. (2019). *Decision Making under Deep Uncertainty*. Springer. Retrieved from http://link.springer.com/10.1007/978-3-030-05252-2 doi: 10.1007/978-3-030-05252-2

McCarthy, M. P., Best, M. J., & Betts, R. A. (2010). Climate change in cities due to global warming and urban effects. *Geophysical Research Letters*, *37*(9), 1–5. doi: 10.1029/2010GL042845

Measham, T. G., Preston, B. L., Smith, T. F., Brooke, C., Gorddard, R., Withycombe, G., & Morrison, C. (2011). Adapting to climate change through local municipal planning: Barriers and challenges. *Mitigation and Adaptation Strategies for Global Change*, *16*(8), 889–909. doi: 10.1007/s11027-011-9301-2

Meijel, M. G. V. (2017). *Stapsgewijs naar een klimaatbestendige stad* (Unpublished doctoral dissertation). Hogeschool van Hall Larenstein.

Miller, J. D., & Hutchins, M. (2017). The impacts of urbanisation and climate change on urban flooding and urban water quality: A review of the evidence concerning the United Kingdom. *Journal of Hydrology: Regional Studies*, *12*(July), 345–362. doi: 10.1016/j.ejrh.2017.06.006

Mirzaei, P. A. (2015). Recent challenges in modeling of urban heat island. *Sustainable Cities and Society*, *19*, 200–206. Retrieved from http://dx.doi.org/10.1016/j.scs.2015.04.001 doi: 10.1016/j.scs.2015.04.001

Nelen&Schuurmans. (2018). *Stresstest Klimaatbestendigheid Hoofddorp en Nieuw-Vennep* (Tech. Rep.). Utrecht: Nelen & Schuurmans.

NEXT Consultancy. (2015). *Exploitatieplan Hooghkamer 2011, 2e herziening* (Tech. Rep.). Gouda: NEXT Consultancy.

Oke, T. (1995). The Heat Island of the Urban Boundary Layer: Characteristics, Causes and Effects. In J. Cermak, A. Davenport, E. Plate, & D. Viegas (Eds.), *Wind climate in cities.* Dordrecht, NL: Springer. doi: 10.1007/978-94-017-3686-2

Patra, J., Kumar, R., & Mani, P. (2016). Combined fluvial and pluvial flood inundation modelling for a project site. *Procedia Technology*, *24*, 93–100. doi: 10.1016/j.protcy.2016.05.014

Powers, J., Klemp, J., Skamarock, W., Davis, C., Dudhia, J., Gill, D., ... Duda, M. (2017). The Weather Research and Forecasting Model. *American Meteorological Society*(August), 1717–1738. doi: 10.1175/BAMS-D-15-00308.1

RIONED. (2006). *Stedelijke Wateropgave* (Tech. Rep.). Ede: Author.

Rosenberg, N., Epstein, D., Wang, D., Vail, L., Srinivasan, R., & Arnold, J. (1999). Possible Impacts of Global Warming on the Hydrology of the Ogallala Aquifer Region. *Climatic Change*, *42*, 677–692.

Rovers, V., Bosch, P., & Albers, R. (2014). *Climate Proof Cities* (Tech. Rep.). Den Haag: TNO. Retrieved from `http://knowledgeforclimate.climateresearchnetherlands.nl/{%}5Cnhttp://knowledgeforclimate.climateresearchnetherlands.nl/climateproofcities` doi: Doi10.1016/S0005-1098(00)00028-5

Schipper, E. L. F. (2006). Conceptual History of Adaptation in the UNFCCC Process. *Reciel*, *15*(1), 82–92.

Schreider, S. Y., Smith, D. I., & Jakeman, A. J. (2000). Climate change impacts on urban flooding. *Climatic Change*, *47*, 91–115. doi: 10.1023/a:1005621523177

Schwarz, N., Schlink, U., Franck, U., & Großmann, K. (2012). Relationship of land surface and air temperatures and its implications for quantifying urban heat island indicators An application for the city of Leipzig. *Ecological Indicators*, *18*, 693–704. doi: 10.1016/j.ecolind.2012.01.001

Stewart, I. D., & Oke, T. R. (2012). Local climate zones for urban temperature studies. *Bulletin of the American Meteorological Society*, *93*(12), 1879–1900. doi: 10.1175/BAMS-D-11-00019.1

Stone, B., & Rodgers, M. (2001). How the Design of Cities Influences the Urban Heat Island Effect. *APA Journal*, *67*(2), 186–196.

Terzaghi, K., Peck, R., & Mesri, G. (1967). *Soil Mechanics in Engineering Practice* (3rd ed.). New York: Wiley. doi: 10.1097/00010694-194911000-00029

Van Buuren, A., Driessen, P. P., Van Rijswick, M., Rietveld, P., Salet, W., Spit, T., & Teisman, G. (2013). Towards adaptive spatial planning for climate change: Balancing between robustness and flexibility. *Journal for European Environmental and Planning Law*, *10*(1), 29–53. doi: 10.1163/18760104-01001003

Van de Ven, F., Luyendijk, E., de Gunst, M., Tromp, E., Schilt, M., Krol, L., ... Peeters, R. (2009). *Waterrobuust bouwen, de kracht van kwetsbaarheid in een duurzaam ontwerp* (Tech. Rep.). Rotterdam: SBR.

Vörösmarty, C. J., Green, P., Salisbury, J., & Lammers, R. B. (2000). Global Water Resources: Vulnerability from Climate Change and Population Growth. *Science*, *289*(July), 284–288. doi: 10.1126/science.289.5477.284

Zhou, Q., Mikkelsen, P. S., Halsnæs, K., & Arnbjerg-nielsen, K. (2012). Framework for economic pluvial flood risk assessment considering climate change effects and adaptation benefits. *Journal of Hydrology*, *414-415*, 539–549. doi: 10.1016/j.jhydrol.2011.11.031

Appendix A

Climate change hazards in Atlas

The following systematizations summarize which climate change hazards are taken into account by the Climate Impact Atlas (water hindrance, drought and heat; in the purple ellipses). It also indicates the primary output criteria used to compose the maps shown in the Atlas (green rounded rectangles) and the data of the most sensitive functions used to compose the maps (blue rectangles).

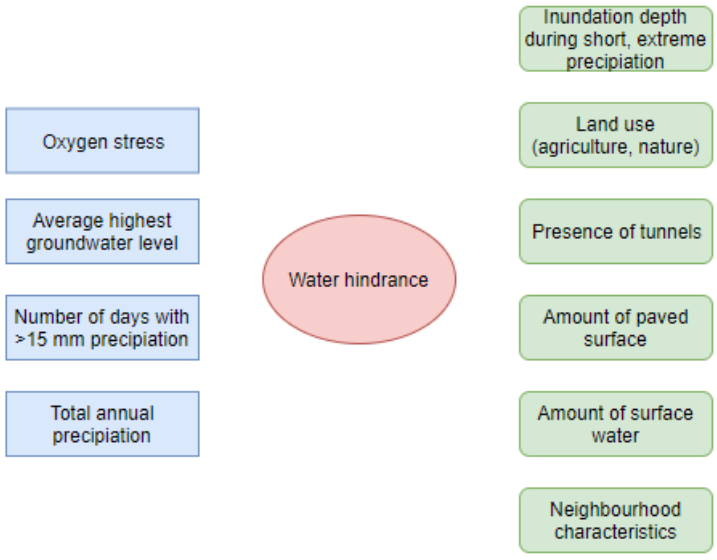

Figure A.1: Overview of the climate effects (blue) and sensitive functions and characteristics (green) used to assess the hazard water hindrance (purple) in the Climate Effect Atlas

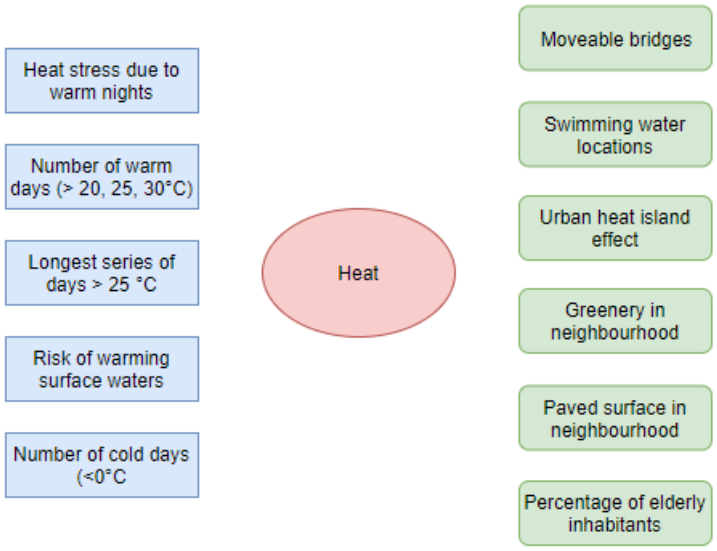

Figure A.2: Overview of the climate effects (blue) and sensitive functions and characteristics (green) used to assess the hazard heat (purple) in the Climate Effect Atlas

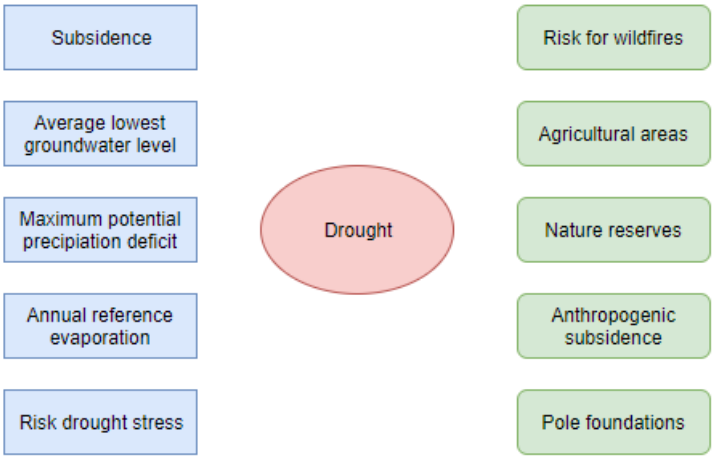

Figure A.3: Overview of the climate effects (blue) and sensitive functions and characteristics (green) used to assess the hazard drought (purple) in the Climate Effect Atlas

Appendix B

Elaborate model descriptions

This appendix serves to provide a more elaborate description of InfoWorks ICM, the model used to simulate pluvial flooding in the case studies.

B.1 InfoWorks ICM

Water which reaches the stormwater sewage is modeled using the 1D module of ICM; surface water flow is simulated using the 2D module.

For 1D flow, InfoWorks ICM employs the Saint Venant's equations (Randall, 2006). The continuity equation can be written as follows:

$$\frac{\partial A}{\partial t} + \frac{\partial Q}{\partial x} = 0 \tag{B.1}$$

and the momentum balance equation as:

$$\frac{\partial Q}{\partial t} + \frac{\partial}{\partial x}\Big(\frac{Q^2}{A}\Big) + gA\Big(\cos\phi\,\frac{\partial y}{\partial x} - S_0 \cdot \frac{Q|Q|}{K^2}\Big) = 0 \tag{B.2}$$

where A is the cross-sectional area [L^2], t time [T], Q the discharge [$L^3\ T^{-1}$], x the horizontal distance [L], g the gravitational constant (9.81 m s^{-2}), ϕ the angle of the sewer bottom with the horizontal plane (degrees), y the vertical distance [L], S_0 the pipe slope (in degrees; equal to ϕ) and K the conveyance [$L^3\ T^{-1}$].

Eqs. B.1 and B.2 are solved for free surface problems. As the sewage is filled with water, this poses a difficulty for which the equations cannot account on their own. A well-known solution that is also applied in ICM is the so-called Preissmann slot (see also Cunge and Wegner (1964)). This comes down to an engineering fix of a practical modeling problem.

Eqs. B.1 and B.2 are solved using the finite difference method that used Pressmann's four-point implicit difference scheme in pipes (for further reading, see Fan et al. (2017)). The water level and flow discharge are subsequently expressed at each conduit junction and solved through an iteration procedure. To overcome the

problem that Preissmann's scheme cannot simulate supercritical flow, critical flows are treated as subcritical by correcting the convective momentum term in Eq. B.2. Again, for more information the reader is referred to Fan et al. (2017).

For 2D surface water modeling, ICM uses the full shallow water equations, written as follows when the Coriolis and wind effects are neglected:

$$\frac{\partial h}{\partial t} + \frac{\partial (hu)}{\partial x} + \frac{\partial (hv)}{\partial y} = q_{1D} \tag{B.3}$$

$$\frac{\partial (hv)}{\partial t} + \frac{\partial}{\partial x}\left(hv^2 + \frac{gh^2}{2}\right) + \frac{\partial (huv)}{\partial y} = -gh(S_{0,x} - S_{f,x}) + q_{1D}u_{1d} \tag{B.4}$$

$$\frac{\partial (hv)}{\partial t} + \frac{\partial}{\partial y}\left(hv^2 + \frac{gh^2}{2}\right) + \frac{\partial (huv)}{\partial x} = -gh(S_{0,y} - S_{f,y}) + q_{1D}v_{1d} \tag{B.5}$$

where h is the water depth [L], u and v the velocities in the x and y directions respectively [L T^{-1}], q_{1D} the source discharge per unit area [L T^{-1}], $S_{0,x}$ and $S_{0,y}$ the ground slope [-] in the x and y directions and S_f the friction slope.

These equations are integrated over the control volume and solved using a second-order backward difference scheme. More details regarding this method can be found in Fan et al. (2017).

Appendix C

Results updated designs Wilderszijde

C.1 Pluvial flooding

C.1.1 Modifications in discharge

C.1.2 Modifications in storage within the study area

C.2 Heat stress

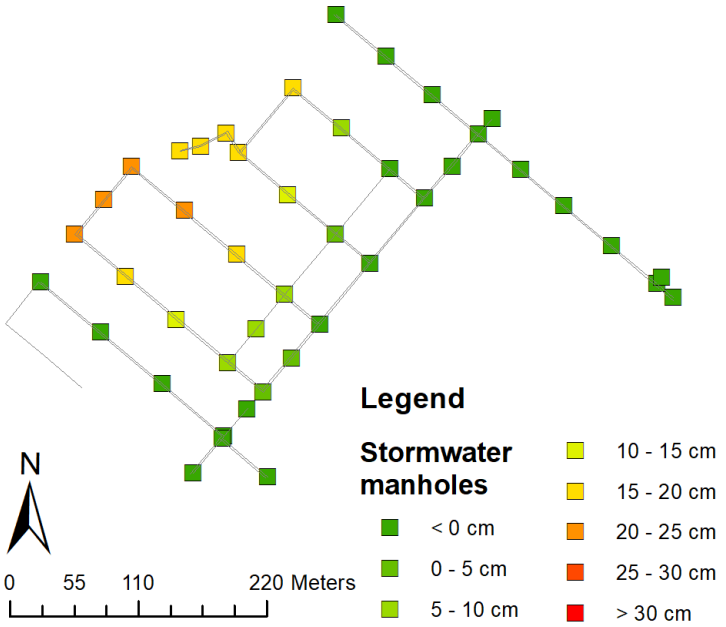

Figure C.1: InfoWorks ICM results showing maximum flood depths at stormwater manholes for a precipitation event of 33 mm in 1 hour. Here the sewer design was adapted so that each pipe's diameter is 100 mm larger than in the design

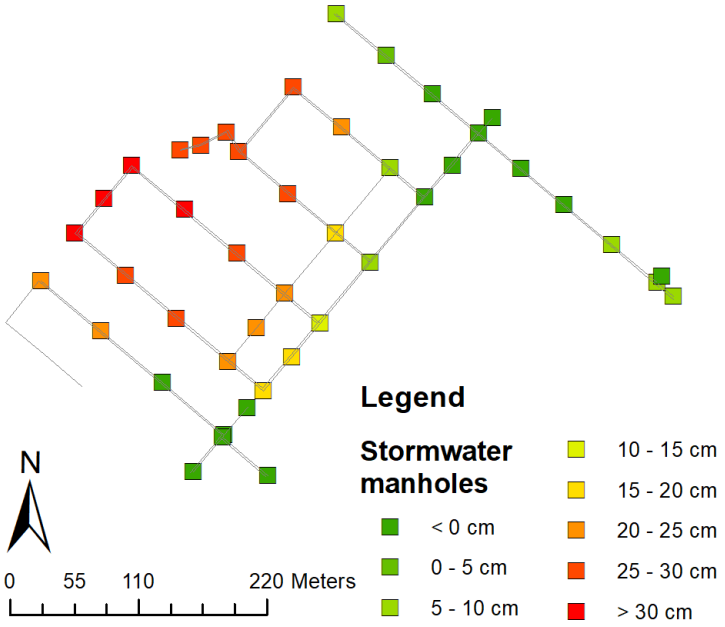

Figure C.2: InfoWorks ICM results showing maximum flood depths at stormwater manholes for a precipitation event of 69 mm in 1 hour. Here the sewer design was adapted so that each pipe's diameter is 100 mm larger than in the design

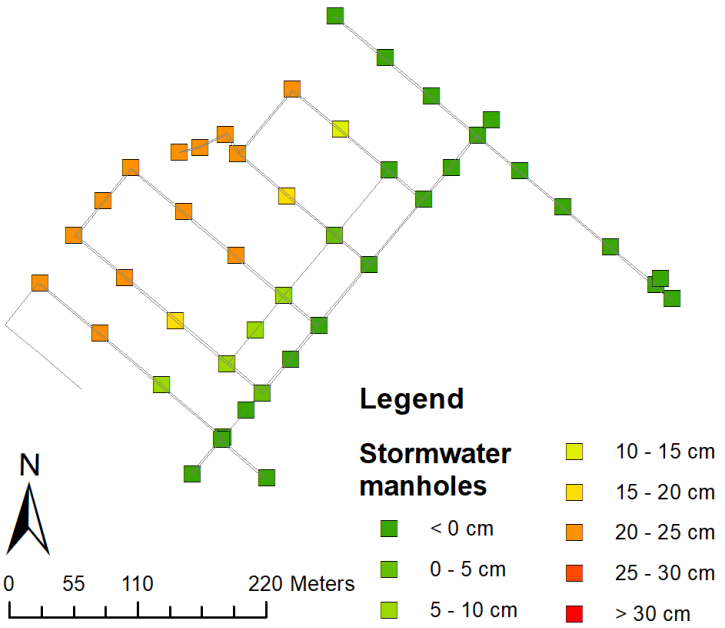

Figure C.3: InfoWorks ICM results showing maximum flood depths at stormwater manholes for a precipitation event of 33 mm in 1 hour. Here the sub-catchments are adapted so that there is 10 % less paved surface

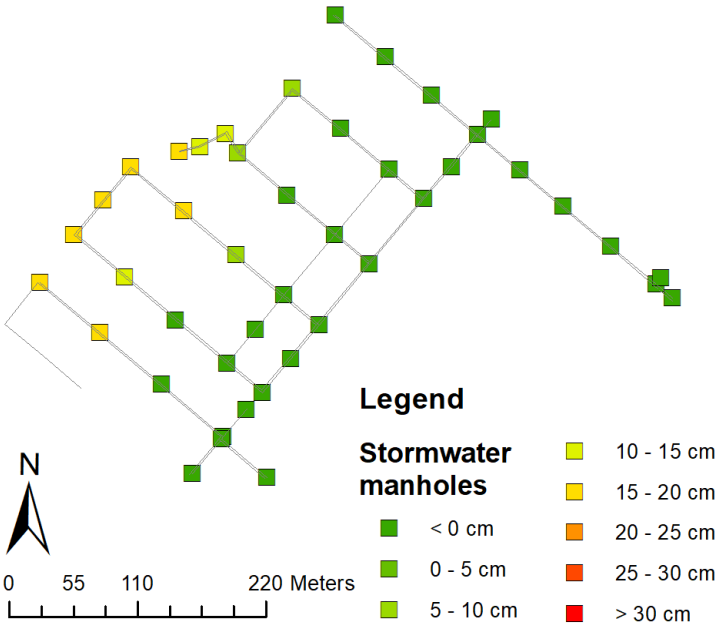

Figure C.4: InfoWorks ICM results showing maximum flood depths at stormwater manholes for a precipitation event of 33 mm in 1 hour. Here the sub-catchments are adapted so that there is 20 % less paved surface

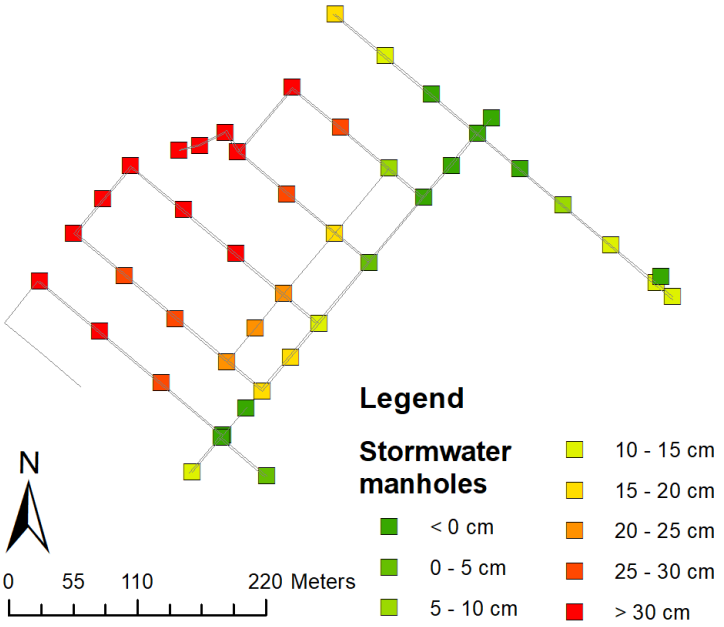

Figure C.5: InfoWorks ICM results showing maximum flood depths at stormwater manholes for a precipitation event of 69 mm in 1 hour. Here the sub-catchments are adapted so that there is 10 % less paved surface

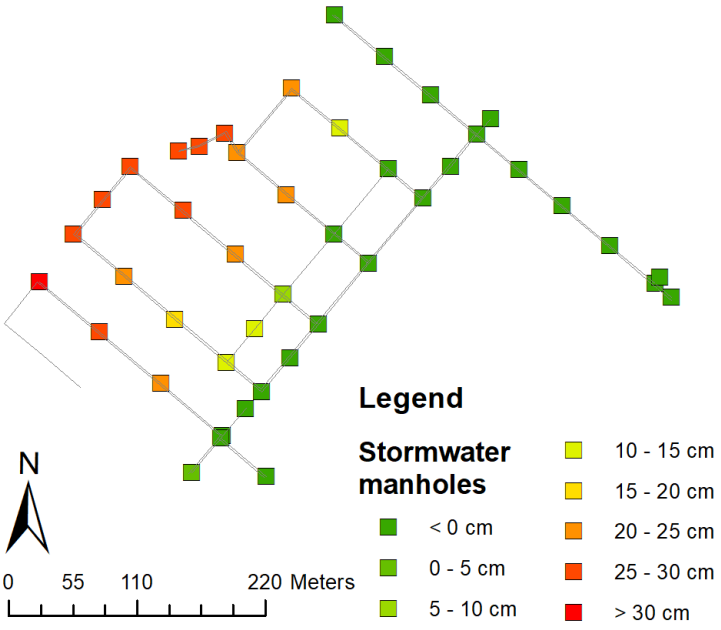

Figure C.6: InfoWorks ICM results showing maximum flood depths at stormwater manholes for a precipitation event of 69 mm in 1 hour. Here the sub-catchments are adapted so that there is 20 % less paved surface

Appendix D

Results updated designs Hooghkamer

D.1 Pluvial flooding

D.1.1 Enlarged sewage capacity

D.1.2 Reduction of paved surface

D.2 Heat stress

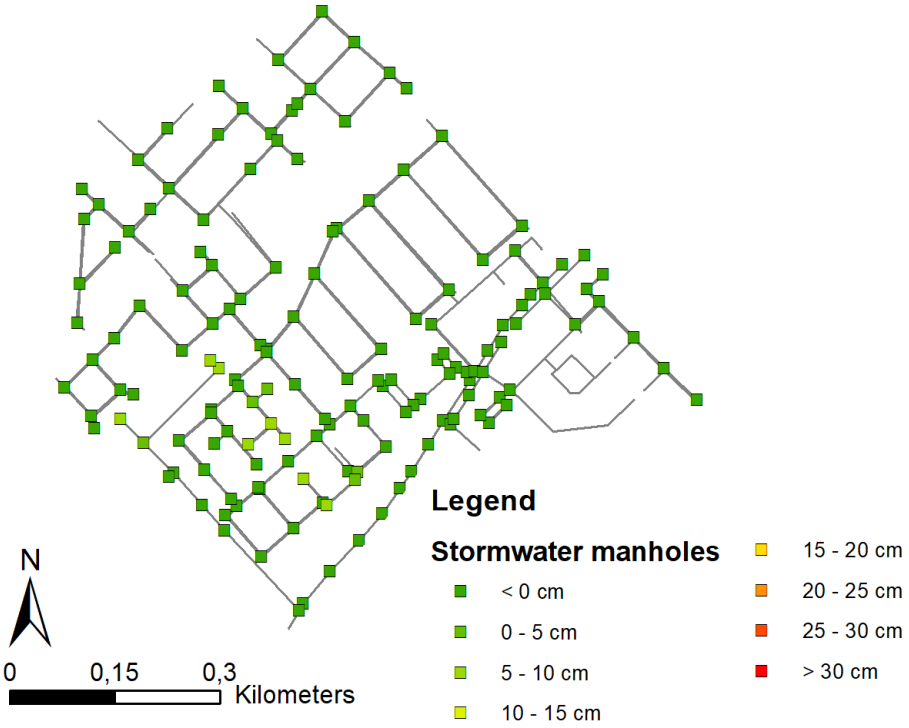

Figure D.1: InfoWorks ICM results showing maximum flood depths at stormwater manholes for a precipitation event of 33 mm in 1 hour in Hooghkamer. Here the sewer design was adapted so that each pipe's diameter is 100 mm larger than in the design

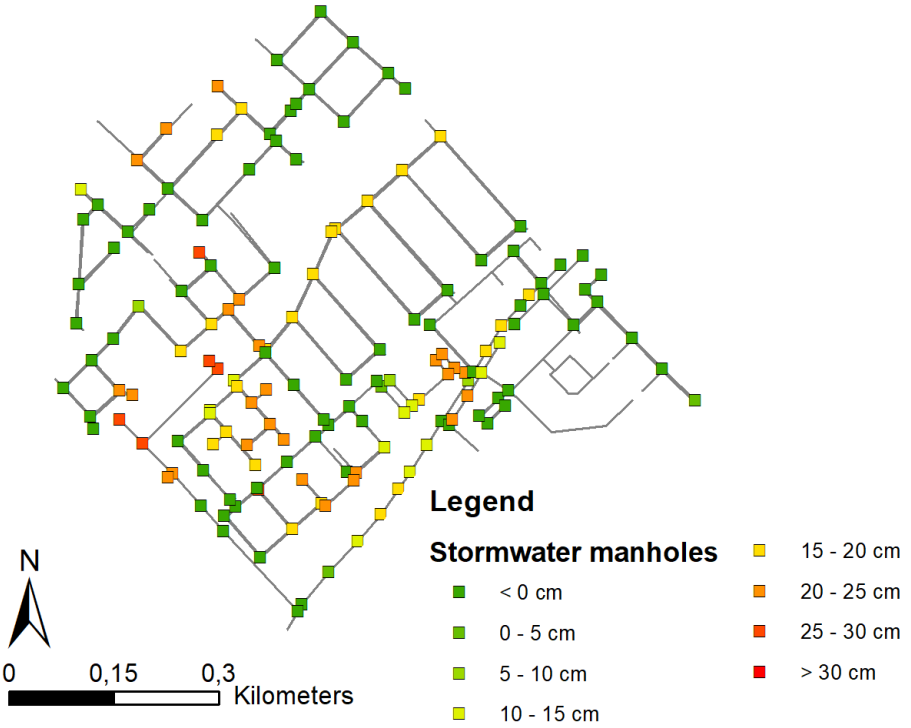

Figure D.2: Identical to Figure D.1, but for a 69 mm h^{-1} event

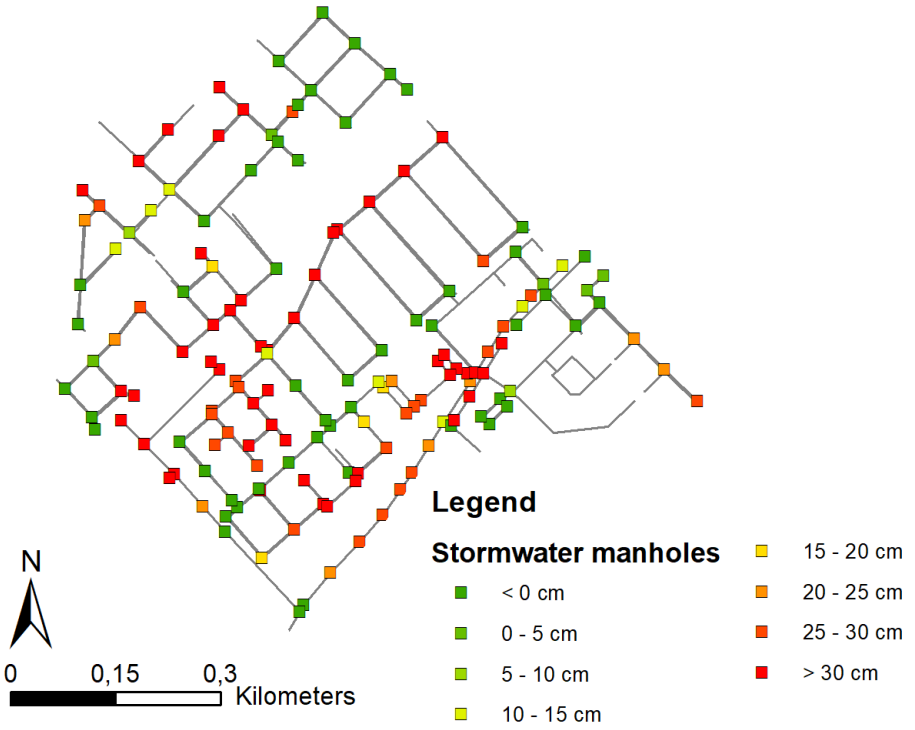

Figure D.3: Identical to Figure D.1, but for a 120 mm h^{-1} event

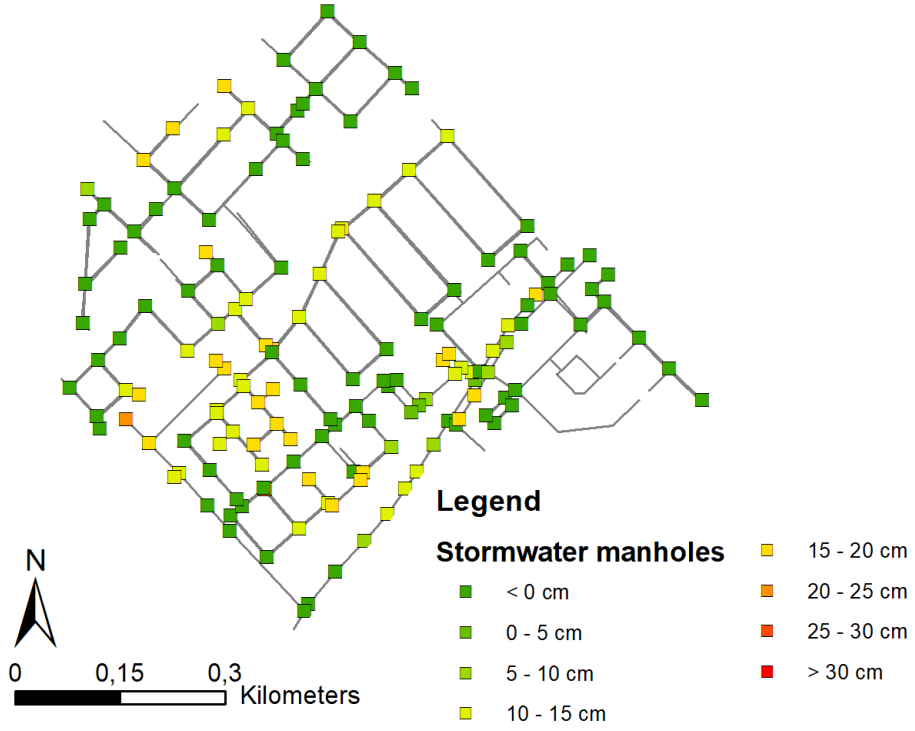

Figure D.4: InfoWorks ICM results showing maximum flood depths at stormwater manholes for a precipitation event of 33 mm in 1 hour in Hooghkamer. Here the amount of paved surface (closed and open paved) was reduced by 10%

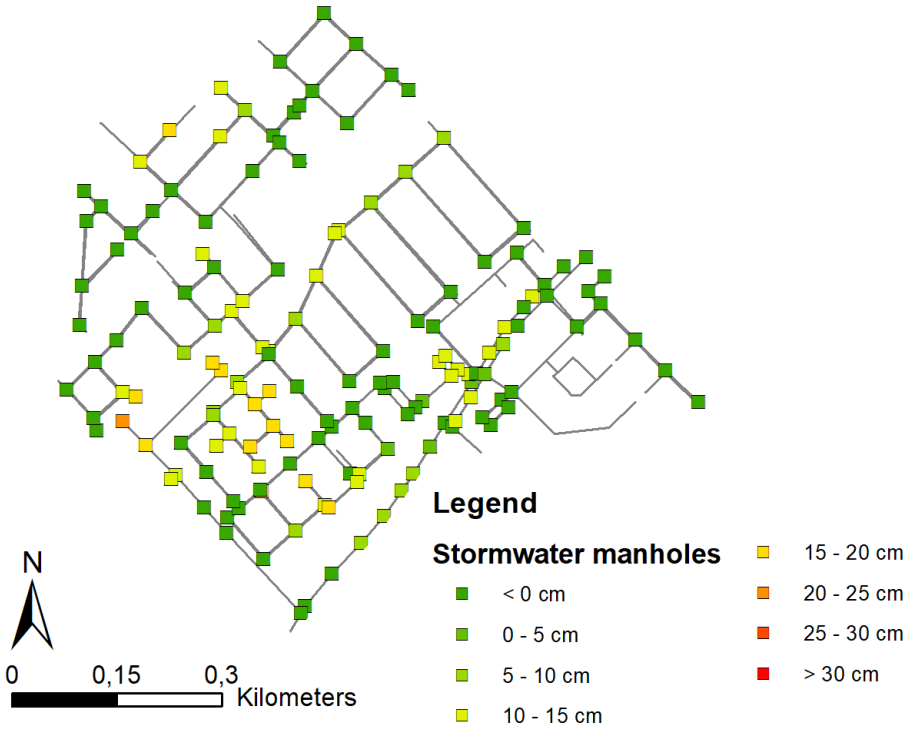

Figure D.5: Identical to Figure D.4, but with a reduction of paved surface by 20%

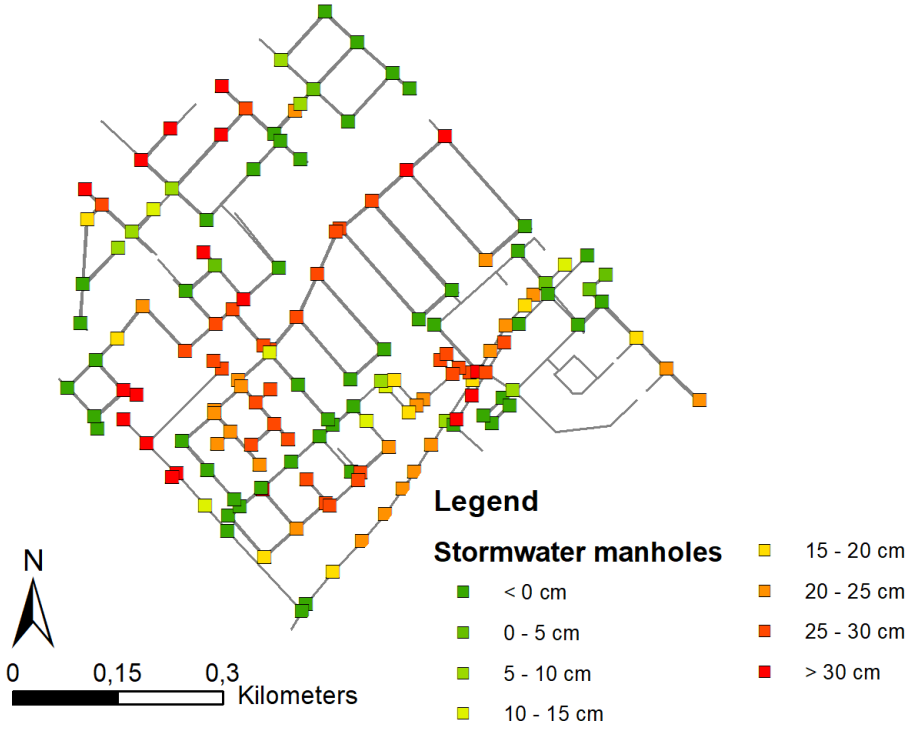

Figure D.6: InfoWorks ICM results showing maximum flood depths at stormwater manholes for a precipitation event of 69 mm in 1 hour in Hooghkamer. Here the amount of paved surface (closed and open paved) was reduced by 10%

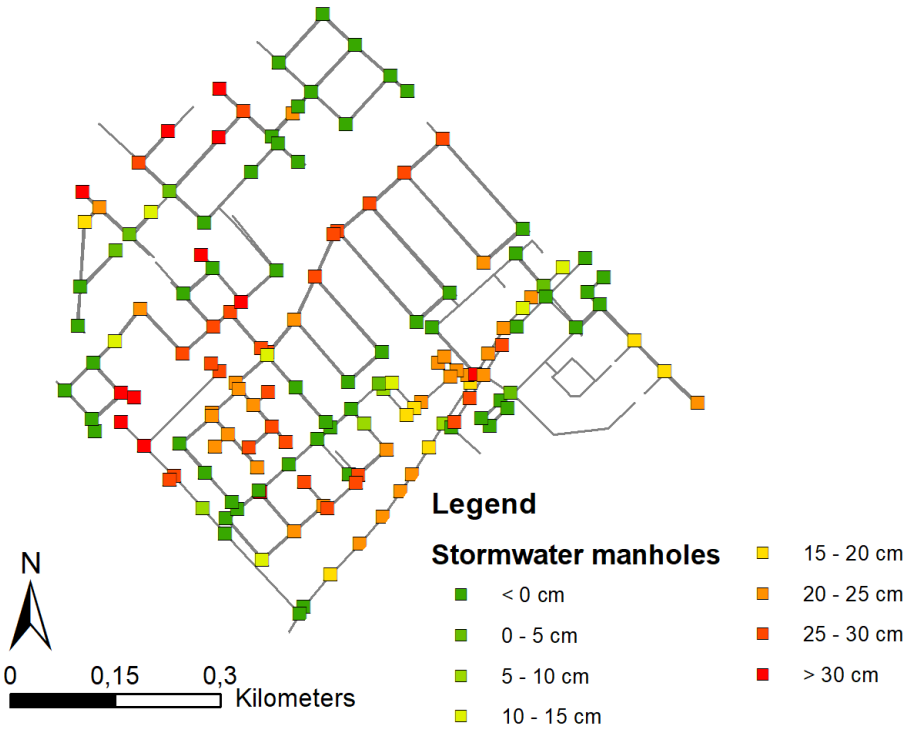

Figure D.7: Identical to Figure D.6, but with a reduction of paved surface by 20%

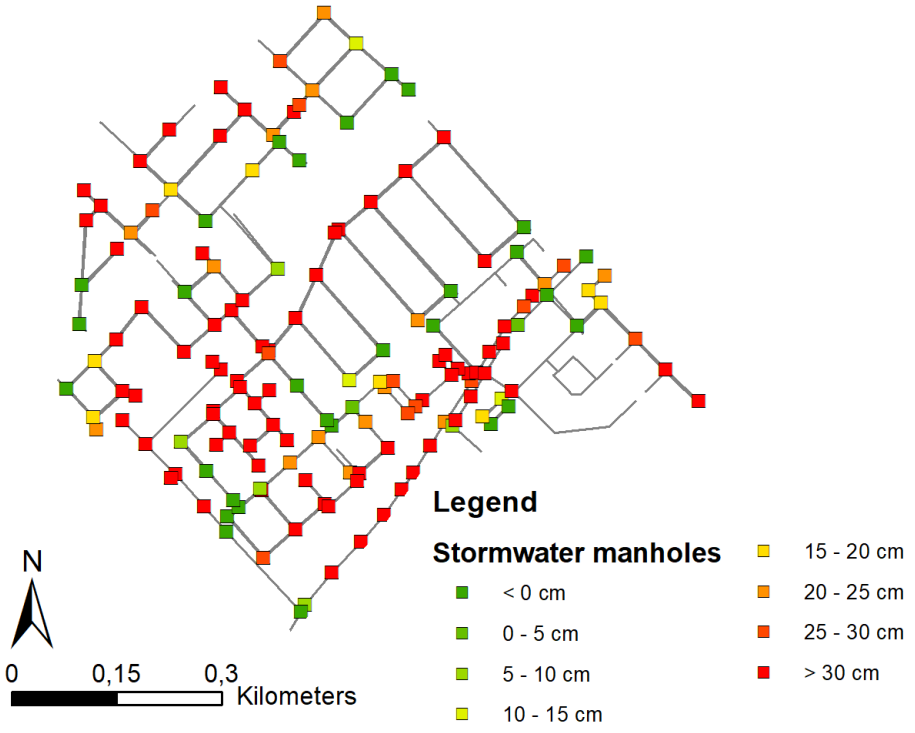

Figure D.8: InfoWorks ICM results showing maximum flood depths at stormwater manholes for a precipitation event of 120 mm in 1 hour in Hooghkamer. Here the amount of paved surface (closed and open paved) was reduced by 10%

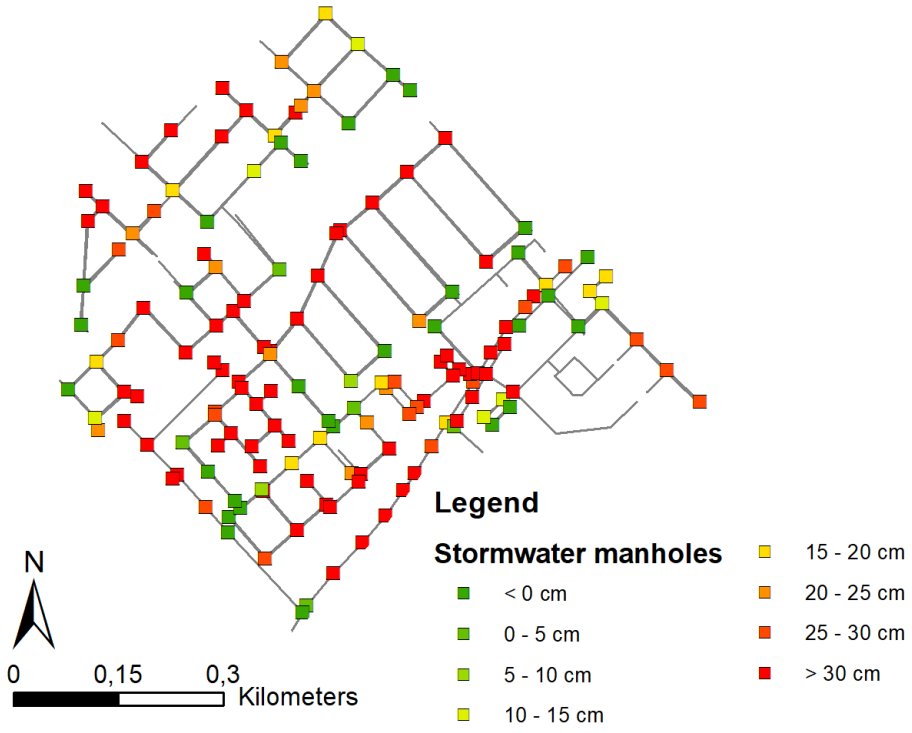

Figure D.9: Identical to Figure D.8, but with a reduction of paved surface by 20%

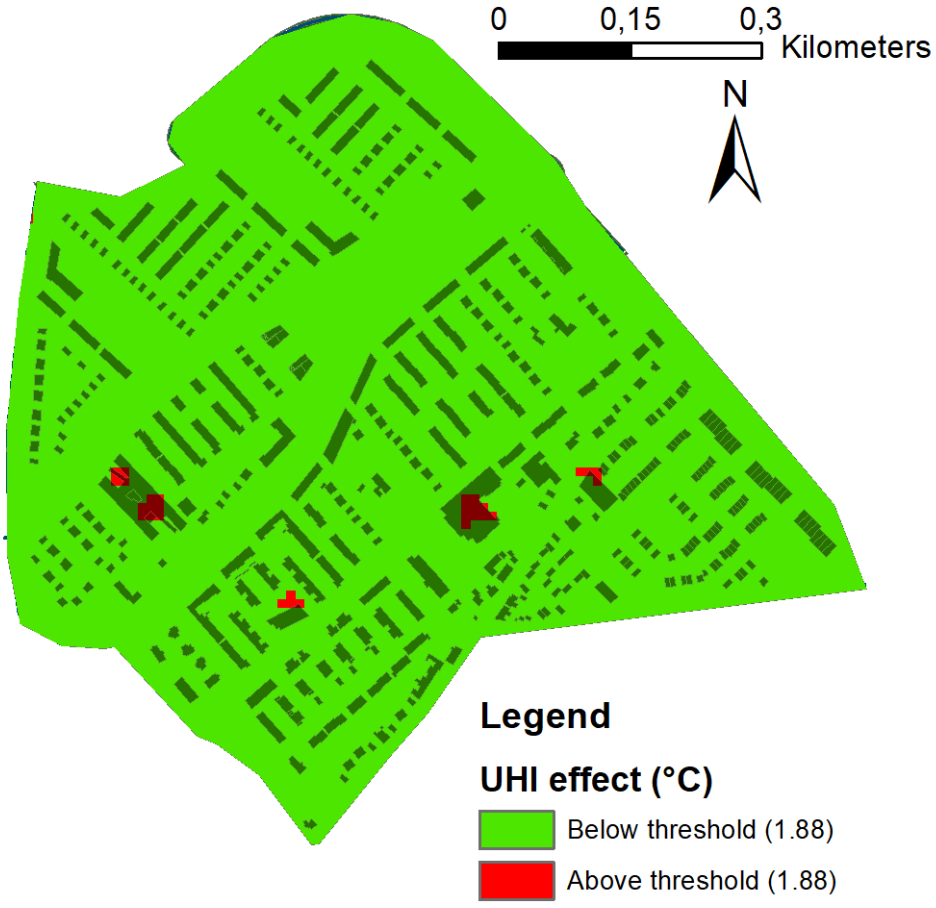

Figure D.10: Detailed and interpolated heat assessment using a threshold value of 1.88 °C for variant 1 (maximum albedo values)

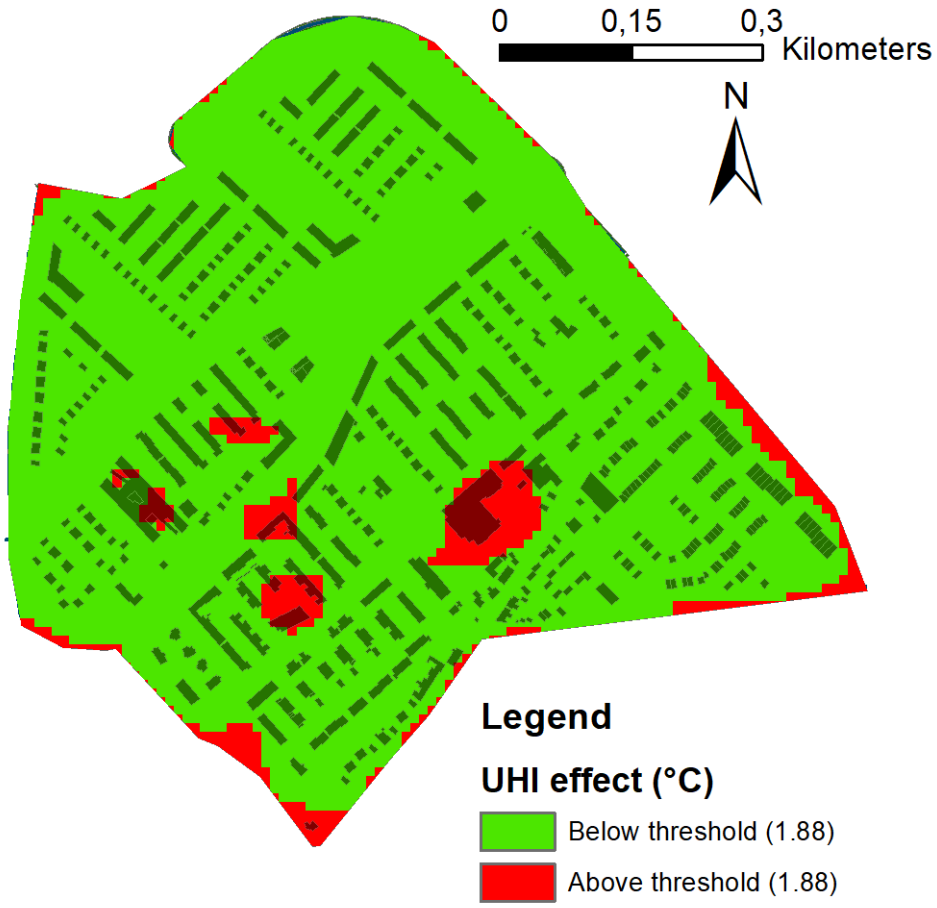

Figure D.11: Detailed and interpolated heat assessment using a threshold value of 1.88 °C for variant 1 (maximum garden vegeation)